MATHEMATICAL MODELING OF CASSAVA WASTEWATER TREATMENT SYSTEM

BY

EZE REMIGIUS ONUKWUGHA (B.ENG; M.ENG.)

REG. NO: 20074587018

A THESIS SUBMITTED TO THE POSTGRADUATE SCHOOL,

FEDERAL UNIVERSITY OF TECHNOLOGY, OWERRI

IN

PARTIAL FULFILLMENT OF THE REQUIREMENTS FOR THE AWARD OF THE DEGREE OF DOCTOR OF PHILOSOPHY (PH.D) IN CIVIL ENGINEERING (WATER RESOURCES ENGINEERING)

JANUARY, 2015

CERTIFICATION

This Thesis, 'Mathematical Modeling of Cassava Wastewater Treatment System' by Eze Remigius Onukwugha, Reg. No: 20074587018 has been read and approved as meeting the requirements of the School of Postgraduate Studies, Federal University of Technology, Owerri for the award of degree of Doctor of Philosophy (PhD) in Civil Engineering (Water Resources Engineering).

_____	_____
Engr. Prof. J.C. Agunwamba (Supervisor)	**Date**
_____	_____
Engr. Prof. B.A. Nwachukwu (Supervisor)	**Date**
_____	_____
Engr. Dr. B.C. Okoro (Supervisor)	**Date**
_____	_____
Engr. Dr. (Mrs.) B. U. Dike (Head, Civil Engineering Dept.)	**Date**
_____	_____
Engr. Prof. E. E. Anyanwu (Dean, School of Engineering and Engineering Technology)	**Date**
_____	_____
Engr. Prof. K. B. Oyoh (Dean, Postgraduate School)	**Date**
_____	_____
External Examiner	**Date**

DEDICATION

To the memory of my Father: Chief Anthony D.I. Onukwugha

ACKNOWLEDGEMENTS

First and foremost I offer my sincerest gratitude to my Supervisors Engr. Prof. J.C. Agunwamba and Engr. Dr. B.C. Okoro who have supported me both in proposing this topic and guiding in the writing of the thesis with their patience and knowledge, while allowing me the room to work in my own way. I attribute the level of my doctoral degree to their encouragement and effort and without them this thesis, too, would not have been completed or written. One simply could not wish for better or friendlier supervisors.

My sincere gratitude goes to the Head of department Engr. Dr. (Mrs.) B. U. Dike and other Lectures: Engr. Dr. J. C. Ezeh, Dr. D. O. Onwuka, Engr. Dr. L. O. Ettu, and all members of staff of Civil Engineering Department, Federal University of Technology Owerri for their contributions and suggestions during my seminars. I am thankful to Engr. Prof. B.A. Nwachukwu for his guidance and also to Engr. Prof. I.L. Nwaogazie and the other lecturers of Civil Engineering Department for their constant encouragement.

In the various laboratories and workshops I have been aided for many months in running the equipment and experiments by Mr. Enyinnia Chibundu of the department of Civil Engineering, Federal Polytechnic Nekede Owerriwho also helped me with sample collections. I also wish to thank Mr. Charles Onyegbula

who assisted me in the importation of the peristaltic pump employed in the experiments.

Thanks to Engr. Obinna Ibeje for his support in certain computer applications for this study. I am unreservedly grateful to Engr. Prof. E. E. Anyanwu, Dean, School of Engineering and Engineering Technology; Engr. Prof. (Mrs.) K. B. Oyoh, Dean, Postgraduate School and Engr. Prof. O.N. Oguoma and Engr. Dr. S. N. Asoegwu for their immense contributions and assistance throughout my postgraduate work.

I wish to express my heartfelt gratitude and appreciation to the entire members of my family for their high-spirited encouragement and patience during the busy period of this work.

Finally, I thank God for his continual mercies, guidance, blessings and protection.

ABSTRACT

The study presented mathematical model for the treatment process of cassava wastewater system. Anaerobic Baffled Reactor (ABR) was used for the analysis of cassava wastewater samples from a cassava processing factory at Imo Polytechnic, Umuagwo, Imo State, Nigeria. The kinetic coefficients for the two processes (with and without inhibition) were determined after the treatments for the obtained values. The characterization of the wastewater showed the pH of the wastewater was high from the measured levels of alkalinity and turbidity obtained. Tests were also conducted to determine cyanide, total solids, dissolved solids, suspended solids, fixed solids, volatile solids contents and the chemical oxygen demand (COD). The results of all these tests and measurements were used for further analyses with mathematical models $\mu_g = \frac{\mu_m S}{K_s + S}$ and $Y = \frac{Y_{max} S}{K_m + S}$, graphs and other mathematical tools available. These aided in the evaluation of seven kinetic coefficients which include endogenous decay coefficient, cell yield coefficient, maximum rate of substrate utilization per unit mass of micro-organisms, half velocity constant, overall COD removal rate, Michaelis-Menten constant and the overall inhibition constant. Graphs were generated which represented the variations of the kinetic coefficients with the base kinetic constant termed the inhibition constant. From the graphs, it was read that the half velocity constant, overall COD removal constant, Michaelis-Menten constant, endogenous decay coefficient and maximum rate of substrate utilization per unit mass of micro-organisms all increase with the inhibition constant. However, the cell yield coefficient was found to vary inversely with the inhibition constant. Finally, a mathematical regression model was generated for the cassava wastewater treatment process as $\mathbf{RE = (0.83038504(L/W)^{0.019319}N_b^{0.0011}) / (K_i^{0.012}Q^{0.016})}$. A COD removal efficiency of 82% was obtained at a cyanide concentration of 110 mg/L. the increase in the aspect ratio from 0.4 to 1.3 produced 81 to 86% increase in COD removal efficiency. However, the increase of number of baffles from 3 to 12 decreased inhibitor constant from 9.9989 to1.610 mgL^{-1}. When the model performance was verified using the coefficient of determination, R^2, it yielded a value of 0.997. This clearly showed that the model was effective in predicting the COD removal efficiency. It is recommended that the developed model be used for the optimal design of pilot plant for treating cassava wastewater.

Keywords: cassava wastewater, ABR, COD, inhibition constant, cell yield, kinetic coefficient, removal efficiency.

TABLE OF CONTENTS

CERTIFICATION	iii
DEDICATION	iv
ACKNOWLEDGEMENTS	v
ABSTRACT	vii
TABLE OF CONTENTS	viii
LIST OF TABLES	xii
LIST OF FIGURES	xiv
LIST OF PLATES	xvi
LIST OF NOMENCLATURE	xviii
CHAPTER ONE-INTRODUCTION	1
1.1 Background Information	1
1.2 Problem Statement	4
1.3 Objectives of Study	6
1.4 Justification of Study	6
1.5 Scope of Study	8
CHAPTER TWO-LITERATURE REVIEW	10
2.1 Cassava Tuber Crop	10
2.1.1 The Processing of Cassava Starch	10
2.1.2 Effluents in Wastewater from Cassava Processing	13
2.2 Cassava Wastewater and Water Pollution	13
2.2.4 Pollution of Water Sources by Cassava Wastewater	16
2.2.5 Cyanide and Cassava Roots	20
2.2.6 Degradation of Glycoside in Cassava Wastewater	21
2.2.7 Effect of Cyanide On Cassava Wastewater Degradation	23
2.2.8 Effect of Cassava Wastewater on Sewage Degradation	24
2.3 Inhibition of Wastewater Treatment	24
2.3.1 Self-Inhibition of Wastewater Treatment	26
2.3.2 Competitive Inhibition of Wastewater Treatment	28
2.3.3 Noncompetitive Inhibition of Wastewater Treatment	30

2.3.4 Decoupling Inhibition of Wastewater Treatment 31
2.4Modelling of Anaerobic Digestion 32
2.5 Anaerobic Treatment of Wastewater 46
2.5.1 Reactor Configurations for Anaerobic Treatment of Wastewater 48
2.5.1.1 Completely Mixed Reactor 48
2.5.1.2 Anaerobic Contact Reactor 50
2.5.1.3 Up flow and Down flow Bed 51
2.5.1.4 Fluidized and Expanded Beds 52
2.5.1.5 Up low Anaerobic Sludge Blanket 52
2.6Anaerobic Baffled Reactor (ABR) 53
2.6.1 Background and theory of ABR 54
2.6.2 Development and Application of ABR 57
2.6.3 Performance and Characteristics of ABR 60
2.6.3.1 Reactor Hydrodynamics 60
2.6.3.2 Effluent Recycles 61
2.7Types of Models 63
2.7.1 Fundamental Models 63
2.7.2 Empirical Models 64
2.7.3 Mixed Models 65
2.8 Classification of Biological Models 66
2.8.1 Unstructured Biological Models 66
2.8.2 Structured Biological Models 68
2.8.3 Segregated Biological Models 69
2.8.4 Material Balance Biological Models 71
CHAPTER THREE-MATERIAL AND METHODS 72
3.1 Materials 72
3.1.1 The Reactor 72
3.1.2 Start-up of ABR 73
3.1.3 Process of Obtaining Cassava Wastewater 75
3.2 Methods 75

3.2.1 Procedure for Experiment-1: Cassava Wastewater Modeling Without Inhibition 75

3.2.2Evaluation of Kinetic Coefficients without Inhibition 76

3.2.3 Monod Model for ABR 76

3.3 Procedure for Experiment-2: Cassava Wastewater Modeling With Inhibition 77

3.3.1 Evaluation of Kinetic Coefficients with Inhibition 78

3.4 Procedures for Wastewater Characterization 79

3.4.1Determination of pH 79

3.4.2 Test for Cyanide 80

3.4.3 Determination of Total Solids 81
3.4.4 Determination of Dissolved Solids 82
3.4.5 Determination of Suspended Solids 82

3.4.6 Determination of Fixed Solids 83

3.4.7 Determination of Volatile Solids 84

3.4.8 Turbidity Determination 84
3.4.9 Alkalinity Determination 86

3.4.10 Determination of Chemical Oxygen Demand 87

CHAPTER FOUR-RESULTS AND DISCUSSIONS 90

4.1 Results of Experiments 90

4.2 Evaluation of Kinetic Coefficients without Inhibition 92

4.3 Evaluation of Kinetic Coefficients with Inhibition 100

4.4 Calibration and Validation of Model for Cassava Wastewater Treatment 117

4.5 Results of Acidity, Alkalinity, Turbidity and pH Determination 121

4.5.1 Results of Acidity, Alkalinity, Turbidity and pH Determination for Reactor 1 121

4.5.2 Results of Acidity, Alkalinity, Turbidity and pH Determination for Reactor 2 123

4.5 Results of Acidity, Alkalinity, Turbidity and pH Determination for Reactor 3 125

4.6 Comparison of results with Other Works 126

CHAPTER FIVE-CONCLUSION AND RECOMMENDATIONS 127

5.1 Conclusion 127

5.2 Recommendations 128

5.3 Contributions to Knowledge 128

REFERENCES 130

APPENDICES 147

LIST OF TABLES

Table 2.1: Composition of Cassava Root per 100g (Edible Portion). 10

Table 2.2: The Volume of Processing Products by Scale 11

Table 2.3: Wastewater Volume per day by Household Scale 13

Table 2.4: Effluents in Wastewater from Cassava Processing at Umuagwo 13

Table 2.5: Quantity and Composition of Cassava Wastewater 16

Table 2.6: Typical Wastewater Composition at Each Stage of Processing 16

Table 2.7: Impact of Release of Starch Factory Wastewater on Surface Water Quality 18

Table 2.8: Models that Assume Substrate-inhibited Monod kinetics (Andrews, 1969) at the Methanogenesis 34

Table 2.9: Models Using H_2 as the Control Parameter 40

Table 2.10: More complicated Models II 45

Table 2.11: More Complicated ModelsI46

Table 2.12: Advantages Associated with the ABR 57

Table 2.13: classification of biological growth models 66

Table 4.1: Definition of the Cases of Cassava Wastewater Treatment 90

Table 4.2: Record of Effluent COD and Suspended Solids for the Different Cases Studied 90

Table 4.3a: Estimation of Parameters for the Various Experimental Cases 91

Table 4.3 b: Estimation of Parameters for the Various Experimental Cases 92

Table 4.4: Determination of Endogenous decay coefficient, k_d and Endogenous decay coefficient, Y 94

Table 4.5: Determination of Maximum rate of Substrate Utilization, k and Half Velocity Constant, k_s 95

Table 4.6: Determination of Overall COD Removal Rate Constant, K_r 97

Table 4.7: Michaelis-Menten Constant, K_m 99

Table 4.8: Phase 1 at particular inhibitor concentration for each of the 10 cases 101

Table 4.9: Phase 2 at particular inhibitor concentration for each of the 10 cases 103

Table 4.10: Phase 3 at particular inhibitor concentration for each of the 10 cases 105

Table 4.11: Phase 4 at particular inhibitor concentration for each of the 10 cases 107

Table 4.12: Computation of Inhibitor Concentration, I 109

Table 4.13: Estimation of COD Removal Efficiency (RE) 110

Table 4.14: Computation of Model Parameters 117

Table 4.15: RE and L/W, N_b, K_i, Q involving the Upper and Lower Limits 118

LIST OF FIGURES

Fig. 2.1: Flow Chart for the Making of Cassava Starch 12

Fig. 2.2: Illustration of How Inhibitions Can Affect the Primary Flow of Electrons and Energy.(After Rittmann and Sóez, 1993). 26

Fig. 2.3: Haldane kinetics and the Relationship between S and Reaction rate (top) and between S and θx. 28

Fig. 2.4: Reaction Rates for Methane and TCE as Governened by Competitive Inhibition Kinetics 29

Fig. 2.5: Block diagram of Hill and Barth (1977) mathematical model 36

Fig. 2.6: Schematic biochemical process stages of anaerobic digestion (Kleinstreuer and Powegha, 1982). 36

Fig. 2.7: Flow chart of Moletta et al. (1986) model 36

Fig. 2.8: Flow chart of Smith et al.(1988) model 37

Fig. 2.9: Flow chart of Hill (1982) model 38

Fig. 2.10: Flow chart of Bryers (1985) model 38

Fig. 2.11: Flow chart of Mosey (1983) and Pullammanappallil et al. (1991) models 41

Fig. 2.12: A schematic of the relationship between each group of bacteria in the anaerobic ecosystem model (Costello et al., 1991) 42

Fig.2.13: Flow chart of Angelidaki et al. (1993) 43

Fig. 2.14: Typical anaerobic configuration 49

Fig. 2.15: Conversion Reaction in the Anaerobic Baffled Reactor 56

Fig. 2.16: Different types of the ABR: B-Biogas, W= wastewater; E = Effluent 58

Fig.3.1: 3-D View of the Anaerobic Baffled Reactor 73

Fig. 4.1: Plot of $Q(S_o-S)/(V_wX_o)$ against 1/SRT 95

Fig. 4.2: Plot of $SRT/(1+k_d*SRT)$ against 96

Fig. 4.3: Plot of $Q(S_o-S)/V_w$ against S 98

Fig. 4.4: Plot of 1/Q against 1/S 99

Fig. 4.5: Plot of 1/Q against 1/S 102

Fig. 4.6: Plot of 1/Q against 1/S 104

Fig. 4.7 Plot of 1/Q against 1/S 106

Fig. 4.8: Plot of 1/Q against 1/S 108

Fig. 4.9: Plot of K_s, K_r, K_m against k_i 111

Fig. 4.10: Plot of k_d, Y, k against K_i113

Fig. 4.11: Effect of Cyanide Inhibitor on COD Removal Efficiency 115

Fig. 4.12: Plot of K_i against I 116

Fig. 4.13: pH behaviour as a function of time 121

Fig.4.14: (a) Alkalinity and (b) Acidity behaviour as a function of time 122

Fig 4.15: Turbidity behaviour as a function of time 123

Fig. 4.16: Influent and effluent alkalinity during reactor operation period 124

Fig.4.17: pH variation profile during reactor operation period 124

LIST OF PLATES

Plate. 3.1: Photo of the Reactor, Researcher 76

Plate 3.2: Experimental Set-up 77

Plate 4.1: Microsoft Visual Basic Program for Estimating Removal Efficiency 120

APPENDICES

APPENDIX 1: Values for Generation of Regression Model 133

APPENDIX 2: Values for Generation of Regression Model 134

APPENDIX 3 : pH Behaviour as a Function of Time 135

APPENDIX 4: Alkalinity Behaviour as a Function of Time 136

APPENDIX 5: Turbidity Behaviour as a Function of Time 137

APPENDIX 6: Influent and Effluent Alkalinity during Reactor Operation Period 138

APPENDIX 7: pH Variation Profile during Reactor Operation Period 139

NOMENCLATURE

A	Glucoside Concentration
ABR	Anaerobic Baffled Reactor
ANN	Artificial Neural Networks
B	Cyanohydrins Concentration
b_{eff}	Effective Endogeneous Decay Coefficient (day^{-1})
BOD	Biochemical Oxygen Demand
C	Cyanide Concentration
COD	Chemical Oxygen Demand
CSTR	Continuous Flow Strained-tank Reactor
FAO	Food and Agricultural Organisation
g	Gram
gm	Gram
HCN	Hydrogen Cyanide
HRT	Hydraulic Retention Time
I	Concentration of Inhibitor
I	Non-competitive (Cyanide) Inhibitor Concentration (mgl^{-1}).
k	Maximum Rate of Substrate Utilization per unit Mass of Micro-organisms, per min
K	Substrate Concentration at which the Rate is one-half of the Maximum Value
k_d	Endogenous Decay Coefficient, per min

K_{eff}	Effective Concentration giving one-half the Maximum Rate (mgL^{-3})
kg	Kilogram
K_i	Inhibition Constant, mg/l
K_1	Inhibition Concentration of the Competitive Inhibitor (M_1L^{-3})
K_{1S}	Inhibition Concentration of the Self-inhibitory Substrate (M_sL^{-3}).
K_m	Michaelis-Menten Constant, mg/l
K_r	Overall COD Removal Rate Constant, per min
k_s	Half Saturation Constant (mgl^{-1})
k_s	Half Velocity Constant, Substrate Concentration at one-half of the Maximum Growth Rate, mg/l
LCFA	Long-chain Fatty Acids
L/W	Length-width Ratio
MABR	Modified Anaerobic Baffled Reactor
m_c	Critical Cell Mass
MMO	Methane Monooxygenase
m^3	Cubic Metre
m^3/l	Cubic Metre per Litre
NA	Data Not Available
NADH	Nicotinamide adenine dinucleotide ion
NAD+	Nicotinamide adenine dinucleotide
N_b	Number of Baffles

OLR	Organic Loading Rate
PABR	Periodic Anaerobic Baffled Reactor
ppm	Parts per Million
Q	Flow Rate, l/min
Q_{app}	Apparent Flow Rate, l/min
q_{eff}	Effective Maximum Specific Rate of Substrate Utilization (mgL^{-3})
Q_{inf}	Influent Wastewater
r_A	Rate of Utilization of Substrate (mg/l.day)
r_{Aeff}	Specific Rate of Electron Flow to the Acceptor ($M_sM_x^{-1}T^{-1}$)
RE	COD Removal Efficiency
r_{ueff}	Effective Rate of Substrate Utilization ($mgL^{-3}day^{-1}$)
RTD	Residence Time Distribution
S	Effluent COD after the First Step of each Case, mg/l
S	Concentration of the Growth Limiting Substrate (mgL^{-3})
S_e	Substrate Concentration in the Effluent (mgl^{-1})
S_i	Substrate Concentration in the Influent (mgl^{-1})
S_o	Influent COD at the start of each of the Experimental Case, mg/l
SRT	Solid Retention Time
SS	Suspended Solids
STP	Standard Temperature and Pressure
TCE	Trichloroethylene

UASB	Upflow Anaerobic Sludge Blanket
UASBR	Upflow Anaerobic Sludge Bed Reactor
VFA	Volatile Fatty Acid
V_r	Reactor Volume, l
VSS	Volatile Suspended Solids
V_{up}	Vertical Upflow Velocity
V_w	Wastewater Volume for each Case, l
X	Effluent Suspended Solids, mg/l
X_a	Concentration of the Active Biomass (mgL^{-3})
X_o	Influent Suspended Solids at the start of each Case, mg/l
Y	Cell Yield Coefficient, Ratio of the Mass of Cells formed to the Mass of Substrate Consumed, mg/mg
Y_{eff}	Effective Yield for Cell Synthesis
μ	Specific Growth Rate,
μ_{eff}	Effective Maximum Specific Growth Rate ($mg.mg^{-1day-1}$)
μ_g	Specific Growth Rate Inhibited by a Non-competitive Inhibitor (per day)
μm	Micrometre
μ_{max}	Maximum Specific Growth Rate

CHAPTER ONE

INTRODUCTION

1.1 Background Information

Industries have long been implicated in the discharge of toxicants into the environment. Over 1.2 billion of the world's city dwellers breathe highly polluted air, 10% of the world's rivers are heavily polluted with discharges from food and allied industries and users of these rivers and streams are constantly exposed to health related risks due to this indiscriminate discharge of industrial effluents (Salami and Egwin, 1997).Wastewater treatment in developing countries is a problem to manage. Some industries such as cassava industries hardly treat their wastewaters. Cassava (Manihot Esculenta Crantz) processing into garri, for instance involves several unit operations vis-à-vis, peeling, washing, grating, pressing and fermenting, sieving, roasting and drying. Traditional garri production is associated with the discharge of large amounts of water, hydrocyanic acid and organic matter in the form of peels and sievates from the pulp as waste products. When these waste products are improperly disposed, they are left in mounds which generate offensive odours and unsightly scenarios (FAO, 2004).The major components of the effluents from garri processing industries is cyanide and starch, and in most cases, these effluents are channeled into pits where they continue to accumulate and gradually percolate into the surrounding soils thereby posing serious health and environmental hazard.

Due to the position of cassava and its derivatives on the average Nigerian daily meal, being common, it is important to take a closer look at the effects its wastewater would have on the degradation of sewage and the environment at large. The wastewater from cassava processing or its derivative (garri) ends up with domestic sewage if processed in small quantities while others end up being carried with industrial wastes if processed in large industrial quantities. Lastly, others percolate into the soil depending on the processors. Tests like coliform counts are used to give indications of the sanitary quality of the waste. The Biochemical Oxygen Demand (BOD), Chemical Oxygen Demand (COD) and suspended solids tests are also used to reveal the level of pollution.

Cassava processing is generally considered to contribute significantly to environmental pollution and aesthetic nuisance. The two major wastes of cassava processing in Nigeria are cassava sievates (a product from garri processing), and cassava offal (wastes from fufu production).

About 10 million tonnes of cassava are processed for garri annually in Nigeria alone (Okafor, 1992). In the processing of cassava fermented products, the roots are normally peeled to rid them of two outer coverings: a thin brown outer covering, and a thicker leathery parenchymatous inner covering. These peels are regarded as wastes and are usually discarded and allowed to rot. With hand peeling, the peels can constitute 20 - 35% of the total weight of the tuber (Ekundayo, 1980). The wastes generated at present pose a disposal problem and would even be more problematic in the future with increased industrial

production of cassava products such as cassava flour and dried cassava fufu. Products of fermentation of cassava peels from such heaps include foul odour and sometimes poisonous and polluted air, which when inhaled by man or animals may result into infection and diseases that may take a long time to manifest. In the same vein, vegetation and soil around the heaps of cassava peels are rendered unproductive and devastated due to biological and chemical reactions taking place between the continuously fermenting peels, soil and the surrounding vegetation. Since these peels could make up to 10% of the wet weight of the roots, they constitute an important potential resource if properly harnessed biotechnologically (Obadina et al., 2006).

During the last 30 years, there has been an increasing demand for more efficient systems for the treatment of wastewater due to increasingly stringent discharge standards now widely adopted by various national and international agencies (Akunna and Clerk, 2000). The treatment of both domestic and industrial wastewater is usually carried out using biological methods due to their lower costs compared to chemical methods (Langenhoff *et al*., 2000). Great advances have been made over the last 20 years in anaerobic reactor design and in understanding the complex process that occur in anaerobic digestion (Langenhoff and Stucky, 2000). The successful application of anaerobic systems to the treatment of industrial wastewater is critically dependent on the development and use of high rate anaerobic bioreactors. These reactors achieve a high reaction rate per unit reactor volumes in terms of $kgCOD/m^3.d$ by

retaining the biomass Solid Retention Time, (SRT) in the reactor independently of the incoming wastewater Hydraulic Retention Time, (HRT), (Barber and Stucky, 1999). Such separation allows the slowgrowing anaerobic bacteria remain within the reactor independent of the wastewater flow. This allows higher volumetric loads and produces significantly enhanced removal efficiencies (Akunna and Clark, 2000). In contrast to domestic wastewater, industrial effluents pose many problems for treatment and such effluents are subjected to daily and sometimes seasonal fluctuations with respect to both their flow and strength (Nachaiyasit and Stucky, 1997a). The characteristics of food-processing wastes show high variation in Biological Oxygen Demand (BOD), Total Suspended Solids (TSS) and flow rate. The wastes may be highly alkaline or highly acidic.

1.2Problem Statement

Wastewater from cassava processing, if released directly into the environment before proper treatment, is a source of pollution. In many areas where traditional processing is practiced, wastewater is normally discharged beyond the "factory" wall into roadside ditches or fields and allowed to flow freely, settling in shallow depressions. Eventually this will percolate into the subsoil or flow into streams. Besides the presence of some quantities of soil in cassava wastewater, there are numbers of other contaminating substances in cassava wastewater. Normally, wastewater discharged from a cassava starch processing factory is acidic with high organic matter content (soluble carbohydrates and

proteins) and suspended solids (lipids and non-soluble carbohydrates). Wastewater also contains cyanide as well as sulphur dioxide if this is used during the extraction process.

Cassava roots contain cyanogenic glucosides in various concentrations depending on the variety and growing conditions. This cyanide is released during peeling, slicing and crushing. The bound cyanide is converted to free cyanide during the milling operation. About 40% to 70% of the total cyanide appears in the water used to wash the starch from the disintegrated tissue. The press water, although produced in relatively low volumes (250 – 300 litres per tonne of roots), is the main problem because of its high biological oxygen demand (BOD) of 25,000 – 50,000 mg/l with a typical cyanide concentration in excess of 400 mg/l (Arguedas and Cooke, 1982).Cyanide, being an acidic component of cassava wastewater will naturally have an inhibiting action on the biological degradation of cassava wastewater especially when applied to designed treatment systems. Cassava wastewaters are often discharged into sewers or allowed to percolate into the soil causing environmental degradation. This effect on the environment is significant as the air we breathe becomes contaminated with the odour emanating from it, an effect yet to be addressed properly in developing countries due to inadequate equipment and lack of research materials. The cassava wastewater may introduce some toxic elements e.g. cyanide in sewage which may inhibit the usual degradation processes.

1.3 Objectives of Study

The main objective of the study is the use of mathematical model to describe cassava wastewater treatment process taking into account solutions to some inhibition properties of cassava wastewater systems.

The other objectives include:

i. To investigate the performance of anaerobic treatment plants using physical models, and use of data from the physical models for calibration and verification of the mathematical models.

ii. To study the effect of variations in input parameters- flow rate and hydraulic retention time (HRT) on the efficiency of the physical models of anaerobic treatment plants.

iii. To determine the extent of inhibition caused by cyanide on the degradation of cassava wastewater.

1.4 Justification of Study

Improper treatment of sewage is a major cause of pollution of surface waters like lakes, rivers and streams. This gives rise to many problems which include drastic reduction of aquatic life, public health hazards especially to swimmers by exposures to various diseases. The study is designed to provide information about the biological effects and chemical characteristics of effluents from traditional cassava wastewater. Chemical characterization involved analysis of effluent for conventional parameters such as BOD, COD, suspended solids (SS)

and cyanide contents. This study will also help the sanitary engineer to design appropriate treatment unit for a community and to effectively monitor the efficiency of such treatment facilities. This will reduce cost and eliminate wastage of treatment chemicals which are likely to be used indiscriminately in the absence of such tests. Summarily, the justification for this study is as follows:

i. ***Increased production of Cassava Products:*** The development of cassava products that meet minimum requirements for incorporation into commercial food production, in cassava producing areas, would certainly relieve the pressure on demand for available cereal grains. Since the presence of cyanogenic glucocides constitutes a major limitation to the safe handling and disposal of cassava wastewater, there is therefore a justified necessity to review current findings for the elimination of the toxic glucoside in cassava products, thus paving way for increased cassava production.

ii. ***Mathematical Model for Cassava Wastewater Treatment:*** Currently there seems not to be a mathematical model for the treatment of cassava wastewater, especially with emphasis on the reduction of cyanide concentration. This study is ultimately aimed at developing such a model which is an approach to solving cassava wastewater problems.

iii. ***Enhanced Performance of Cassava Wastewater Treatment Process:*** Cassava wastewater treatment would be more efficient by the integration

of the developed mathematical model into the treatment process. Cost of treatment would be reduced if a mathematical model for cassava wastewater is developed and less poisonous effluent would be achieved. Thus, the environment would be saved from the poisonous discharge containing cyanogenic glucosides.

1.5 Scope of Study

This work is limited to the steady state flow condition in which case, the flow rate had a constant value at every time. The study excludes all observations made when the flow varied with time.

The reactor used in the study was observed only under anaerobic conditions. Aerobic events were not considered in the reactor treatment process.

The cassava wastewater that was fed to the reactor excludes sludges. This is because the wastewater that was used in the work was the supernatant wastewater obtained from the filtration of raw wastewater. Therefore, the concept of sludge hydrolysis, acidogenesis and methanogenesis was not included in the synthesis of the mathematical model.

The Anaerobic Baffled Reactor (ABR) that was used in the study was a continuous stirred tank reactor and not the plug flow batch reactor. This means that the associated mathematical model included the use of mass balance equation for a continuous stirred tank reactor without effluent recycle.

Cyanide was considered as a non-competitive inhibitor in the modelling of the cassava wastewater treatment. Other forms of inhibition such as self-inhibition, competitive inhibition as well as mixed inhibition are beyond the boundaries of this research.

Ultimately, the specific effects of various processing techniques like peeling, chopping, grating, soaking, drying, boiling and fermentation on the cyanide content of cassava excluded from frame of this research.

CHAPTER TWO

LITERATURE REVIEW

2.1 Cassava Tuber Crop

Cassava, the source of garri production gives the highest source of starch per hectare of land of all known crops. The bye-product, garri is the 90% fermentable carbohydrate while the protein content is about 3.55% (Odunfa, 1985). Table 2.1 shows the composition of cassava root per 100g (edible protein).

Table 2.1: Composition of Cassava Root per 100g (Edible portion).

Item	Fresh Cassava/100g	Unit
Food energy	146.0	gm
Water	62.5	gm
Carbohydrate	34.7	gm
Protein	1.2	gm
Fat	0.3	gm
Calcium	33.0	gm
Iron	0.7	gm
Vitamin A	Trace	-
Vitamin C	36.0	mg
Niacin	0.6	mg

Source: FAO, (2004).

There are certain known variations in the chemical composition of cassava. Cassava contains a protein amount less than 1% which can lead to malnutrition (Kwashiokor), if not supplemented. Odunfa (1985) also, noted that useful amounts of vitamins and calcium are contained in cassava.

2.1.1 The Processing of Cassava Starch

Processing activities take place from September to March when the cassava roots are harvested. At first, the roots are cleaned. Then they are peeled and

ground. The mixture of cassava starch and water is then left for about eight hours to separate the water (starch deposition process). The black starch found floating on the surface is afterwards eliminated to get pure cassava starch. Fig.2.1 illustrates how cassava starch is made. On average, households can get around 450 kg of processed product from one tonne of cassava roots as shown in Table 2.2 This amount was not significantly different among the household groups.

Table 2.2:Volume of Processing Products by Scale

Household Scale	Indicator	Product volume/1tonne of root (kg)	Production volume per processing day (kg)	Total product volume (kg)s
Small –scale	Mean Std deviation	447.2 13.7	702.3 148.6	66,440.6 18,600.1
Medium-Scale	Mean Std deviation	450.0 15.2	904.6 118.4	106,000.8 8,539.6
Large-Scale	Mean Std deviation	450.3 8.8	1,567.3 629.6	202,023.6 91,025.2
All	Mean Std deviation	449.1 12.8	1,047.6 524.5	123,104.6 77,737.5

Source: Odunfa (1985)

However, there existed a great difference in product volume per processing day among the household groups. The processed volume of the small-scale households is around 702 kg per day while it is 904 kg for the medium-scale households and 1,567 kg for the large-scale households. The total annual product of the small-scale households was around 66 tonnes, while for the medium and large-scale households, it is 106 tonnes and 202 tonnes, respectively (Odunfa, 1985).

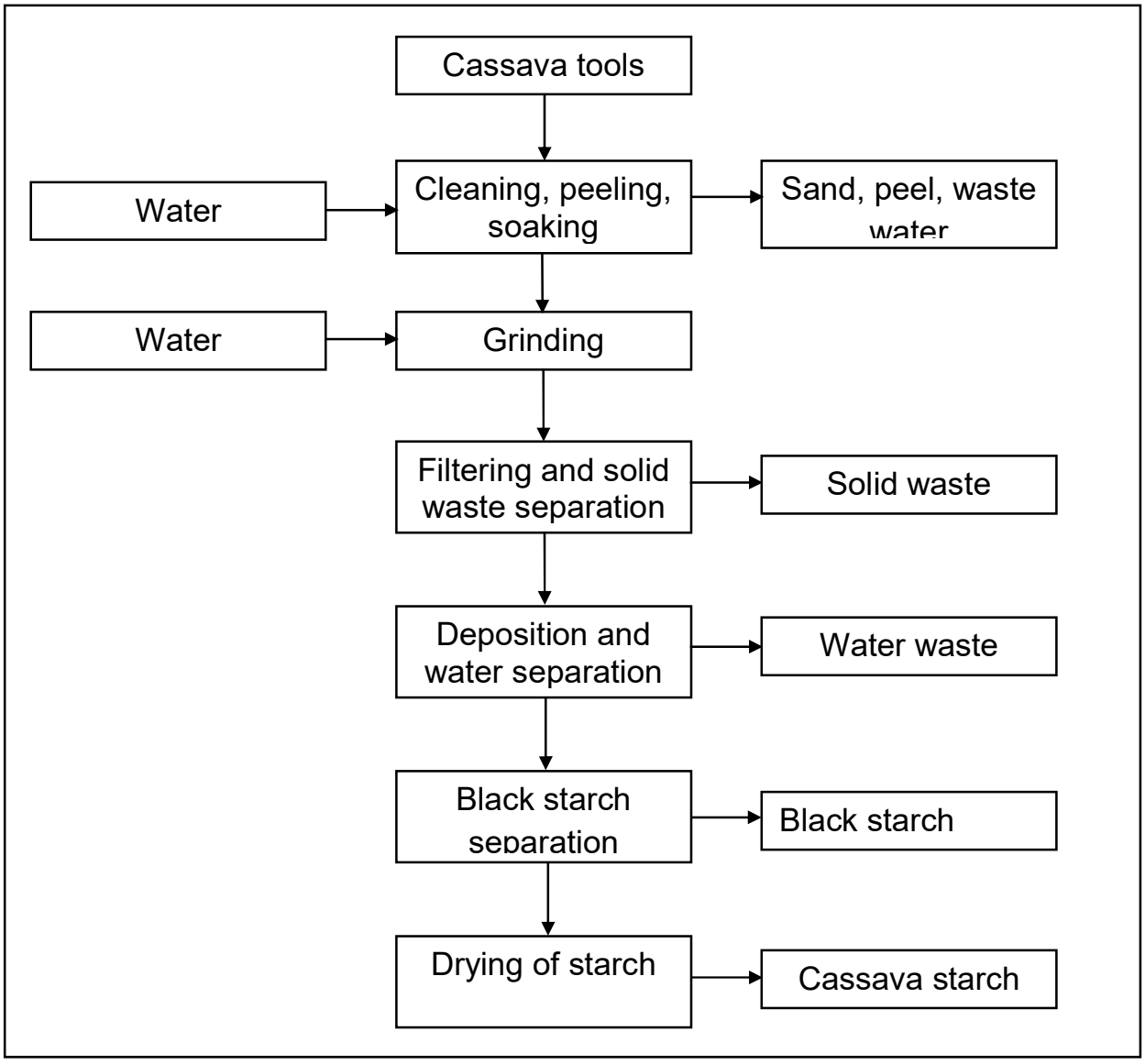

Fig. 2.1: Flow Chart for production of Cassava Starch

Source: Odunfa (1985)

The discharged wastewater volume per day vary across the different household groups. On average, one small-scale household discharge nearly $10m^3$ of wastewater per day while the medium and large-scale ones discharge $12.3m^3$ and $21.8m^3$ per day. The minimum wastewater volume is $5m^3$ per day while the maximum is $50m^3$ per day (Table 2.3).

Table 2.3: Wastewater Volume per day by Household Scale

Household sale	Mean (m^3)	Minimum (m^3)	Maximum (m^3	Std. Deviation
Small –scale	9.7	5.00	14.00	2.60
Medium-scale	12.25	7.00	18.00	2.30
Large-scale	21.76	10.00	50.00	9.34
All	14.41	5.00	50.00	7.67

Source: Odunfa (1985)

2.1.2 Effluents in Wastewater from Cassava Processing

Tests at the Imo State polytechnic Umuagwo in 2003 found that the concentrations of COD, BOD, and SS in wastewater from all the processing steps were over the standards (Table 2.4). These effluents were especially high in wastewater separated from deposited starch. The COD and BOD concentrations in the wastewater from cleaning and soaking were around 10 to 12 times higher than the standards while the wastewater from the starch deposition process had COD and BOD concentrations of more than 120 times higher. The free discharge of untreated wastewater, especially from the starch deposition process, thus led to environmental pollution.

Table 2.4: Effluents in Wastewater from Cassava Processing at Umuagwo

		Wastewater production produced per processing step		
Indicators	Unit	Wastewater from cleaning and peeling	Wastewater from soaking roots after peeling	Wastewater from starch deposition
pH	-	6.8	6.5	3.9
COD	Mg/l	856	982	12.289
BOD	Mg/l	550	660	6,400
SS	Mg/l	42	52	1,186

Source: Akunna and Clark (2000)

2.2 Cassava Wastewater and Water Pollution

Water released from cassava during squeezing can have potentially harmful effects on the environment, especially if generated in large amounts. The main

products of squeezing cassava are garri and farinha. Wastewater is generated from two operations: pressing and washing. The press water, although produced in relatively low volumes (250-300 liters per tonne of roots), is the main problem because of its high biological oxygen demand (BOD) of 25,000-50,000 mg/1 and a typical cyanide concentration of more than 400 mg/l (Table 2.5). In contrast, the BOD of wash water can be on the order of 500-2,500 mg/l. Starch is the main product of aqueous extraction. Wastewater is generated at three stages: Root washing, Primary settling of starch milk, Secondary settling of starch milk.

In the processing of starch, about 85% of the average 30 m^3 of water required to produce one tonne of starch is discharged as liquid waste; the remainder is lost through evaporation. The average amount of wastewater discharged from all sources during starch extraction is between 20-40 m^3/tonne starch for a modern factory, and about 20-100 m^3 water/tonne starch for a medium-scale factory. A rigorous review of the literature is difficult because of differences in reporting formats, choice of analytical methods and sampling strategies. However, within these limitations general observations can be made.

The composition of wastewater varies among different scales of processors (Table 2.5) and extraction methods. Total solids in the wastewater from small-scale processors in north Vietnam are about 1,500 mg/1 and the total nitrogen content about 15 mg/1. These values reflect a tendency to maximize starch yield at the expense of quality. By comparison, wastewater released by medium-scale

processors (India) contains about 4,100 mg/1 total solid, 70 mg/1 total nitrogen and has a BOD of 4,900 mg/1. Changing the extraction technology can markedly affect starch quality, as shown by the comparison of wastewater measurements from Thai cassava processors, taken 25 years apart; the earlier when sedimentation was the main method for starch extraction and the later one from a fully automated modern factory. Wastewater from the more technologically sophisticated processors is purer. For a modern factory, typically found in Thailand or Indonesia, the composition of combined waste waters will be similar to that shown in Table 2.5.Each stage of starch extraction creates wastewater with different amounts of contaminating materials. For example, wastewater from decanters is high in organic substances and contains starch, fat and protein. The chemical oxygen demand (COD) of wastewater from the decanters is 30,000 mg/l, and the combined wastewater 15,000 mg/l. Problems created from wastewater occurs when this is removed from the factory, especially if handled incorrectly. Wastewater generated by starch and farinha processors is sometimes directed into pits (starch processors in Brazil) for conversion, but depending on the soil characteristics, partial leaching may contaminate the groundwater, while overflow may affect surface water. Wastewater is also released directly to neighboring land (Vietnam, India), or is returned directly to streams and other surface water sources (sour starch producers in Brazil and Colombia).

Table 2.5: Quantity and Composition of Cassava Wastewater

	Brazil	Brazil	Vietnam	India	Colombia	Thailand	
	1)	**1)**	**2)**	**3)**	**4)**	**Late 1970s**	**1995**
Scale	Small	Large	Small	Medium	Small	Medium (intermediate technology)	Large (continuous process)
Wastewater (m^3/l starch)	71	40	40	31	60-75	20	25-45
pH	NA	3.8-5.2	NA	4.5-5.6	3.9-4.7	3.4-6.5	4.5-6.5
Total solids (mg/1)	5,000	5,800-56,460	1,500	4,000-6,600	2,680-10,020	234-2592	7,604
Suspended solids (mg/1)	NA	950-16,000	NA	1,868-2,960	NA	NA	2,642
Total dissolved solids (mg/1)	NA	4,900-20,460	NA	3,425-3,680	NA	1.3-30.1	6,483
BOD(mg O_2/1)	5,000	1,400-34,300	NA	4,600-5,200	1,500-8,600	2,508-16,880	3,608
COD(mg O_2/1)	NA	6,280-51,200	NA	5,631-6,409	4,000-12,800	4,950-36,840	8,842
Total nitrogen (mg N/1)	NA	140-1,150	15	66-72	29-233	84-375	172
HCN (mg CN^- /1)	60	22.0-27.1	NA	NA	1.2-4.0	NA	9.0

Source: Cereda and Takahashi (1996)(Note: NA = data not available)

Table 2.6: Typical Wastewater Composition at Each Stage ofProcessing

	Rooting washing	**Primary setting**	**Secondary settling**
pH	6.5-7.5	4.3-5.4	4.5-4.7
Total solids (mg/1)	550-700	4,200-4,400	4,000-6,600
Suspended solids (mg/1)	400-500	680-730	1,868-2,960
Total dissolved solids (mg/1)	150-200	3,520-3,670	2,132-3,620
BOD (mg/1)	40-60	4,800-5,700	3,500-6,018
COD (mg/1)	100-150	5,760-6,840	3,870-6,670
Total nitrogen (mg/1)	30-38	70-75	65-74

Source: ERM (1996)

2.2.4 Pollution of Water Sources by Cassava Wastewater

Groundwater Pollution: Contamination of groundwater is often the outcome of seepage of untreated effluent into shallow and deep aquifers. From the limited information it is clear that open wells and bore holes in close proximity to starch processors can be contaminated by high levels of suspended solids and high BOD. Nevertheless, even in areas of intensive starch processing, the proportion of contaminated sites is minimal, with the majority not affected. Geology and

soil characteristics are important in determining if the groundwater supply will become contaminated; porosity and degree of saturation are the principal factors. Cyanide contamination, even site-specific, of groundwater seems not to be a problem. In areas close to intensive cassava processing, the cyanide concentration in the groundwater was found to be below detectable levels. Despite this apparent low incidence of contamination, it is still important to know the frequency of site-specific impacts and be able to predict problem sites. It should be noted that studies are limited and the same conclusions may not be true of a site with geology/soil characteristics that promotes seepage of wastewater. Depending on the geology, groundwater supplies can remain protected from contamination. However, where physical conditions permit, untreated effluent reach groundwater in sufficient quantities to pollute open well and bore holes. If such conditions prevail, groundwater quality may be affected, leading to health problems of nearby communities.

Surface Water Pollution: Surface water includes all rivers, streams, canals, ditches, lakes, reservoirs, lagoons, estuaries and coastal waters. Environmental impact on surface water may be due to the addition of substances, heat or microorganisms to the water. This leads to temperature changes and/or increases in microbial populations. The main problem originating from cassava processing is through the addition of organic substances. This results in eutrophication, which in-turn is responsible for an increase in the number of microorganisms and the growth of algae. This can alter water quality and/or

change the aquatic ecology, affecting plants and animals, human health and visual aspects. The impact to surface water will depend on environmental conditions during the processing season; in the dry months the effects are most apparent. The magnitude depends on the concentration of processors and their distance from water bodies capable of facilitating rapid dispersal. Streams, slow flowing rivers, ponds and lakes are therefore most at risk. Surface water can remain contaminated (high BOD levels) even after dispersal downstream from a factory (Table 2.7). In extreme cases, surface water can become anaerobic due to the formation of a thick crust forming on the water surface. However, usually the main effect is that water becomes eutrophic from excessive organic matter loading. Contamination of surface water has been reported to be severe-in several areas of Vietnam (Viet, 1998). No measurements are available, but reports suggest a high degree of eutrophication.

Table 2.7: Impact of Release of Starch Factory Wastewater on Surface Water Quality

	COD (mg/1)	**BOD (mg/1)**	**Suspended solids (mg/1)**	**pH**	**HCN (mg/1)**
Supernatant liquor	14,778	3,370	4,979	5.38	62
Wash water	3,475	618	1,797	6.21	0
River water (down-stream from factory)	79	3,052	3232	6.43	0

Source: Pick-Ford (1977)

The water used in aqueous extraction methods will help to dilute the cyanide. Hence, there is little risk of water contamination from cyanide on a broad scale. However, site-specific effects can be significant. For example, high cyanide content in wastewater discharged by sour starch processors in Brazil

(representing 50-60% of the total cyanide content of the roots) was not present in river water downstream of the factory; in fact, no cyanogens could be detected. In comparison, when microtox and tropical duckweed were exposed to untreated effluent from a cassava starch factory in Thailand, the waste was found to be toxic to the plants. The toxicity was thought to be associated with the high cyanide content and to a lesser extent other components (Bengtsson and Triet, 1994). Cyanide content in by-products and wastes also depends on the cassava variety. The high yield varieties used throughout Asia generally contain high amounts of HCN. For production of 200 tonnes of starch/day, about 800 tonnes of roots are required, which will contain about 32 kg of HCN. Generally, the HCN concentration of fresh peeled roots varies from 6-250 mg/kg fresh weight. The factory with a process discharge of 2,323 tonnes of wastewater will also discharge about 30 kg HCN, equivalent to 13 mg HCN per liter of wastewater. In Vietnam, small-scale processors released 28 mg HCN per liter of wastewater (Bengtsson and Triet, 1994).

The significance of surface water contamination should be interpreted from the perspective of seasonal variation. It is most acute in an extended dry season. Care should be exercised to identify all possible sources of contamination, as starch processing may only be a minor contributor. This is especially difficult when examining the impact of cassava processing on river water quality. It is also not easy to determine the number of lakes and ponds affected by starch processing because of problems in distinguishing between starch effluents,

agricultural run-off and domestic sewage. Reports suggest that in some cassava processing areas, where increasing agricultural intensification has taken place, many water bodies have become progressively more eutrophic. The contribution to this problem from cassava processing is difficult to assess, except for a few areas where cassava processing is the only source of effluent to the body of water. Environmental problems from cyanide in wash water or expressed liquid can occur if the water is used, without dilution, for irrigation (e.g. young stages of rice, vegetables) (Bengtsson and Triet, 1994). Negative effects on local agriculture and sensitive stages of fish and crustacean populations in receiving water bodies can also be expected if the concentration of cyanide increases above 0.3 mg/I. However, this has never been documented. Starch effluents may have significant environmental effects on lakes and ponds, ultimately affecting local communities. Effluent from the Brazilian sour starch processors is claimed to kill fish and other animals. Reports concerning contaminated water courses in processing areas increase towards the middle and end of the dry season. Further research is required to substantiate such claims, as there has not been any systematic monitoring.

2.2.5Cyanide from Cassava Tubers

Linamarin is a form of glucose extracted from cassava roots (tuber). The hydrogen cyanide released during the hydrolysis of linamarin is a poisonous substance. It has a boiling point of 25.7%. Akinrele (1986), reviewed the work of Woffside and Shifter (1959) and showed that hydrocyanic acid and the

cyanides are true protoplasm poison combining in the tissue with the enzymes associated with cellular oxidation. Cytochrome oxidase is the substance involved in the respiratory process and causes ultimately the electron transfer to molecular oxygen. Cyanide thereby renders the oxygen unavailable to the tissues causing death through asphyxia. Cyanide is readily absorbed from the gastrointestinal tract. It exerts inhibitory action on metalloenymes. Cyanide specifically, by forming a complex table with cytochrome oxidase causes death. This is called cellular anoxia. Swyen and Wiston (1971) observed that Cyanide can produce neurological problems.

2.2.6 Degradation of Glycoside in Cassava Wastewater

Cassava is an important staple food crop in tropical Africa. It is produced in large quantity in Nigeria. Garri, a variant of the South American Farinha de Mandioca, is by far the most popular form in which cassava is consumed in West Africa. For its preparation, cassava tuber is grated, fermented for 3-4 days, then dewatered and fried to a moisture content of about 9-12%. It is utilized for the production of several useful products in food and textile industries (Ihekoronye and Ngoddy, 1985).

Spontaneous release of HCN from the plant depends on the presence of a specific glycosidase and water. The enzymes are extra – cellular and gain access to the glycosides after physical disruption of the cell. Auto hydrolysis is enhanced by dilution. The release of HCN depends on pH, temperature and other physical conditions. It boils at 26^0C and storage in hot humid conditions

leads, to gradual loss. The compound, cyanide exists in cassava as aliphatic Cyanogenic glucosides, linamarin and lotaustralin often referred to as bound cyanide and the free non – glucosidic cyanide, HCN. The bound form accounts for approximately 90% of the total cyanide content (Nartey, 1973). Glucoside is first broken down to glucose and cyanohydrins, Cyanogenic glucoside, linamarin and lotastralin under enzymzatic action. Cyanohydrin then breaks down to HCN reversibly and ketone if pH>5.5. At lower pH (<5.5), cyanohydrin is very stable, little HCN is released and HCN dissociates spontaneously into cyanohydrins. However, liberation of HCN can be achieved at low pH through the action of bacteria. Because most cassava tubers are rich in cyanide, the wastewater resulting from its processing will also contain cyanide. Cyanide is known to interfere with some treatment processes. Earlier research has shown the possibility of co-treatbility of both cassava wastewater and sewage (Agunwamba et. al., 2001). Combination of sewage and cassava wastewater mixed in certain proportion resulted in better degradation than either cassava wastewater or sewage treated alone anaerobically. (The previous research did not analyze the role of cyanide in the degradation of cassava wastewater and its relationship with the other parameters. Knowledge of these aspects will not only give a better insight into the optimal conditions for degradation but will also ultimately facilitate better design of treatment works).

The rate of cyanide release from cassava seems not to have attracted the interest of many researchers. The rate of cyanide release is very important for estimate

of the period within which it affects cassava wastewater degradation. The only available literature on cyanide release is by Agunwamba (2004). The Kinetic equations describing the release were expressed as follows:

$$\frac{dA}{dt} = K_1 A \qquad (2.1)$$

$$\frac{dB}{dt} = k_1 A + k_3 C - k_2 B \qquad (2.2)$$

$$\frac{dC}{dt} = K_2 B - K_3 K_1 \qquad (2.3)$$

The equations were solved by Laplace transformation, calibrated with experimental data and verified with an independent set of data.

2.2.7 Effect of Cyanide on Cassava Wastewater Degradation

Glucoside degrades to form cyanide in cassava wastewater. A result from research carried out at the University of Nigeria, Nsukka Civil Engineering Laboratory showed that the concentration of cyanide in cassava wastewater was poorly correlated with pH, BOD and COD but positively and highly correlated with coliform. There seems to be an evidence of no inhibition of cassava wastewater degradation by cyanide (Agunwamba, 2004) as far as E – Coli and coliform bacteria is concerned. The presence of cyanide seems to enhance bacteria growth and cyanide may not be toxic to these groups of bacteria.

Experiments have been conducted by researchers for determination of the BOD kinetic constants for both fermented and garri wastewaters. Result gave these constants as $0.432d^{-1}$ and $0.152d^{-1}$ for garri and fermented cassava wastewaters

respectively. These constants will be useful in the design of units for the treatment of cassava wastewater.

2.2.8 Effect of Cassava Wastewater on Sewage Degradation

In some communities, fermented wastewater is poured periodically into pit latrines. This is claimed to aid degradation of bacteria and organics in sewage. Hence, a study aimed at determination of the effect of cassava wastewater on degradation was performed. The rates of degradation of sewage mixed with 5%, 10% 20% 30% and 50% of fermented cassava wastewater were monitored for 25 days. The sewage was collected from the treatment plant at the University of Nigeria, Nsukka, Nigeria. The preliminary results showed that the optimum percentages of cassava wastewater are 0%, 5% and 20% for COD, BOD_5, suspended solids and coliform bacteria removal respectively (Agunwamba et al. 2001).

2.3 Inhibition of Wastewater Treatment

The rates of substrate utilization and microbial growth can be slowed by the presence of inhibitory compounds. Examples of inhibitors are heavy metals, pesticides, antibiotics, aromatic hydrocarbons, and chlorinated solvents. Sometimes these materials are called toxicants and their effects termed toxicity. Here, the terms inhibitor and inhibition are used, because they imply one of several different general phenomena affecting metabolic rates. The range of possible inhibitors and their different effects on the microorganisms can make inhibition a confusing topic. In some cases, the inhibitor affects a single enzyme

active in substrate utilization; in such a case, utilization of that substrate is slowed (Wrenn and Rittmann, 1995). In other cases, the inhibitor affects some more general cell function, such as respiration; then, indirect effects, such as reduced biomass levels may slow utilization of a particular substrate. Finally, some reactions actually are increased by inhibition, as the cell tries to compensate for the negative impacts of the inhibitor. Fig.2.2 shows the key places that inhibitors affect the primary flows of electrons and energy. Inhibition of a particular degradative enzyme may occur during the initial oxidation reactions of an electron-donor substrate. The immediate effect is a slowing of the degradation rate. In addition, the reduced electron flow can lead to a loss of biomass or slowing of other reactions requiring electrons (ICH_2) or energy (ATP). At the other end of the electron-transport chain, inhibition of the acceptor reaction prevents electron flow and energy generation, thereby leading to a loss of biomass. Interestingly, inhibition of the acceptor reaction can lead to a buildup of reduced electron carriers (ICH_2) and increased rates for reactions requiring reduced electron carriers as a cosubstrate (Wrenn and Rittmann, 1995). Decouplers reduce or eliminate energy generation even though electrons flow from the donors to the acceptor. Decoupling inhibits cell growth and other energy-requiring reactions. In some cases, decoupling inhibition leads to an increase in acceptor utilization per unit biomass as the cells attempt to compensate for a low energy yield by sending more electrons to the acceptor. How an inhibitor affects growth and substrate-utilization kinetics can be

expressed succinctly by using effective kinetic parameters. The kinetic expressions for substrate utilization and growth remain the same as Monod equation, but the effective kinetic parameters depend on the concentration of the inhibitor (Goldsteen and Spencer, 1985).

$$R_{ut,eff} = -\frac{q_{eff}}{K_{eff} + S} X_a \tag{2.4}$$

$$\mu_{ff} = Y_{ff}\left(-r_{ut,e_{ff}}\right) - b_{eff} \tag{2.5}$$

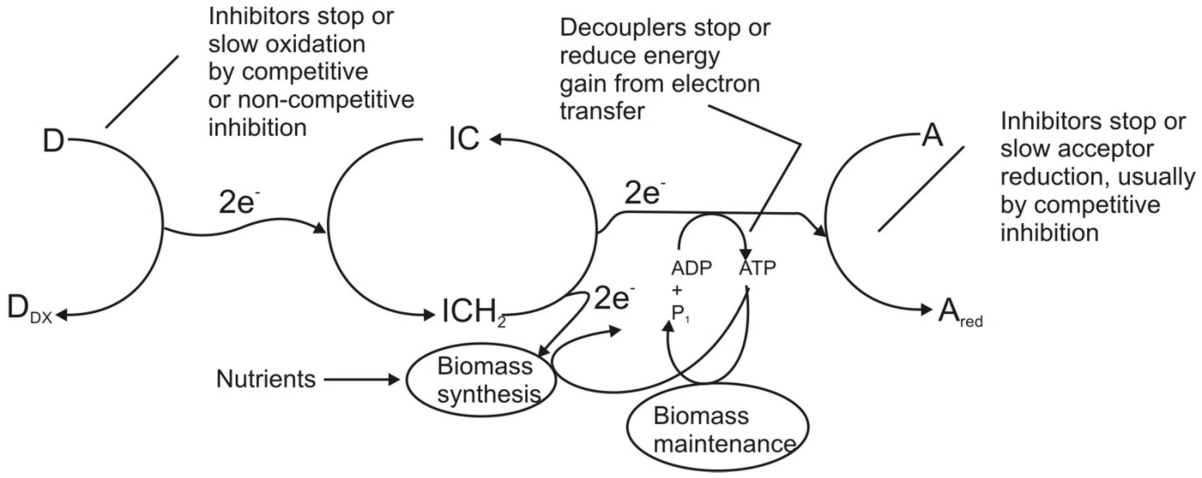

Fig. 2.2: Illustration of How Inhibitions Can Affect the Primary Flow of Electrons and Energy
Source: Rittmann and Sóez (1993)

How q_{eff}, y_{eff}, and b_{eff} are controlled by the inhibitor concentrations depends on the location and mode of the inhibition phenomenon. The most common types of inhibition and their effective parameters are reviewed here.

2.3.1 Self-Inhibition of Wastewater Treatment

A common type of inhibition for aromatic hydrocarbons and chlorinated solvents is self-inhibition, which also is called Haldane or Andrew's kinetics. In

this case, the enzyme-catalyzed degradation of the substrate is slowed by high concentrations of the substrate itself. It is not clear whether the self-inhibition occurs directly through action on the derivative enzyme or indirectly through hindering electrons or energy flow after the original donor reaction, in either situation, the effective parameters for self-inhibition are (Andrews, 1968);

$$q_{eff} = \frac{q}{1 + \frac{S}{K_{IS}}} \tag{2.6}$$

$$K_{eff} = \frac{K}{1 + S/K_{Is}} \tag{2.7}$$

Y_{eff} and b_{eff} are not affected and remain Y and b, respectively. Fig. 2.3 contains two graphical presentations of the effect of substrate self- inhibition on reaction kinetics. The left figure illustrates how the reaction rate ($-r_{ut}$) varies with substrate concentration. At low substrate concentrations, the rate increases with an increase in S. However, a maximum rate is reached, and substrate concentrations beyond this become inhibitory, causing a decrease in reaction rate. When the Haldane reaction rate model is substituted for the Monod relation in the CSTR mass balances, the effect of k_s on effluent substrate concentration is illustrated by the right graph in Fig. 2.3. The reactor population would continue to increase, and the value of S in the reactor would continue to decrease until the microbial population size and substrate concentration reached their steady-state concentrations, about 1 mg/l for the substrate. The value of Fig. 2.3, then, is not only to indicate what this steady-state concentration would

be for a well-operating reactor, but also to indicate upper limits on substrate concentration beyond which reactor start-up cannot proceed (Wrenn and Rittmann, 1995).

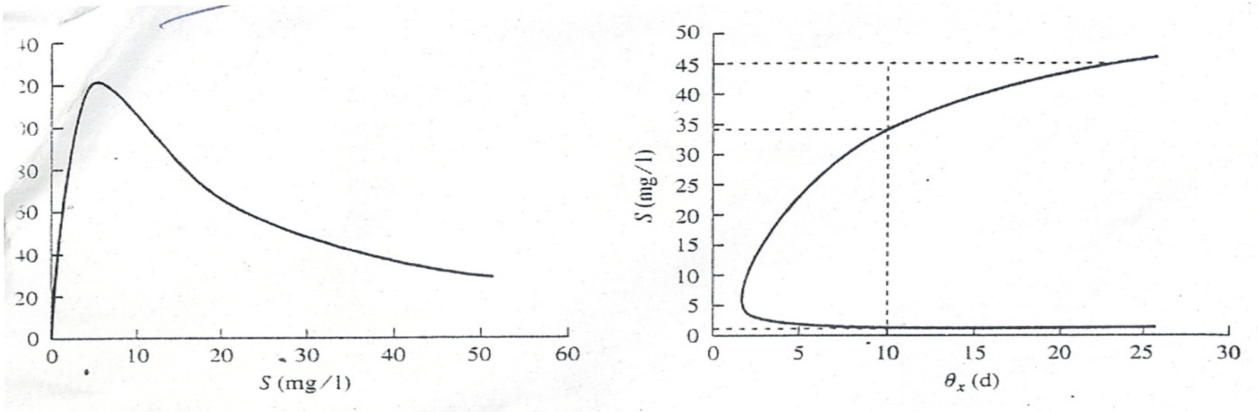

Fig. 2.3 Haldane kinetics and the Relationship between S and Reaction rate (top) and between S and θ_x
Source: Wrenn and Rittmann(1995)

2.3.2 Competitive Inhibition of Wastewater Treatment

The second type of inhibition is competitive, and a separate inhibitor is present at concentration I (M_TL^{-3}). The competitive inhibitor binds the catalytic site of the degradative enzyme, thereby excluding substrate binding in proportion to the degree to which the inhibitor is bound. The only parameter affected by I in competitive inhibition is K_{eff}:

$$k_{eff} = K\left(1 + \frac{I}{K_I}\right) \qquad (2.8)$$

A small value of K_I indicates a strong inhibitor. The rate reduction caused by a competitive inhibitor can be completely offset if S is large enough. One example of competitive inhibition that is of interest in environmental

engineering practice is that of co-metabolism of trichloroethylene (TCE) by microorganisms that grow on substrates such as methane. Here, the first step in methane utilization is its oxidation to methanol by an enzyme called a methane monooxygenase IMMO), which replaces one hydrogen atom attached to the methane carbon with an -OH group. With TCE, MMO interacts to place an oxygen atom between the two carbon atoms to form an epoxide. The key factor is that methane and TCE compete for the same enzyme (Noguera, 1991). The presence of TCE affects the rate at which methane is consumed and, in turn, the presence of methane affects the reaction rate of MMO with TCE. This is illustrated in Fig. 2.4. The presence of 20 mg/I TCE reduces the rate of methane utilization considerably over that given by the Monod model, which does not involve competitive inhibition. Similarly, the rate of TCE utilization is greatly reduced as the methane concentration increases. The rate expression for TCE is similar to that for methane, except that the roles of the substrate and the inhibitor are reversed.

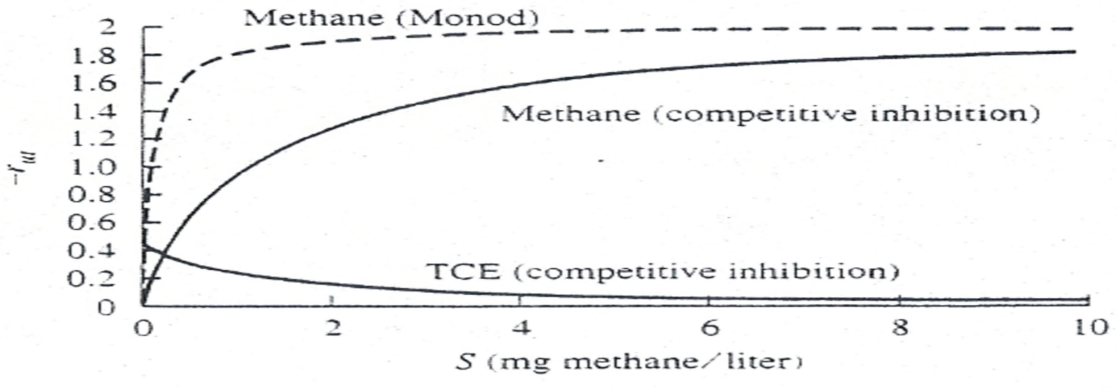

Fig. 2.4: Reaction Rates for Methane and TCE as Governed by Competitive Inhibition Kinetics

Source: Wrenn and Rittmann (1995)

2.3.3 Noncompetitive Inhibition of Wastewater Treatment

A third type of inhibition is noncompetitive inhibition by a separate inhibitor. A noncompetitive inhibitor binds with the degradative enzyme (or perhaps with a coenzyme) at a site different from the reaction site, altering the enzyme conformation in such a manner that substrate utilization is slowed. The only parameter affected is q_{eff};

$$q_{eff} = \frac{q}{1 + \frac{1}{k_1}} \qquad (2.9)$$

In the presence of a noncompetitive inhibitor, high S cannot overcome the inhibitory effects, since the maximum utilization rate is lowered for all S. This phenomenon is sometimes called allosteric inhibition, and allosteric inhibitors need not have any structural similarity to the substrate.

Fig. 2.4 illustrates the different effects that competitive and noncompetitive inhibitors have on reaction rates, in comparison with the Monod model. The values of I, K, and K_I are assumed to be the same, 1 mg/I, making the value $(1 + I/K_I) = 2$. With a competitive inhibitor, the impact is primarily on K, and the inhibitor causes the effective K to increase (from I to 2 as indicated by the horizontal line in the middle of the graph). If the substrate concentration (S) is high enough, the reaction rate eventually approaches q. With the noncompetitive inhibitor, the effect is on causing the apparent value to decrease as the inhibitor concentration increases (from 2 to 1 as indicated by the upper

and middle horizontal lines in the illustration). The value of K, the substrate concentration at which the rate is one-half of the maximum value, in effect, remains unchanged. In some cases, competitive and noncompetitive impacts occur together. This situation is termed uncompetitive inhibition. Both effective parameters, q_{eff} and K_{eff}, vary as they do for the individual cases (McCarty, 1975):

$$q_{eff} = \frac{q}{1 + 1/k_1} \tag{2.10}$$

$$K_{eff} = K\left(1 + \frac{1}{K_1}\right) \tag{2.11}$$

Mixed inhibition is a more general form of uncompetitive inhibition in which the K_1 values in Equations 2.10 and 2.11 can have different values.

2.3.4 Decoupling Inhibition of Wastewater Treatment

The last inhibition type considered is decoupling. Decoupling inhibitors, such as aromatic hydrocarbons, often act by making the cytoplasmic membrane permeable for protons. Then, the proton-motive force across the membrane is reduced, and ATP is not synthesized in parallel with respiratory electron transposed. Sometimes, decouplers are called protonophores. A decrease in Y_{eff} and/or an increase in b_{eff} can model the effects of decoupling inhibition:

$$Y_{eff} = \frac{Y}{1 + \frac{1}{k_1}} \tag{2.12}$$

$$b_{eff} = b\left(1 + \frac{1}{1/k_1}\right) \tag{2.13}$$

The other parameters are not necessarily changed. An interesting aspect of decoupling is that the rate of electron flow to the primary acceptor and per unit active biomass can increase. This is shown mathematically for steady state (Wrenn and Rittmann, 1995):

$$r_{A.eff} = \frac{q_{eff}S}{K_{eff} + s}\left[1 - y_{eff}\left(1 - \frac{f_d b_{eff}\theta_x}{1 + b_{eff}\theta_x}\right)\right] \tag{2.14}$$

in which $r_{A\ eff}$ specific rate of electron flow to the acceptor ($M_s M_x^{-1} T^{-1}$) and units of mass are proportional to electron equivalents (e.g., COD). Equation 2.14for all types of inhibition and shows how self-, competitive, and noncompetitive inhibitions normally slow $r_{A,\ eff}$. However, $r_{A,\ eff}$ increases when decoupling b_{eff} and /or decreases Y_{eff}. Sometimes products of a reaction act as inhibitors. The classic example of conduct inhibition is in alcohol fermentation, where ethanol is produced as an end product from sugar fermentation. In wine manufacture, fermentation of sugar can occur until the ethanol concentration reaches 10 to 13 percent, at which point the alcohol becomes toxic to the yeast, and fermentation stops. This is why the alcohol content of wines normally is in the range of 10 to 13 percent (Monod, 1948).

2.4 Modelling of Anaerobic Digestion

Anaerobic digestion is a process that converts organic matter into a gaseous mixture mainly composed of methane and carbon dioxide through the concerted action of a close-knit community of bacteria. It has been traditionally used for waste treatment but there is also considerable interest in plant-biomass-fed digesters, since the produced methane is a useful source of energy. Anaerobic digestion is a multistep process involving the action of multiple microbes. Usually, such processes contain a particular step, the so called rate-limiting or rate-determining step, which, being the slowest, limits the rate of the overall process (Hill, 1977). Lawrence (1971) defined as limiting step "that step which will cause process failure to occur under imposed conditions of kinetic stress". The first attempts for modelling anaerobic digestion led to models describing only the limiting step. However, during a wide range of operating conditions, the limiting step is not always the same. It may depend on wastewater characteristics, hydraulic loading, temperature, etc. (Speece, 1983). Andrews (1969, 1971) for example considered acetogenic methanogenesis as the limiting step, O'Rourke (1968): the conversion of fatty acids to bingas, and Eastman and Ferguson (1981): the hydrolysis of biodegradable suspended solids. It is apparent that the "limiting step hypothesis" leads to simple and readily usable models. Such models, however, do not describe very well the digester behaviour, especially under transient operating conditions. The Graef and Andrew's model (1974) involves only the acetoclastic methanogens. The

conversion of fatty acids into binges is considered limiting. Volatile fatty acids are expressed as acetic acid and the methanogens composition is assumed to be $C_5H_7N0_2$. The overall reaction, according to this model, may be represented as follows:

$$CH_3COOH + 0.032\ NH_30.032\ C_5H_7N0_2 \pm 0.92\ CO_2 + 0.92\ CH_4 + 0.096\ H_20 \quad (2.15)$$

Monod kinetics with substrate inhibition are assumed (Andrews, 1969), i.e.

$$M = \mu = \frac{\mu_{max}}{1 + \frac{K_s}{S} + \frac{1}{K_i}} \quad (2.16)$$

Table 2.8: Models that Assume Substrate-inhibited Monod kinetics at the Methanogenesis

Model by Authors	Limiting step	Predicted causes of digesters failure	Suitable for the digestion of
Graef and Andrews (1974)	Methanogenesis	VFA accumulation	Soluble for the digestion of
Hill and Barth (1977)	Methanogenesis	Heavy organic loading VFA accumulation	Animal waste
Kleinstreuer and Powegha (1982)	Methanogenesis	Heavy organic loading VFA accumulation	Various substrates
Moletta et al. (1986)	Methanogenesis		Easily fermentable substrates
Smith et al. (1998)	Methanogenesis	VFA accumulation	Biodegradable organic particulate

Source: Andrews, (1969).

- Graef and Andrews (1974) used their model for simulating digester start-up, and digester response to organic and hydraulic overloading, and entry of an inhibitor. To date, no experimental verification of this model has been made. Other models (Table 2.8) that also assume substrate inhibited Monod kinetics (Andrews) of the methanogens are:
- Hill and Barth (1977), who also considered hydrolysis, acidogenesis and ammonia inhibition (Fig. 2.5).

- Kleinstreuer and Powegha (1982), which involves hydrolysis of biodegradable solids, acetogenesis and methanogenesis, dependent on pH and temperature (Fig. 2.6).
- Moletta et al. (1986) which involves also an acidogenesis step, that forms acetate from glucose, and are inhibited by undissociated acetic acid (Fig. 2.7).
- Smith et al. (1998). A slow and a fast hydrolysis step are assumed, whereas acidogenesis of the soluble intermediates and methanogenesis are also taken into account (Fig. 2.8).

The model of Hill (1982) assumes that methanogenesis depends on the total fatty acids. This model was specially developed for describing digestion of manure and animal wastes. The model assumes inhibition by the total fatty acid concentration.

The following bacterial groups are assumed to participate in the overall digestion process (Fig. 2.9):

(a) acidogenic, which give on glucose (considered as the dissolved organics less the volatile fatty acids) form a mixture of acetic, propionic and butyric acids,

(b) hydrogenogenic, which have a slow growth rate, convert propionic and butyric acid into acetic acid arid H_2,

(c) homoacetogenic produces acetate from H_2 and CO_2,

(d) H_2-methanogenic reduces CO_2 into CH_4 and

(e) acetate-triethanogenic converts acetic acid into biogas (CH_4 and CO_2).

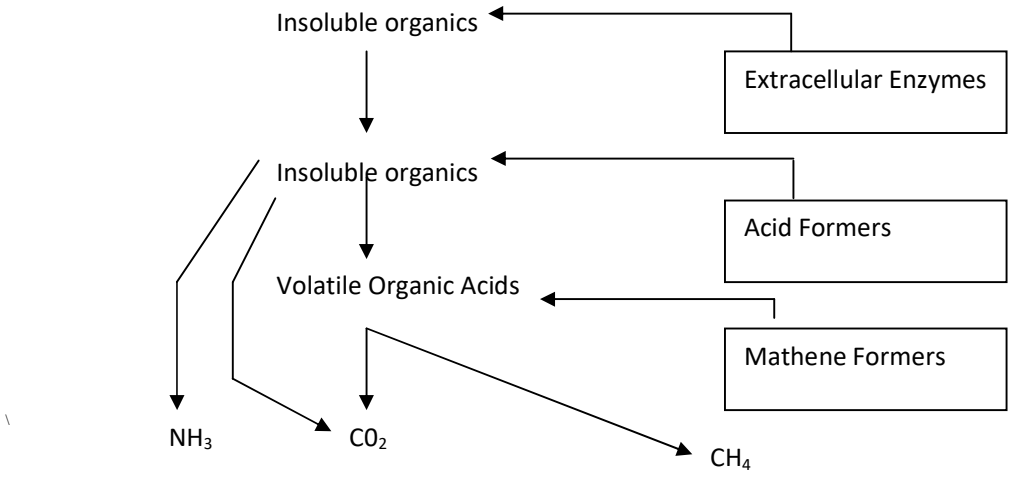

Fig. 2.5: Block Diagram of Mathematical Model

Source: Hill and Barth (1977)

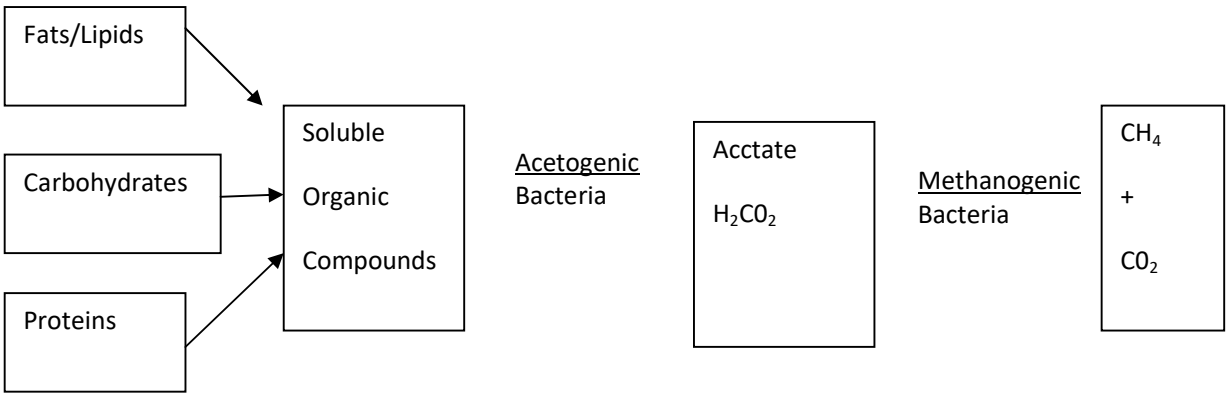

Fig. 2.6: Schematic Biochemical Process Stages of Anaerobic Digestion
Source:Kleinstreuer and Powegha (1982)

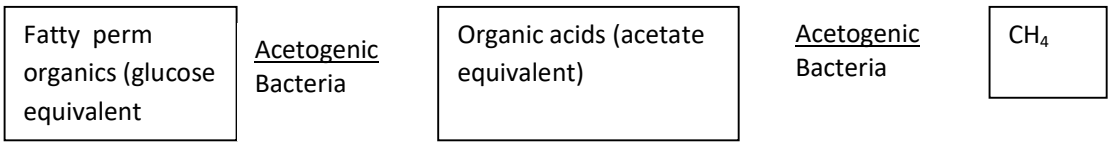

Figure 2.7: Flow Chart of Model 1

Source: Moletta et al. (1986)

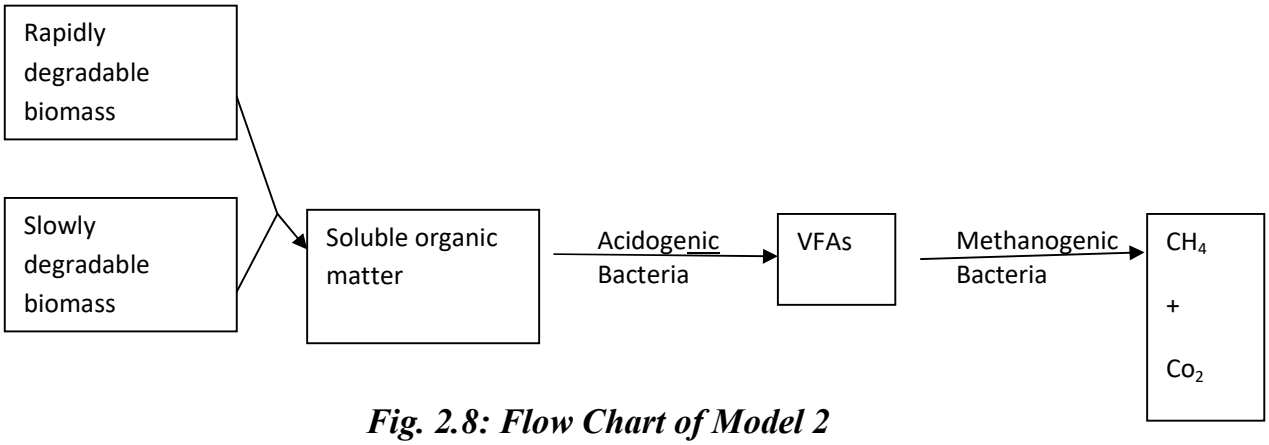

Fig. 2.8: Flow Chart of Model 2

Source: Smith et al. (1998)

Another model, which also considers total volatile fatty acid concentration as a key parameter but also accounts for the influence of other parameters such as the pH, is that of Bryers (1985) (Fig. 2.10).

Mosey (1983) considered the hydrogen partial pressure as the key regulatory parameter of the anaerobic digestion of glucose (Table 2.9). This influences the redox potential in the liquid phase. The model considers four bacterial groups (Fig. 2.11) to participate in the conversion of glucose to CO_2 and CH_4:

(a) The acid-forming bacteria, which are fast-growing and ferment glucose to produce a mixture of acetate, propionate and butyrate,

(b) The acetogenic bacteria convert the propionate and butyrate to acetate,

(c) The acetoclastic methane bacteria convert acetate to CO_2 and CH_4, and

(d) The hydrogen-utilizing methane bacteria reduce CO_2 to CH_4. The fatty acid relative production is assumed to depend on the redox potential or equivalently, on the ratio [NADH] /[NAD+].

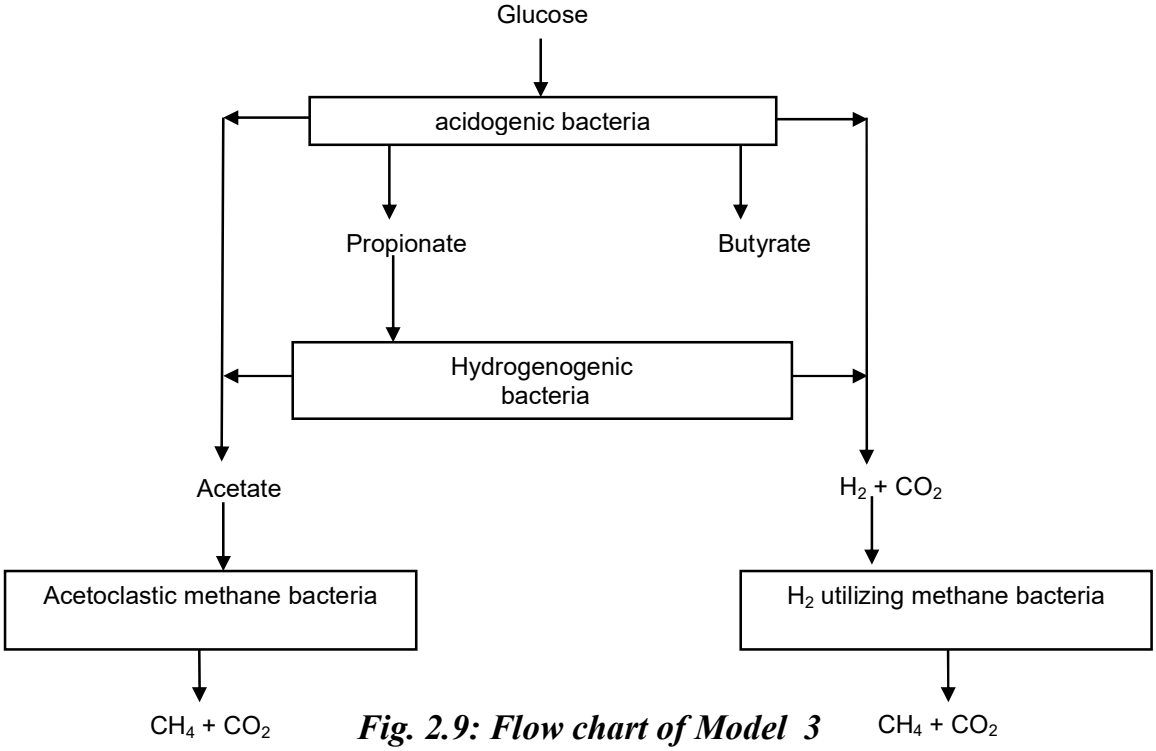

Fig. 2.9: Flow chart of Model 3

Source: Hill (1982)

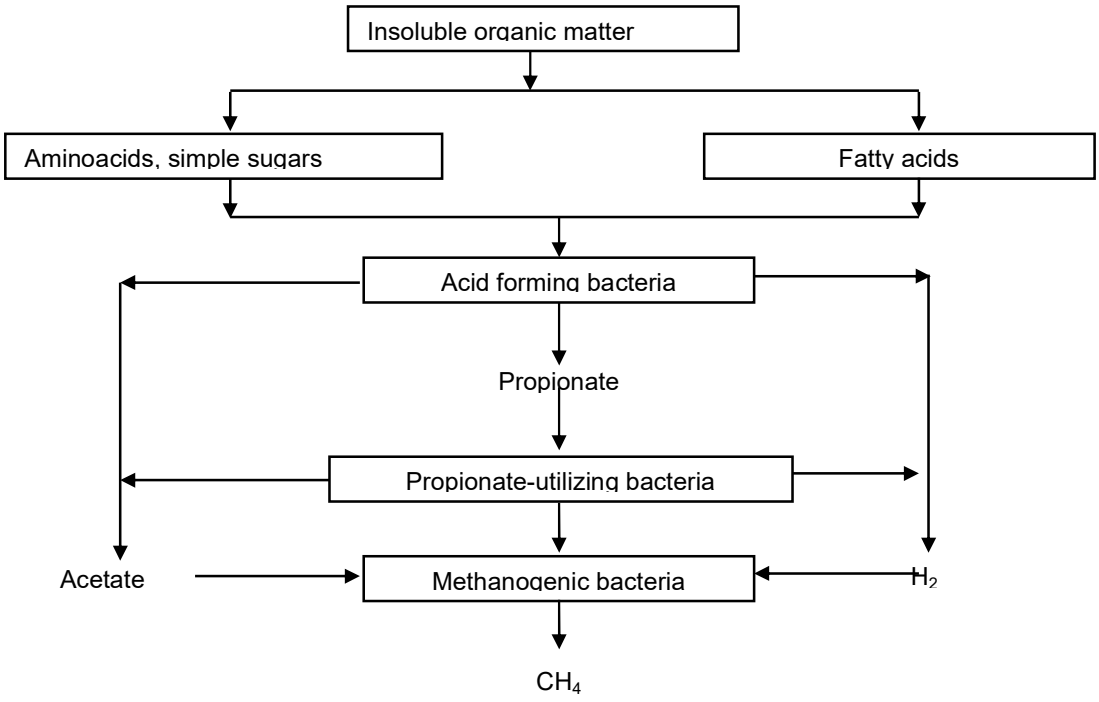

Fig. 2.10 Flow Chart of Model 3

Source: Bryers (1985)

This ratio is made a function of the hydrogen partial pressure in the gas phase.

Considering that the acidogenic bacteria follow the glycolytic metabolic pathway, the factor that regulates the relative amounts of fatty acid generation is the liquid phase redox potential, or equivalently the ratio [NADH] /[NAD+] inside the bacterial mass. This ratio may be expressed as a function of the hydrogen partial pressure, based on the following assumptions:

(1) Inside the bacteria, a neutral pH is maintained, despite variations in the liquid medium.(2) Hydrogen was freely and readily diffused through the bacterial membrane, so that its partial pressure inside the cell is the same as its partial pressure in the digester gas phase. The redox potential inside the cell is equal to that of the liquid medium. Apart from the acidogenic bacteria, hydrogen partial pressure also influences the acetogenic growth rate, since high values inhibit (thermodynarnically) the generation of propionic and butyric acids Finally, low pH values (<6) are expected to be inhibitory to all the bacteria. According to the Mosey model, a sudden increase and the organic loading rate is expected to cause an accumulation of VFAs, since the acetogens grow at a slower rate than the acidogens. The subsequent drop in the pH inhibits in turn the hydrogen utilising methanogenic bacteria, causing a rise in the hydrogen partial pressure, which causes further accumulation of propionic and butyric acids Methane generation is stalled when the pH drops to particularly low levels (< 5.5).

Table 2.9: Models Using H_2 as the Control Parameter

Model	Bacterial group (substrates)	Processes	Kinetics (function of)	Accounted inhibition
Mosey (1983)	Acid-forming bacteria (glucose)	Acidogenesis	Monod (pH)	H_2 partial pressure
	Propionic acid bacteria (propionate)	Acetogenesis	Monod (pH)	H_2 partial pressure
	Butyric acid bacteria (butyrate)	Acetogenesis	Monod (pH)	H_2 partial pressure
	Acetoclastic methane bacteria (acetate)	Methanogenesis	Monod (pH)	
	Hydrogen-utilizing methane bacteria (H2 and CO_2)	Methanogenesis	Monod (pH)	
Pullammanappallil et al. (1991)	Acidogenic bacteria (glucose)	Acetogenesis	Monod (H_2)	
	Propionate-utilizing acetogens (propionate)	Acetogenesis	Monod	H_2 partial pressure
	Butyrate-utilizing acetogens (butyrate)	Acetogenesis	Monod Monod Andrews	H_2 partial pressure Unionized propionate and butyrate
Costello et al. (1991)	Acid-forming bacteria (glucose)	Acidogenesis	Monod	H_2 partial pressure pH product
	Lactic acid bacteria (lactate)	Acidogenesis	Monod	H_2 partial pressure pH product
	Propionic acid bacteria (propionate)	Acetogenesis	Monod	H_2 partial pressure pH product
	Butyric acid bacteria (butyrate)	Acetogenesis	Monod	H_2 partial pressure pH product
	Acetoclastic methane bacteria (acetate)	Methanogenesis	Monod	pH
	Hydrogen-utilizing methane bacteria (H_2 and CO_2)	Methanogenesis	Monod	pH

Source: Lyberatos and Skiadas (1999)

Based on the work of Mosey followed the models of Pullammanappailil et al (1991) and Costello et al. (1991a, 1991b) (Tables 2.10 and 2.11) Pullammanappailil at al. (1991) (Fig. 2.11) allowed description of the gas phase

and acetoclastic inhibition by undissociated fatty acids. Costello et al. (1991a, 1991b) assumed that glucose is first converted into acetic, butyric and lactic acids, followed by conversion of lactate into propionate and acetate by another bacterial group.

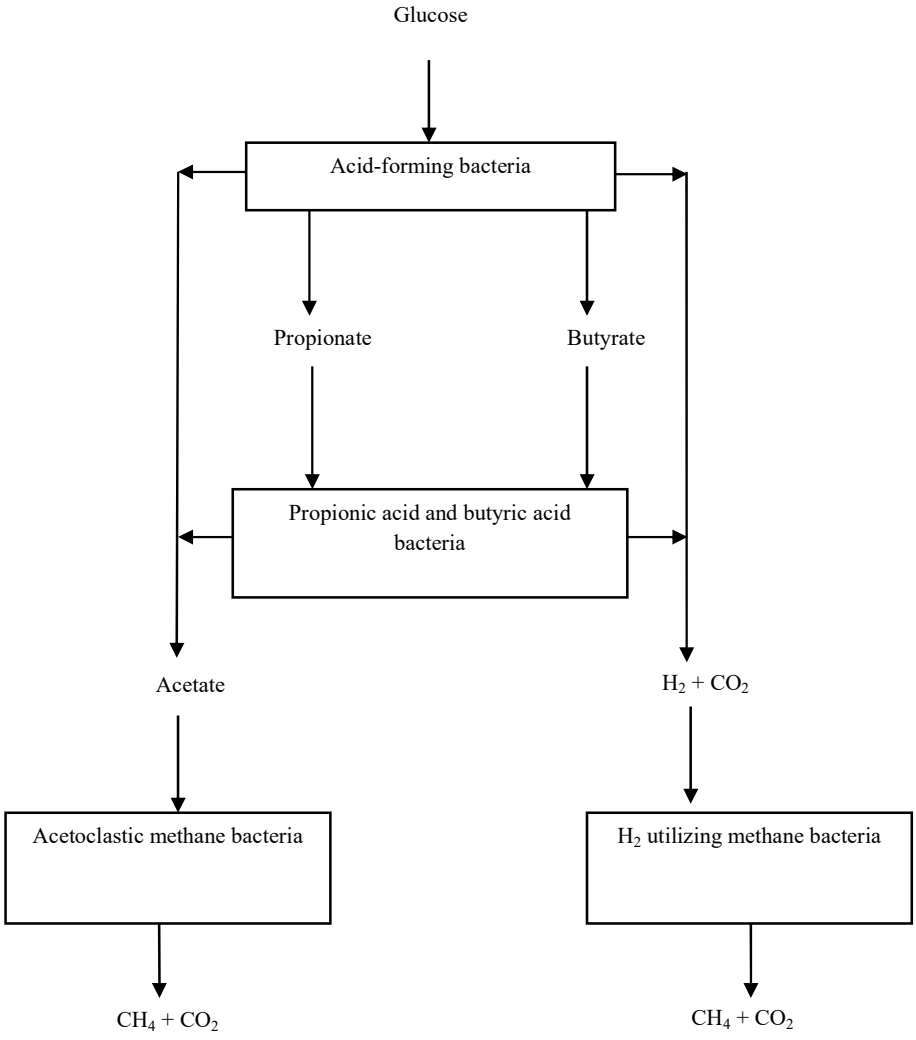

Fig. 2.11 Flow Chart of Model 4

Source: Mosey (1983) and Pullammanappallil et al. (1991)

All the models described thus, are capable of predicting digester failure, caused by a specific disturbance, either through a drop in the pH, and/or through accumulation of volatile fatty acids. Such is a commonly observed behaviour in

digesters treating municipal sludge and/or high organic content industrial wastewaters.

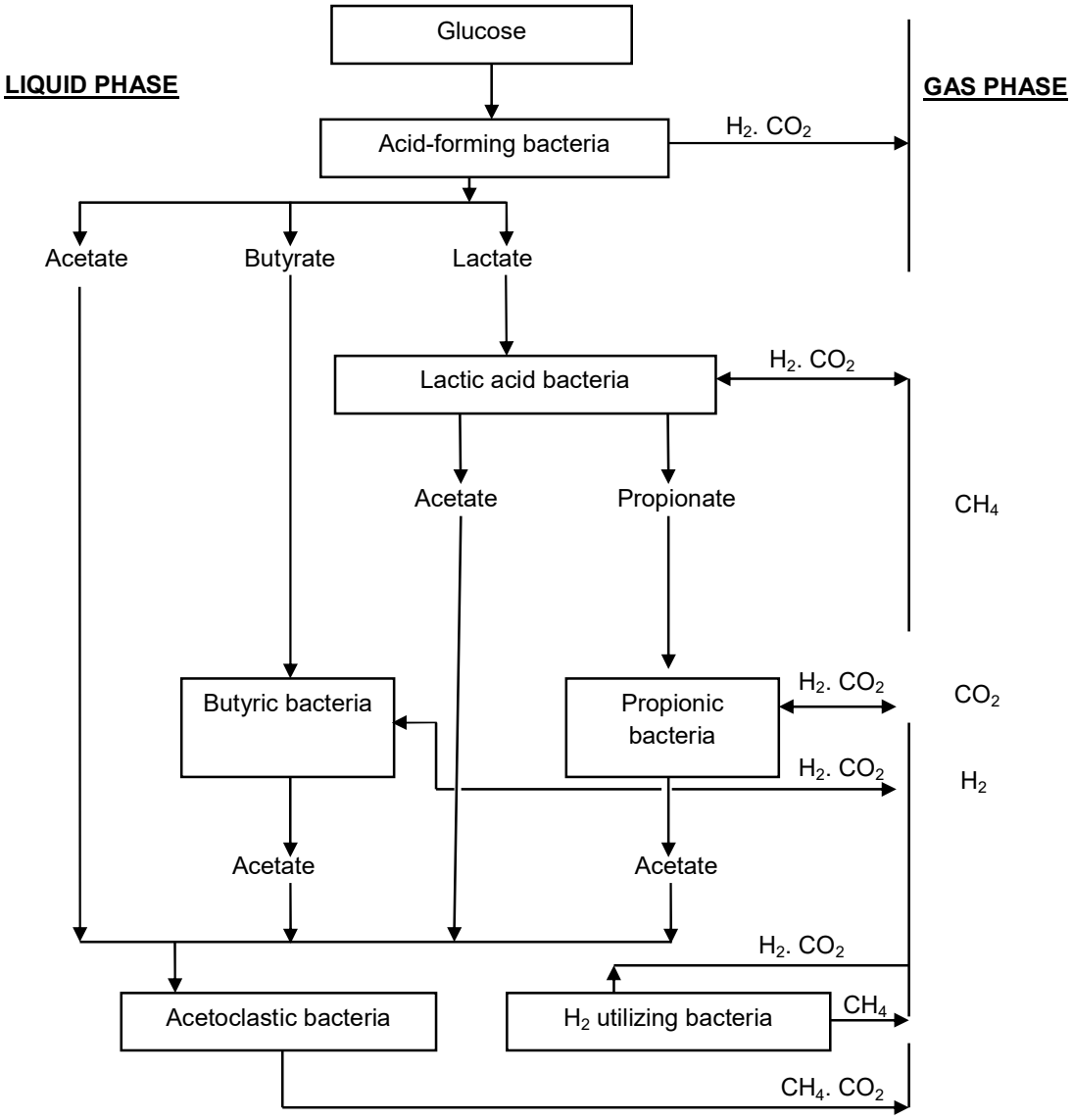

Fig. 2.12: A Schematic of Relationship Bacteria in Tanaerobic Ecosystem Model

Source: Costello et al. (1991)

None of these models, however, can adequately describe anaerobic digestion of manure (Angdlidaki, 1992). Digesters fed with manure, exhibit a self-regulation of the pH, attributed to the generated ammonia. The model of Angelidaki et al.

(1993) considers hydrolysis, acidogenesis, acetogenesis and methanogenesis (Fig. 2.13).

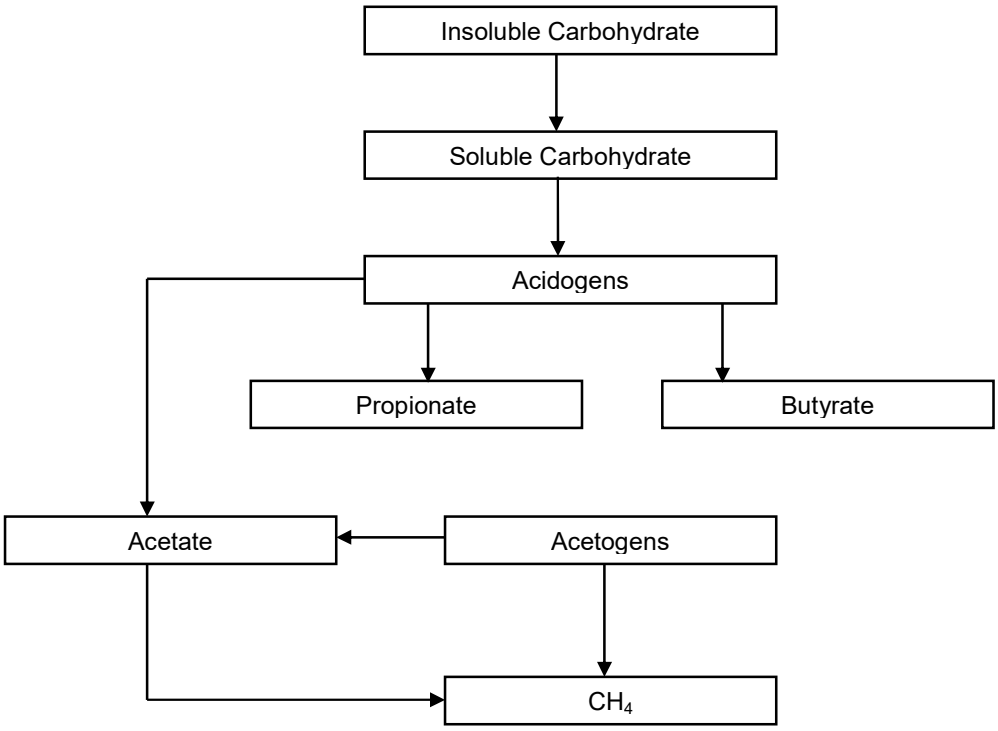

Fig. 2.13: Flow chart of Model 6

Angelidaki et al.(1993)

Free ammonia is assumed to inhibit methane- genesis, acetic acid is assumed to inhibit acetogenesis, and total VFA is assumed to inhibit acidogenesis (Table 2.11). The maximum specific growth rate of the bacteria and the degree of ionisation of ammonia are assumed to depend on the temperature and the pH. The pH self-regulation mechanism is as follows. Whenever free ammonia (high for high pH) inhibits methanogenesis, acetic acid is accumulated. This causes an inhibition to acetogenesis, and a consequent accumulation of propionic and butyric acids, leading to inhibition of acidification. The model is very good for describing the behaviour of manure fed digesters. VFA accumulation reduces

the pH, causing a decrease in the free ammonia concentration and the inhibition of methanogenesis. The process is thus self-regulatory, unless the magnitude of the disturbance is larger than the system can withstand. When this occurs, the pH drops significantly, causing digester failure. All models described so far consider organic matter as a whole and do not account for the nature of the organic macromolecules in the fed composition A modelling approach that takes the complex feed composition (breakdown in carbohydrate, protein, VFAs and other organics) into account has been recently proposed (Gavala et al., 1996). Some of the mechanisms involved in the hydrolysis and biodegradation of complex organic molecules were already elucidated but there was no appropriate kinetic modelling framework available. Thus, it was known that lipids are first hydrolysed into glycerol and long-chain fatty acids (LCFAs). The LCFAs are further degraded into acetate and hydrogen (Weng and Jeris, 1976). Acetate and hydrogen are then finally converted tobiogas (Bryant, 1979). Lipids can cause inhibition of the process (Angelidaki and Abring, 1992). The model of Gavala et al. (1996), describes the codigestion process of agroindustrial wastewaters It is assumed that the wastewaters consist of carbohydrates and proteins (undissolved and dissolved) and other dissolved organic matter. The conversion of organic matter to biogas is carried out by the simultaneous action of three groups of bacteria: acidogens (hydrolysis and acidogenesis), acetogens and methanogens. In the hydrolysis step, the undissolved carbohydrates and proteins are hydrolysed to dissolved carbohydrates and proteins, respectively; in

the acidogenesis step, the dissolved carbohydrates, proteins and other organic matter are converted to acetate and propionate; while in the acetogenesis step, propionic acid is converted to acetate. Finally, hydrolysis of undissolved proteins and carbohydrate is assumed to proceed with first-order kinetics, while Monod kinetics are assumed for the acidogenesis, acetogenesis and methanogenesis steps. The consumption of propionate and acetate proceeds under substrate inhibition. The model is capable of predicting adequately the COD and fatty acidsdependence on the operating conditions, and should be useful for designing codigestion processes (Lyberatos et al.,1997).All the existing detailed anaerobic digestion models do not take into account the particular nature of the developed granular sludge in high rate systems, such as an Upflow Anaerobic Sludge Bed Reactor (UASBR) or an Anaerobic Baffled Reactor (ABR). Some kind of a general approach was suggested for modelling of a UASB reactor (Kalyuzhnii and Fedorovich, 1997).

Table 2.10: More Complicated Models II

Model	**Limiting step**	**Predicated causes of digesters failure**	**Suitable for the digestion of**
Angelidaki et al. (1993)	Acetogenesis	pH break down	Manure
Siegriest et al. (1993)	Acetogenesis	Rise of NH_3 content of the feed hydraulic load increase	Sludge

Source: Lyberatos and Skiadas (1999)

Table 2.11: More Complicated Models I

Model	Bacterial group (substrate)	Processes	Kinetics (function of)	Accounted inhibition
Angelidaki et al. 1993	(insoluble carbohydrate)	Enzymatic hydrolysis	First order	
	Acidogens (soluble carbohydrate)	Acidogenesis	Monod (temperature, pH)	Total VFA
	Acetogens (propionate and butyrate)	Acetogenesis	Monod (temperature, pH)	Acetate
	Acetoclastic methanogens (acetate)	Methanogenesis	Monod (temperature, pH)	Free NH^3
Siegriest et al. (1993)	(biopolymers)	Hydrolysis	First order (temperature)	
	Acidogens (aminoacids and sugars)	Fermentation of aminoacids and sugars	Monod (temperature)	
	Acetogens (fatty acids)	Anaerobic oxidation of fatty acids	Monod (temperature)	H_2 partial pressure acetate
	Acetogens (propionate)	Anaerobic oxidation of propionate	Monod (temperature)	H_2 partial pressure Acetate
	Acetoclastic methanogens (acetate)	Acetate conversion to methane	Monod (temperature)	pH free NH_3
	Hydrogen-utilizing methanogens (H2 and CO_2)	Hydrogen conversion to methane	Monod (temperature)	pH pH

Source: Lyberatos and Skiadas (1999)

2.5 Anaerobic Treatment of Wastewater

Anaerobic treatment by methanogenesis is widely used for the stabilization of municipal wastewater sludge and municipal solid wastes. This application is gaining popularity in the developing world. Particularly where the climate is warm for most of the year. Anaerobic treatment of sewage is not practiced in the developed world, where other technologies like activated sludges already are in place and effluent standards are strict. The chemistry and microbiology of

anaerobic treatment are, indeed, more complex than for aerobic systems and for this reason the operator of an anaerobic treatment system must have a solid understanding of the factors of importance in operation and control. Anaerobic treatment can offer yet significant advantages over aerobic treatment for industrial organic wastes (Bachmann et. al., 1985). First, the factor of waste BOD_L synthesized into biological solids is much less in anaerobic treatment, as the energy yield from transferring electrons from BOD_L to methane is low. With aerobic treatment, up to half of the waste BOD_L is converted into bacterial cells which represent a significant and costly disposal problem. In anaerobic treatment, only 5 percent of the BOD_L is converted into biological solids, thus reducing this disposal problem considerably. Secondly, synthesis of the biomass requires essential nutrients, such as nitrogen and phosphorus. With some industrial wastewaters, nutrients are in limited supply and must be added. With the smaller biomass production in anaerobic systems, the nutrient requirements are proportionally less. A third major advantage of anaerobic treatment is in the methane gas produced which constitutes a readily available energy source that can be used for heating or to generate electrical power. The energy value of CH_4 is 35.8 kJ/1 at STP. Anaerobic treatment is generally a net producer of energy.

Another advantage of anaerobic treatment is that organic loading per unit reactor volume can be very high compared with aerobic treatment. A typical loading for an anaerobic system may be 5 to 10 kg COD per day per m^3 of reactor volume; whereas it is less than 1 kg COD per day per m^3 for aerobic

systems in which transferring O_2 is a major limitation (Lawrence and McCarty, 1969).

2.5.1 Reactor Configurations for Anaerobic Treatment of Wastewater

Several excellent summaries are available for those wishing an expanded knowledge of the methanogenic processes and their applications. One of the most extensive, with emphasis on industrial wastewater treatment. is a textbook on the subject by Speece (1996). A less extensive, but nevertheless thorough overview of the process with emphasis on municipal sludge treatment is Parkin and Owen (1986). Other valuable summaries include: Jewell (1987), McCarty 1964a, l964b, l964c, 1981), McCarty and Smith (1986), and Speece (1983). Many reactor configurations are used for treatment of municipal and industrial wastewaters or sludges. Several described by Speece (1983) are illustrated in Fig.2.14and discussed here.

2.5.1.1 Completely Mixed Reactor

The completely mixed process represents the basic anaerobic treatment system that has been used for treatment of municipal sludges since the first separate heated anaerobic digester was built in 1927 at the Essen-Rellinghausen plant in Germany Heating of digesters with the methane gas produced to an optimum mesophilic temperature about 35^0C, is used at most municipal wastewater treatment plants, since heat recovery can be done economically and results in the more stable operation.

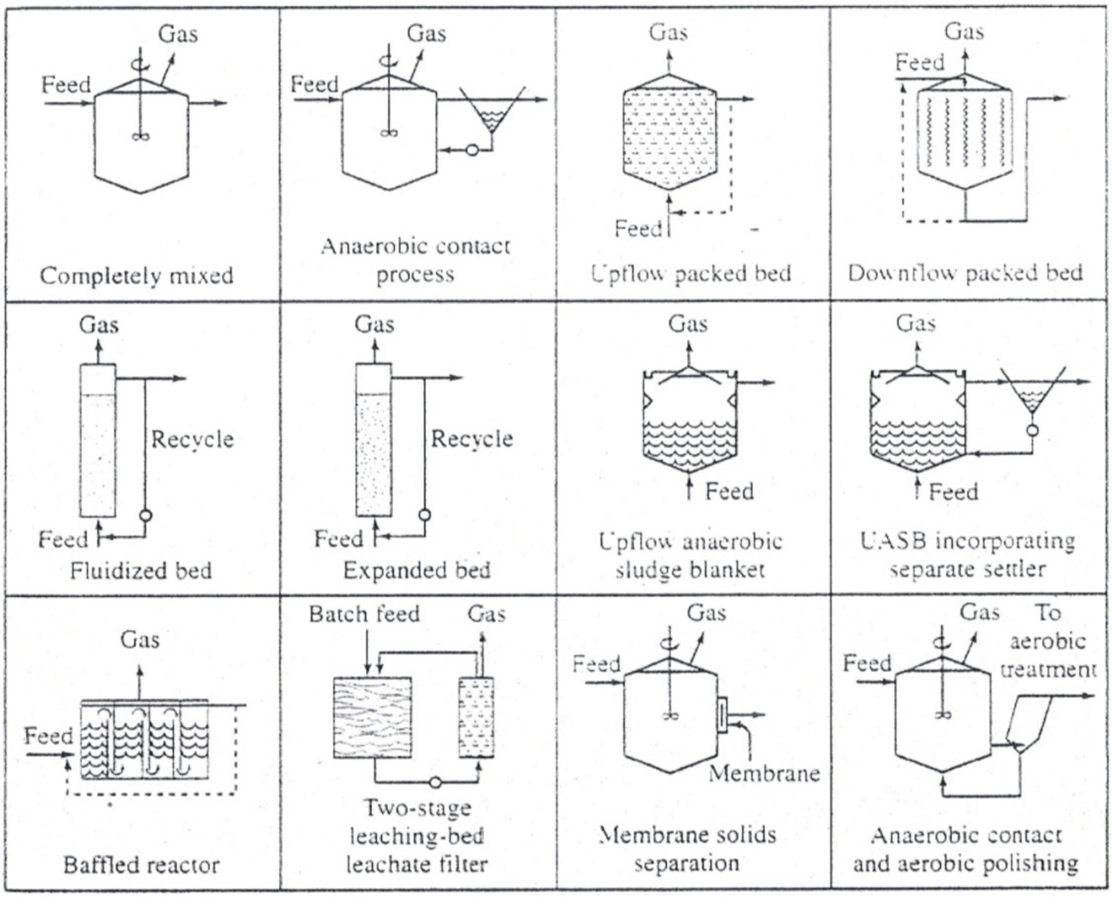

Fig. 2.14: Typical Anaerobic Configuration
Source: Speece (1983)

Municipal primary and secondary sludges entering an anaerobic sludge digester normally have concentrations from 2.5 to 15 percent total solids. According to Parkin and Owen (1986), a detention time of about 20days, the organic loading to a well-mixed digester of the continuous flow strained-tank reactor (CSTR) type is 1 to 4 kg biodegradable COD per day per m^3 of digester volume. (This calculation assumes that 65 percent of the influent suspended solids are volatile and that 50 percent of the volatile solids are biodegradable.) This is a loading comparable to but higher than the volumetric loading achieved in aerobic systems. In addition, the digester produces energy, rather than consuming it. It is easy to see why so many municipal treatment plants employ anaerobic

treatment for waste sludges. A disadvantage of the CSTR for anaerobic treatment is that a high loading per unit volume is obtained only with quite concentrated waste streams similar to municipal sludge, which has a biodegradable COD content of 8,000 to 50,000 mg/1. (Parkins and Owens 1986). However, a great many waste streams are much more dilute. If they were treated in a CSTR with a detention time of 15 to 25 d. the COD loading per unit volume would be very low, reducing or eliminating the cost advantage of anaerobic treatment. The secret to treating such wastes economically is to use reactor systems that separate the detention time of the liquid passing through the reactor from that of the biomass, as is accomplished in the aerobic activated sludge and biofilm systems. In other words, θ_x/θ must be made substantially greater than I (Schroepfer, 1955).

2.5.1.2 Anaerobic Contact Reactor

The anaerobic contact process is an analogy to the aerobic activated sludge system. The first such system was developed and described in 1955 by Schroepfer and his co-workers (Schroepfer et al., 1955) for the treatment of relatively dilute packing house wastes with COD of about 1,300 mg/I. By adding a settling tank and recycle of the biomass back to the reactor, they separated θ_x from θ and achieved a hydraulic detention time of about 0.5 d, which is significantly less than the 4-d of the acetoclastic methanogens. They obtained 91 to 95 percent BOD removals at loading rates of 2 to 2.5 kg/m^3-d.Although the anaerobic contact process has seen many applications, one

recurring problem is a tendency for the biosolids in the settling tank to rise due to bubble generation and attachment in the settling tank. Biosolids loss to the effluent is a more severe problem than in aerobic systems because the quantity of microorganisms produced is so much less; hence, a small biosolids loss can significantly reduce θ_x and adversely affect process stability, as well as effluent quality. This problem is present in all anaerobic treatment systems and has been addressed in different ways. One solution is applying a vacuum to the water passing to the settling tank in order to remove some of the gas supersaturation (Schroepfer, 1955).

2.5.1.3 Upflow and Downflow Bed

The upflow packed bed process, also commonly called the anaerobic filter, was developed through laboratory studies in the late l960s (Young and McCarty, 1969). This system is similar to a trickling filter system in that, originally, a rock medium was used for attaching the biosolids. The anaerobic filter was used for treating soluble substrates with COD from 375 to 12,000 mg/l and had detention times of 4 to 36days. Because of low void volume and specific surface area with rock media most of the subsequent applications used plastic media, just as the aerobic biological towers do today. The anaerobic filter is excellent for the retention of biosolids and has seen wide application. The main concern with this system is clogging by biosolids influent suspended solids, and precipitated minerals.

2.5.1.4 Fluidized and Expanded Beds

The fluidized-bed anaerobic reactor is a unique system that was originally conceived for the removal of nitrate from wastewater through biological denitrificaaon. However, it also is well suited for methanogenic treatment of wastewaters. The fluidized-bed reactor contains small media such as sand or granular activated carbon to which bacteria attach. A relatively high upflow velocity of wastewater causes the biofilm carriers to rise to a point where the carriers' negative buoyancy is just countered by the upward force of friction from the water (Jewel, 1987). Then, the height of the fluidized bed stabilizes. Normally, a portion of the effluent is recycled back to the influent to maintain the high upward velocity, even when wastewater flow rates are low. The high flow rate around the particles creates good mass transfer of dissolved organic matter from the bulk liquid to the particle surface. Bed expansion creates relatively large pore spaces even though the carriers are small. The large pores mean that clogging and short-circuiting of flow through the reactor are much less than in the packed-bed systems. The small carrier size gives a very high specific surface area for biofilm, even when the bed is fluidized to open up the pores. All these features make fluidized beds highly efficient in terms of loading per unit volume.

2.5.1.5 Uplow Anaerobic Sludge Blanket

Lettinga, et al. (1979) developed an important new anaerobic reactor, the upflow anaerobic sludge blanket (UASB), which has had wide application for

the treatment of industrial wastewaters and has been used to some extent for the treatment of relatively dilute municipal wastewaters as well. This system was first described in the late l970s and saw extensive full-scale application in the 1980s. The formation of granules depends upon characteristics of the waste stream, the substrate loading, and operational details such as the upward fluid velocity. Serious problems that occur at times are the formation of granules that float and the lack of granule formation both of which result in loss of biomass from the system. Thus, knowledge of factors affecting granulation is key to successful use of the UASB system. Many UASB systems are being used which a great deal of success on many food- processing industry wastewaters as well as on wastewaters from the paper and chemical industries (Lettinga at al., 1988). Design loading typically is in the range of 4 to 15 kg COD/m^3/d. Because the UASB system at times forms granules or biosolids that do not settle well within the reactor, a separate settler can be provided as a safeguard against excessive loss of biosolids from the reactor.

2.6 Anaerobic Baffled Reactor (ABR)

Increase stringent standards for wastewater discharge drove the demand for more efficient wastewater treatment systems. Over the last decade, anaerobic digestion has proven to be a better alternative than aerobic processes, especially in the treatment of high-strength wastewaters. These high rate reactors amend the principal drawback of anaerobictreatment, which is the long hydraulic retention time (HRT). High-rate reactors separate the HRT from the solid

retention time(SRT) there by allowing the slow growing anaerobic bacteriato remain within the reactor independently of the wastewater flow. The reactor's high SRT keeps the H RT to a minimum which allows higher volumetric load, significantly enhanced removal efficiencies (Skiadas and Lyberatos, 1998).

2.6.1 Background and Theory of ABR

One type of high-rate reactor is the anaerobic baffled reactor (ABR), the ABR is described as a series of upflow anaerobic sludge blanket reactors (UASBS) because it is divided into several compartments. A typical ABR consists of a series of vertical baffles that direct the wastewater under and over the baffles as it passes from the inlet to the outlet. The over and under flow of the liquid reduce bacteria washout, which enable the ABR to retain active biological mass without the use of any fixed media. The bacteria within the reactor tend to rise and settle with gas production in each compartment, but they move down the reactor horizontally at a relatively slow rate, giving rise to a SRT of 100 days at a HRT of 20 hours. The slow horizontal movement allows wastewater to come into intimate contact with the active biomass as it passes through the ABR with short HRT(6-20) hours. Anaerobic digestion that takes place in an ABR consists of different groups of organisms. The first group of organisms is the hydrolytic fermentative (acidogenic) bacteria that hydrolyze the complex polymer substrate to organic ads, alcohols, sugars, hydrogen, and carbon dioxide. The second group is hydrogen producing and acetogenic organisms that convert fermentation products of the previous step (hydrolysis and acidogenesis) into

acetate and carbon dioxide. The third group is the methanogens that convert simple compounds such as acetic acid, methanol, and carbon dioxide and hydrogen into methane. The four main steps that usually determine the organisms' reaction in an anaerobic process are: hydrolysis, acidogenesis, acetogenesis, and methanogenesis. Fig. 2.15 is a schematic showing the conversion reaction in the anerobic digestion.

Although not commonly developed on a large scale, the ABR has several advantages over other well established systems. These advantages are summarized in Table 2.12. Due to the many advantages of the ABR, the reactor had been researched and applied in different low strength waste waters of chemical oxygen demand (COD) < 1000 mg/l.

Probably the most significant advantage of the ABR is its ability to separate acidogenesis and methanogenesis longitudinally down the reactor, which allow different bacterial groups to develop under the most favorable conditions. This specific advantage also allows there actor to behave as a two-phase system without the associated high cost and control problems. Two-phase operation permits acidogenesis to dominate in the first compartment and methanogenesis to dominate in the subsequent section.

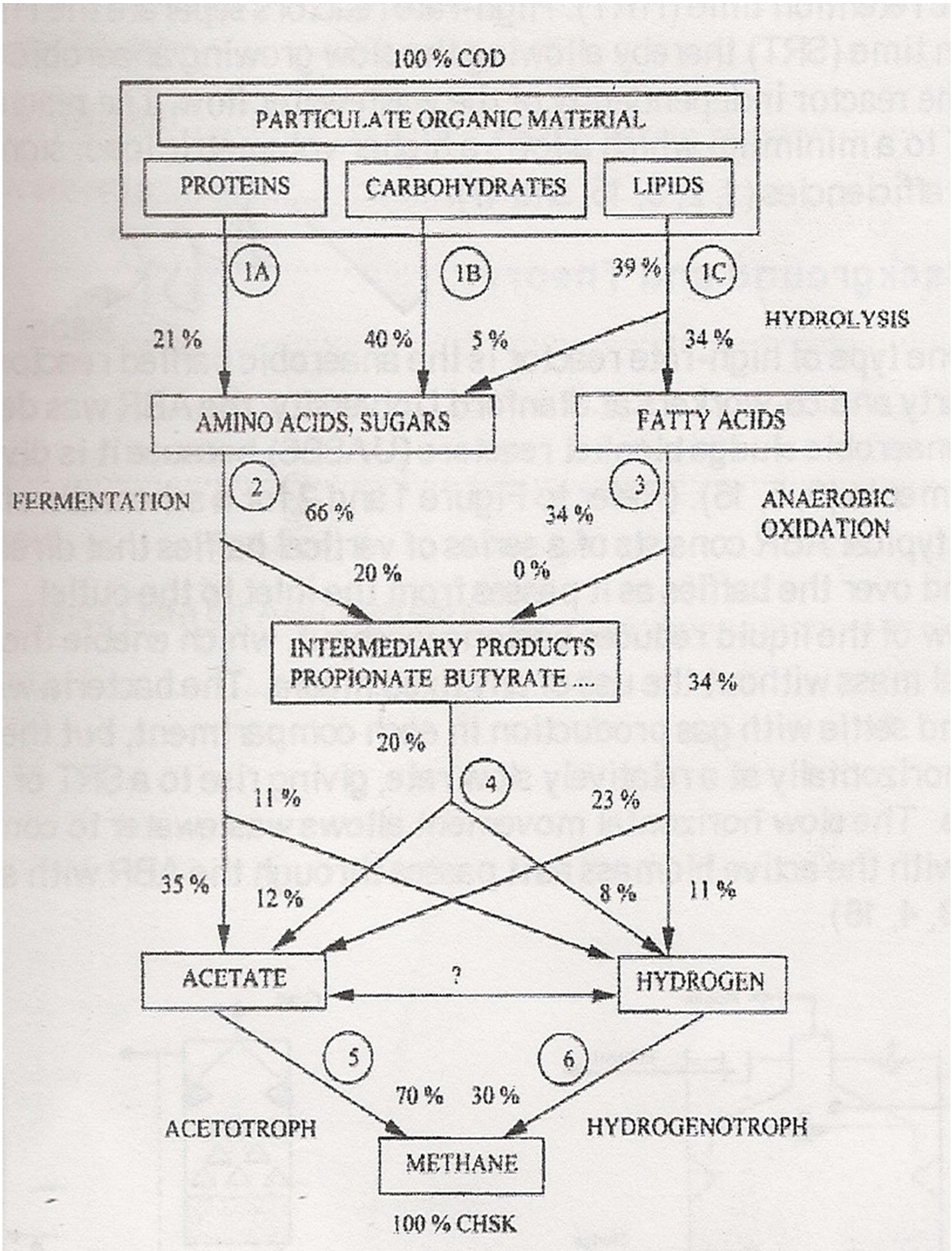

Fig. 2.15: Conversion Reaction in the Anaerobic Baffled Reactor

Source: McCarty (1975)

Table 2.12: Advantages Associated with the ABR

i.	**Simple design**	**No requirement for biomass with unusual settling properties**	**Low hydraulic retention times (HRT)**
ii.	**No moving parts**	**Low sludge generation**	**Intermitten operation possible**
iii.	**No mechanical mixing**	**High solids retention times (SRT)**	**Extremely stable to hydraulic shock loads**
iv.	**inexpensive to construct**	**Retention of biomass without fixed media or a solid settling chamber**	**Protection from toxic materials in influent**
v.	**High- void vo1ume**	**No special gas or sludge separation required**	**Long operation times without sludge wasting**
vi.	**Reduced dogging**		**High stability to organic shocks**
vii.	**Reduced sludge bed expansion**		
viii.	**Low capital and operating costs**		

Source:Barber and Stuckey (1999)

This can increase acidogenic end methanogenic activity by a factor of four because the separation of the two phasescausesan increase in protection against toxic materials and higher resistance to-changes in environmental parameters (i.e. pH, temperature, and organic loading rates)(Barber and Stuckey,1999).

2.6.2 Development and Application of ABR

Since the original design of ABR was developed for wastewater treatment, many modifications have been made in reactor design in order to enhance both the efficiency and reliability of the reactor. The treatment efficiency of ABR was closely related to the solids retention capacity.

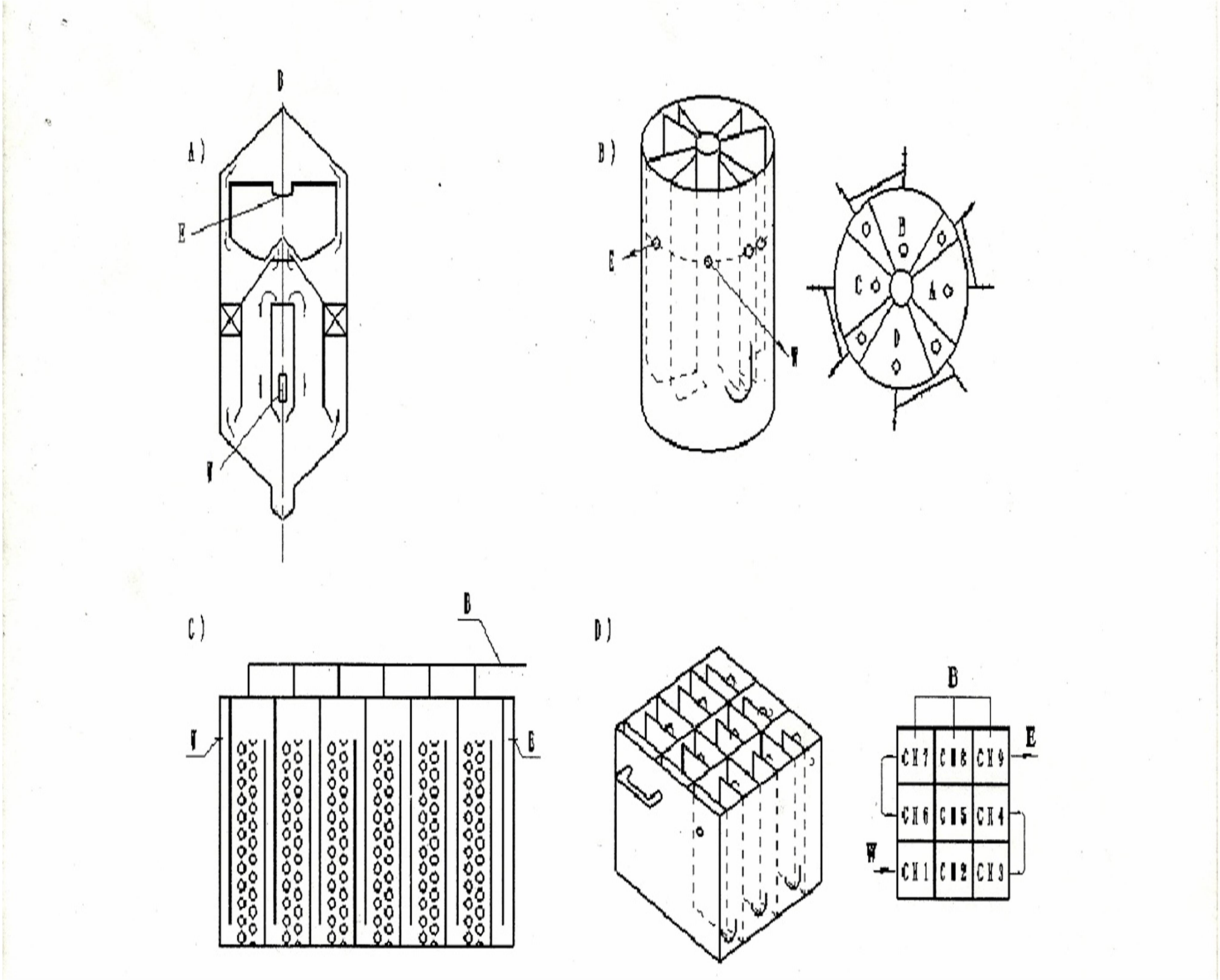

B-Biogas, W= wastewater; E = Effluent

Fig. 2.16 Different Types of the ABR

Source: Barber and Stuckey (1999)

Many researches have been conducted into modifications to the configuration of ABR in order to enhance the solids retention capacity, treat refractory wastewater and reduce capital costs. A summary of the main alterations was well documented by Barber and Stuckey (1999).In 1993, vertical baffled anaerobic sludge bed as a baffled reactor was used to treat wastewater distillers, the structure is shown in Fig. 2.16A. It combined the function of anaerobic contactor reactor, anaerobic filter and UASB simultaneously (Li et al., 2001).

The latest modification of ABR is periodic anaerobic baffled reactor (PABR) developed in 1998. The structure is shown in Fig. 2.16B. The main advantage of PABR is its random operation: different operation periods were chosen to get optimum treatment efficiency under favorable working conditions according to the influent concentration and quantity (Skiadas and Lyberatos, 1998).In order to avoid or at least decrease clogging and sludge washout of biomass in attached form, enhance the bacterial activity together with better mixing to ensure high-rate contact between the cells and their substrate (Faisal and Unno, 2001), the carrier anaerobic baffled reactor (CABR) was developed to treat sewage at 28 ± 1 °C. It combines the advantages of ABR with the characteristics of biofilm reactor and is a suitable technology for decentralized domestic sewage treatment for rural areas of China (Feng et al., 2008). The structure is shown in Fig. 2.16C.A study has focused on basic configuration modification of ABR to obtain improved treatment efficiency. A nine- chambered modified anaerobic baffled reactor (MABR) was developed to evaluate its suitability for the treatment of municipal wastewater and to establish the understanding of the relationship between reactor design and operational parameters. A long-term operation (375 d) of MABR indicated that the reactor configuration can be exploited for treatment of dilute wastewaters such as municipal wastewater at lower HRT of 0.25 d. The MABR can be useful as an onsite compact wastewater treatment plant for individual houses or small colonies in Indian climatic conditions (Bodkhe, 2009). The structure is shown in Fig. 2.16D.The

performance of the ABR while treating a variety of wastewaters has been well reviewed in the literature (Barber and Stuckey, 1999). In recent years, application of ABR for treatment of wastewater has received considerable attention. The ABR can be used to treat various wastewaters, in particular, low and high strength wastewater and other refractory wastewaters.

2.6.3 Performance and Characteristics of ABR

2.6.3.1 Reactor Hydrodynamics

The hydrodynamics and occurrence of mixing within an ABR strongly influence the extent of contact between substrate and bacteria, thus affecting the whole reactor's treatment efficiency. Previous studies indicated that the ABR has low levels of dead space in comparison with other anaerobic designs. Dead space consists of both hydraulic and biological dead spaces. Hydraulic dead space is a function of the flow rate and the number of compartments in the reactor and the biological dead space is a function of the biomass concentration and activity. An increase in the (hydraulic) dead space was expected with a decrease in HRT while creating less (biological) dead space. However, no direct correlation between hydraulic dead space and HRTs could be drawn.In the last decade, several studies have focused on residence time distribution (RTD) of ABR. Using the calculated dispersion numbers in the ABR, it can be concluded that the intermediate was between plug-flow and perfectly mixed (Langenhoff and Stuckey, 2000); It was also indicated that the intermediate was closer to plug flow than completely mixed flow (Krishna et al., 2008, Kong and Wu,

2008). RTD studies were carried out at different temperatures to determine whether the rate of gas production and viscosity affected the hydrodynamics of the ABR. The results indicated that the volume of dead space was relatively constant at the temperatures used, even though less gas was produced at low temperature due to the lower COD removal (Langenhoff and Stuckey, 2000).By splitting the feed for ABR, the flow pattern changed corresponding to a higher degree of mixing within the reactor. The mixing pattern produced by the proper ratio was considered to represent an appropriate intermediate between plug-flow and completely mixed reactors (Sallis and Uyanik, 2003).Liu et al. (2007) studied hydrodynamic characteristics of a four-compartment PABR. The results showed that the dead space in PABR was similar to that in ABR. The flow patterns within the PABRs were intermediate between plug-flow and perfectly mixed under all conditions tested (Liu et al., 2007). RTD studies of ABR for treatment of low-strength soluble wastewater were carried out at 8 and 10 h HRTs. The results showed that the volume of dead space decreases with decreasing HRT. This conclusion seemed contradictory to others as this might be due to biological dead space established as the major contributor to overall dead space, the variation of HRT had no significant effect on hydraulic dead space (Krishna et al., 2007).

2.6.3.2 Effluent Recycles in ABR

The advantages and disadvantages of effluent recycle have been well summarized in the literature and will not be discussed here. However, with plug

flow characteristics, high substrate loading in the front part of the reactor can leading to the accumulation of volatile fatty acid (VFA) and a concomitant decrease in pH, affecting its efficiencies in pollutant removals. High strength wastewater is more likely to expose sensitive bacteria in front compartments to toxic levels of inorganic and organic compounds (Baloch et al., 2007; Yu et al., 2002). To lessen such negative effects, dilution of incoming wastewater can be accomplished by effluent recycle (Kennedy and Barriault, 2005). Additionally, the addition of a recycle stream could also alleviate the problem of low pH caused by high levels of VFA at the front part of the ABR reactor (Baloch et al., 2007). Also, the organic removal performances have been improved by the effluent recycling. When the effluent recycle was applied to treat high sulfate wastewater in ABR, the effect was opposite. In effluent recycle, its positive effects as mentioned by other works were not realized; instead it caused a reduction in organic removal and methane yield. Operation at longer HRT and lower effluent recycle ratios could generate the biogas with higher methane content and yield. Effluent recycle also provided an additional alkalinity for a pH control purpose and toxicity (Saritpongteeraka andChaiprapat, 2008). A modified anaerobic baffled bioreactor (MABR) was studied under steady-state conditions for treating palm oil mill wastewater. The stability was achieved by the recycling of 30 times feed flow rate. By recycling the effluent to the influent, the alkalinity in the effluent was recovered (Faisal and Unno, 2001).Therefore, it was found that the overall effects of recycle are unclear. In

practice, the ultimate use of recycle will depend on the type of wastewaters. The effluent recycle will be beneficial if pH problems are severe. The influent with high levels of toxic material, or high loading rates are preferred. The application of effluent recycling should be cautious and only when absolutely necessary.

2.7 Types of Models

A model is a mathematical representation of a physical process, and it attempts to capture the relationship between the inputs and outputs for the system under study. In general, models do not fall into distinct categories but here exists a continuum for models, varying from fundamentally derived models based on process physics, to purely empirical models developed from input-output data.

2.7.1 Fundamental Models

Fundamental models, (also called first-principle models) are based on the underlying physics occurring in the system and are generally preferred model structure for developing process representations for model based control systems. These models are developed by applying mass and energy balances over the components or states and may also include a fluid description of the fluid flow and transport processes that occur in the system (Marquardt, 1995). A number of fundamental models have been developed to model processes ranging from a single cell (Jeong et al.,1990; Domach et al., 1984; Steinmeyer and Shuler, 1989), to a complex two phase pulp digester (Wisnewski et al.,1997). Fundamental models offer several potential benefits. Since they include details about the physics of the system, they can better represent the

nonlinear behavior and system dynamics; this allows the model to be used beyond the operating range in which the model was constructed. Another benefit of utilizing the first-principles approach is that the states are generally physical variables such as temperature or concentrations of the system components that can be measured. However, these models are time consuming to develop and they often have a high state dimension. The involved mathematical description may result in a model with a large number of equations with many parameters that need to be estimated. Many of these parameters can be obtained experimentally or from previous reported data available in literature. In some cases, regression analysis is used or adjustable parameters are employed to adequately represent the system behavior. The considerable effort required in order to develop a first-principle model often leads to the utilization of a simpler model structure for control applications.

2.7.2 Empirical Models

In many cases, the actual system may be complex and the underlying phenomena are not well enough understood to develop a first-principle model. Empirical models are useful in this scenario and actual plant data are used to capture the relationship between the process inputs and process outputs using a mathematical framework such as Artificial Neural Networks (ANN), polynomial models such as Aoyama et al. (1995), Agrawal et al. (1989) and Parker and Doyle III (2001). The parameters describing the model are then identified by a regression analysis of the process data (Maner and Doyle III,

1997). As an example of the empirical modeling framework, Parker and Doyle III (2001), utilized a second order Volterra series model framework to capture the dynamic behavior exhibited by continuous cultures of *Klesbsiella pneumonia*. Although the time requirement to obtain these models is often significantly reduced, these models generally can be used with confidence only for the operating range in which they are constructed. Since these models do not account for the underlying physics, practical insight into the problem may be lost as a physical variable of the system such as temperature and concentration are generally not the states of the empirical model (Ljung, 1987).

2.7.3 Mixed Models

Mixed models are developed, as the name suggests, by combining the fundamental and empirical models, thus utilizing the benefits of both. As an example, mixed models have been used to model polymerization reactors in which the known mass balances for the reactants are modeled using fundamental models, whereas, the unknown rates of the reactions taking place are modeled using empirical models (Tholudor and Ramirez, 1996; De Azevedo et al.,1997). In some cases, mixed models have also been used to determine time-varying parameters that model the nonlinear process behavior. Another approach as suggested by Henson (1998) is to use a fundamental model to capture the key process dynamics and then utilize an empirical model to capture the modeling error between the model and the actual plant.

2.8 Classification of Biological Models

In the literature, biological models have been classified based on the level of detail in the description of the cell and its intra-cellular processes. Considering biomass, Tsuchiya et al.(1996) described the model as segregated if all cells are treated differently, i.e., they may be in different stages of growth. If the cells are all treated alike then the model is a non-segregated model. Further, if the intra-cellular processes are explicitly accounted for the model is a structured model, whereas if the model relies only on lumped cellular input-output behavior it is an unstructured model. A compact representation is presented in Table 2.13.

Table 2.13: Classification of Biological Growth Models

MODELS	Unstructured	Structured
Unsegregated	**Cells indistinguishable; lumped metabolic and physiological processes**	**Cells indistinguishable; *distinct physiological and metabolic processes***
Segregated	**Cells may be in different states of growth. Lumped metabolic and physiological processes**	**Cells may be in different states *distinct physiological and metabolic processes***

Source : Tsuchiya et al.(1996)

2.8.1 Unstructured Biological Models

Unstructured models are the simplest of all modeling philosophies used to describe the biological model. They consider the cell mass as a single chemical species and do not consider any intracellular reactions occurring within the cell. Unstructured models typically describe the growth phenomena based on a single limiting substrate and consider only substrate uptake, biomass growth, and

product formation in the modeling framework. Thus the biological component of the system depends directly on the macroscopic reactor variables. These models give an adequate representation of the biological growth phenomena in relative simple cases, when the cell response time to environmental changes is either negligibly small or much longer than the batch time (Bailey and Ollis,1986). The most commonly used unstructured model in the literature is the Monod model (Monod, 1949) and it is one of the earliest attempts at modeling biological systems. In this model the growth kinetics are expressed in terms of the specific growth rate, μ. The Monod model is used to express growth based on a single limiting substrate, $\boldsymbol{S}$ and can qualitatively describe growth phenomena for relatively simple systems. A drawback of this model is that it does not capture the initial growth which is observed in most batch cultures and also fails to capture the sequential consumption of glucose and ethanol as multiple substrates, as observed in cultures of *Saccharomyces cerevisiae.* There are variants to the Monod model that have also been used, such as the models by Karl-Heinz Bellgardt (2000).These models differ in their substrate dependence and some include terms to account for saturation due to high substrate concentration and inhibition due to product or a competing inhibitor. However, these models do not differ significantly from the Monod model in the fact that they are empirical and represent all of the cellular processes with just a single equation for the specific rate. As an example, Yang and Humphrey (1975) showed that for yeast cultures with phenol as the limiting substrate, five

different equations with inhibition terms represented the data equally well. Monod type models are a helpful tool for a preliminary analysis of the system, but they fail in more complex cases owing to the simplified description of the cell's biochemical machinery.

2.8.2 Structured Biological Models

In contrast to the unstructured models, structured models include a greater level of detail about the biochemical phenomena occurring within the cell. The biological detail is no longer lumped into a single biomass variable. In structured models, the biomass is structured into several components or functional groups that are interconnected with each other and with the macroscopic reactor environment by material balances. The functional groups that represent the biomass can themselves vary based on the level of detail included in their description. Theses functional groups could be reaction networks including details about known intracellular reactions, as is employed in the single cell models(Marquardt, 1995; Jeong et al.,1990; Domach et al.,1984) or they could have a lumped representation of the actual detailed networks as in case of two-compartment model of Williams (1967).

Single cell models have been successful in describing cellular events in a mathematical format. Generally, these models have been developed with a specific purpose. Jeong et al.(1990)have captured the lag phases of growth for *Bacilus Subtilis*and have included a detailed representation of various metabolic pathways in the cell, most notably, purine metabolism. This is a good model

structure for understanding cellular regulation and also gives valuable insight into the mechaniosm by which sporulations occurs. Similarly, the model by Domach et al. (1984) can predict changes in the cell size, cell shape and the time at which chromosome synthesis initiates as a function of the limiting external glucose concentration for Escherichia coli. In an extension of this work, Peretti and Bailey (1985) formulated a model that can describe the kinetics and control of transcription and translation. Steinmeyer and Shuler (1989) also utilized a single cell model to capture the dynamic growth behavior of yeast cultures in batch mode. This model structures the biomass into twelve distinct pools and has over a hundred parameters. Determination of these parameters is not a trivial task and although many of these parameters can be obtained experimentally, there also exists an element of empiricism in the choice of the parameter value.

2.8.3 Segregated Biological Models

Segregated models take into account the fact that a culture can have cells in different stages of growth, and they account for these stages using population balances. These models can be broadly grouped into two main types, age structured or mass structured. If the intracellular chemical structure is described in terms of a mass conversation then the population balance is mass-structured, whereas if age is used to differentiate cells in a population, then the model is referred to as an age structured model. Mantzaris et al. (2002)utilized a mass structured segregated model in a continuous bioreactor. Cell cycle is assumed to

occur in two stages and the product formation is considered only in the second stage of the cell cycle. Substrate concentration is used as the manipulated input to control the productivity of a described product. A mass structure cell population balance model has also been used by Zamamiri et al.(2002)to capture the experimentally observed oscillatory dynamics exhibited by continuous cultures of yeast, using unstructured biological model. The key variable that characterize the cell cycle is the critical cell mass m_c . Cells with a mass greater than m_c *are*mother cells whereas those with a mass lower are known as daughter cells. The origin of the cell cycle known "Start" is the point when the cell attains the critical mass m_c . Bud formation takes place once the cell has grown for a particular time and the budding cells continue to grow until the cell division stage is reached. At this division stage, the bud separates forming a new daughter cell of smaller mass than the mother cell which is returned to the "Start" point and has its age set to zero. Daughter cells become mother cells once they reach m_c and continue their growth until the budding stage is reached at which point they become mother cells.

With the use of population balances for model formulation, segregated models can no longer be described by ordinary differential equations. The constitutive equations are now described by partial differential equations in age-structured and integral-partial differential equations in mass structured segregated models. In most cases analytical solutions of these equations are difficult to obtain and solution has to be accomplished numerically. This makes the computations

associated with these models significantly more challenging. Additionally, identifying and mathematically expressing the intrinsic physiological state functions such as growth rates, the stage-to-stage transition rates, that are parameters in these models is itself a difficult exercise.

2.8.4 Material Balance Biological Models

Wang and Cooney(1977) have reported the control of bioreactors using a model based on material balances. They treat the biomass as a compound with a fixed elemental composition consisting of Carbon, Hydrogen, Oxygen, and Nitrogen. Based on a stoichiometric balance of these elements and the uptake and evolution of Oxygen and Carbon Dioxide gases, the state of the fermenter is obtained. This state information is somehow related to the physiological state of the growing cells and its relationship is usually determined empirically. Material balance models, (also known as stoichiometric models) were very popular in the 1970s and 1980s when computational resources were expensive and sensor technology was not well developed. However, these models do not account for the biomass as an actual living species and are thus only a chemical approximation to the biology. Although these models have been successfully used, they suffer from most of the disadvantages of empirical and unstructured models.

CHAPTER THREE
MATERIALS AND METHODS

3.1 Materials

The study makes use of anaerobic baffled reactor ABR in the treatment of cassava wastewater, i.e. starch wastewater, organic loading of COD and hydraulic was used; process of experimental set-up, wastewater characteristics, analysis of mathematical regression model was done and program was written using Microsoft Visual Basic.

3.1.1 The Reactor

The laboratory scale ABR was constructed from 6mm thick stainless steel, with external dimensions of lengths, widths, depths and working volumes. Fig. 3.1 shows a schematic diagram of the reactor. The reactors were divided into different number of equal compartments by vertical baffles with each compartment of each the reactors having downcomer and riser regions created by a further vertical baffle. For each of the reactors, the widths of upcomers were multiples of the widths of downcomer. The lower parts of the downcomer baffles were angled at 45^0 in order to direct the flow evenly through the upcomer. This produced effective mixing and contact between the wastewater and anaerobic sludge at the base of each riser. Each compartment was equipped with sampling ports that allowed biological solids and liquid samples to be withdrawn. The operating temperature was maintained constant at 35 ± 0.5°C by putting the reactor in a water bath equipped with a temperature regulator. The

influent feed was pumped using variable speed peristaltic pump. The outlet was connected to a glass U-tube for level control and to trap solids.

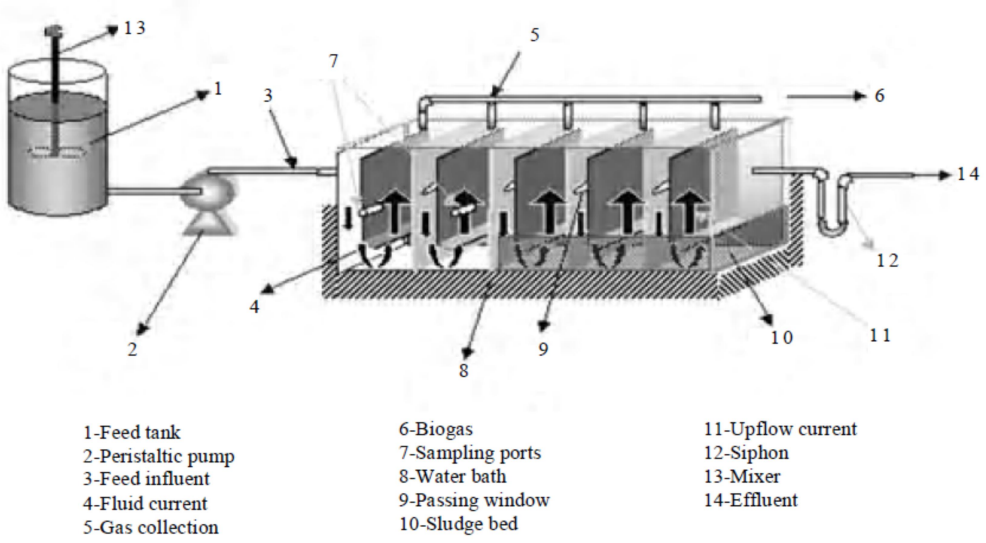

Fig. 3.1: 3-D View of the Anaerobic Baffled Reactor

Source: Draaijer et al., (1992)

3.1.2 Start-up of ABR

Start-up without seed sludge was rather difficult and time consuming for suspended growth anaerobic reactors. The following 3 steps were taken: (i) the reactor was filled with cassava wastewater and allowed to rest for 15 days (ii) the sludge bed was allowed through a process of sludge accumulation by settling and sludge improvement and (iii) after 15 days, feeding of the wastewater was resumed at a flow rate of 5.33litres per day and HRT of 6days with a very low organic loading rate (OLR) of 0.067kgCOD/m^3.day. The resumed wastewater feeding helped the development of sludge bed at the bottom of individual chambers of the ABR. This process of feeding the system followed by two weeks rest is based on the experiment made in Kanpur (India)

for the start-up of a UASB plant without inoculum (Draaijer et al., 1992). The reactor exhibited S-shaped acclimatization curve with three distinct phases during the acclimatization period. During phase I of acclimatization period of 25 d (l6th-40th day), the observed SS and COD removal may be attributed to the interception of organics in the sludge bed. During second phase of 30 d (41st-70th day), a significant gain of up to 90% was observed in COD removal. The steady state of increase in efficiency signified the adequate quantum of biosludge accumulation in the reactor (Hutnan et al., 1999). Third phase of acclimatization lasted for 20 day (7lst – 90th day). Last five consecutive observations revealed consistent COD removal efficiency of 97%. At this stage the reactor was reckoned as matured or acclimatized. Hence, start-up period for ABR without inoculum was adjudged to be 90 days. Lettinga et al. (1993) took 84 days for the start-up whereas, Kalogo et al. (2001) required a period of 140days of self-inoculated UASB. A full scale UASB plant needed 70days for start-up without inoculation (Draaijer et al., 1992). The anaerobic contact filter was started-up by feeding cow dung slurry and sewage sludge by Vijayaraghavan and Ramanujan (1999) and observed 160days to complete the start-up operation. The analysis of requirements of start-up periods without inoculation showed that the time consumed by the ABR for self inoculation was favorably comparable.

3.1.3 Process of Obtaining Cassava Wastewater

The cassava wastewater from a cassava processing factory at Imo Polytechnic Umuagwo in eastern Nigeria was used as feed. The supernatant of the

wastewater after the simple gravity settling, used in the investigation, had low TSS that was approximately 90% of the solids removed. The supernatant wastewater was diluted to achieve the COD concentration required for each loading rate with water. In order to achieve pH and alkalinity adjustment, the supernatant was neutralized by NaOH and $NaHCO_3$. A COD:N:P ratio of 300:5: 1 was kept during operation using NH_4C1 and K_2HPO_4. The micro-nutrient deficiency was added occasionally to correct growth conditions according to Angenent et al. (2002).

3.2 Methods

3.2.1 Procedure for Experiment-1: Cassava Wastewater Treatment without Inhibition

The wastewater was collected twice a day from the cassava processing plant, and it was intermittently mixed to feed the reactor with a consistent quality. The wastewater came from processing cassava specie (bogot) that had no cyanide content. The wastewater was fed to the reactor with the help of a variable speed peristaltic pump. The ABR was operated at various hydraulic retention times (HRTs) by varying the flow rate of influent wastewater (Q_{inf}), thereby varying the organic loading rate (OLR). The wastewater flowed from the downcomer to the upcomer within an individual chamber through the sludge bed formed at the bottom of the individual chambers. After receiving treatment in the particular chamber, wastewater entered the next chamber from the top. Due to the specific design and .positioning of the baffle, the wastewater is evenly distributed in the

upcomer and the vertical upflow velocity (V_{up}) could be significantly reduced. The treated effluent was collected from the outlet of the 3rdcompartment (C3). The reactor was kept in a temperature controlled chamber maintained at 35 ^{O}C.

Plate 3.1: Photo of the ReactorSystem and Researcher in the Laboratory at Imo Polytechnic, Umuagwo, Nigeria.

3.2.2Evaluation of Kinetic Coefficients without Inhibition

3.2.3 Monod Model for ABR

The Monod model is described as

$$r_A = \frac{ds}{dt} = \frac{Q}{V}(S_i - S_e) = \mu.X \qquad (3.1)$$

$$= \frac{\mu_{max} S_e}{K_s + S_e} X$$

$$\frac{XV}{Q(S_i - S_e)} = \frac{K_s}{\mu_{max}} \frac{1}{S_e} + \frac{1}{\mu_{max}} \qquad (3.2)$$

$XV/(S_i\text{-}S_e)$ is plotted against $1/S_e$ in equation (3.2)

3.3Procedure for Experiment-2: Cassava Wastewater Treatment with Inhibition

After the start-up stage has been completed; the steady-state operation was conducted. The ABR (reactor 2) was operated at various cyanide concentrations by using influent wastewater from different cassava species as listed in Table 3.2.The steady-state performance was evaluated under hydraulic retention time of 3 to 10 days. (Organic loading rate of 1.60 to 5.33 g-COD (l day). At any given loading rate, the bioreactor was continuously operated until steady-state condition is achieved, when effluent COD, VSS and gas production rate in bioreactor become constant. Then samples were collected and subjected to the analysis of the following parameters, i.e., influent and effluent COD, total alkalinity: total volatile fatty acid, suspended solids and volatile suspended solids, reactor pH, according to standard methods (APHA, 1998).

Plate 3.2: Experimental Set-up

3.3.1Evaluation of Kinetic Coefficients with Inhibition

Monod kinetics with substrate inhibition are assumed (Andrews, 1968), i.e.

$$\mu_g = \frac{\mu_{max}}{1 + \frac{K_s}{S_e} + \frac{I}{K_i}} \tag{3.3}$$

Substituting Equation 3.3 into Equation 3.2, by replacing μand μ_g gives

$$\frac{ds}{dt} = \frac{Q}{V}(S_i - S_e) = x.\mu \tag{3.4}$$

$$\frac{Q}{V}(S_i - S_e) = x\left[\frac{\mu_{max}}{1 + \frac{K_s}{S_e} + \frac{I}{K_i}}\right] \tag{3.5}$$

Expanding Equation 3.5, gives

$$\frac{Q}{V}(S_i - S_e) = \frac{x\mu_{max}}{1 + \frac{K_s}{S_e} + \frac{I}{K_i}} \tag{3.6}$$

Taking inverse of both sides of the Equation 3.6, results in;

$$\frac{1}{\frac{Q}{V}(S_i - S_e)} = \left[\frac{x\mu_{max}}{1 + \frac{K_s}{S_e} + \frac{I}{K_i}}\right]^{-1} \tag{3.7}$$

Simplifying Equation 3.7 gives

$$\frac{V}{Q(S_i - S_e)} = \frac{1 + \frac{K_s}{S_e} + \frac{I}{K_i}}{x\mu_{max}} \tag{3.8}$$

Multiplying both side of Equation 3.8 by x and taking the inverse of both sides results in

$$\frac{xV}{Q(S_i - S_e)} = \frac{1 + \frac{K_s}{S_e} + \frac{I}{K_i}}{\mu_{max}} \qquad (3.9)$$

Simplifying Equation 3.9 further results in

$$\frac{xV}{Q(S_i - S_e)} = \frac{1}{\mu_{max}} + \frac{K_s}{\mu_{max}} . \frac{1}{S_e} + \frac{1}{\mu_{max} K_i}(I) \equiv y = c + mx \qquad (3.10)$$

$$where, \qquad y = \frac{xV}{Q(S_i - S_e)} = plot\ on\ y - axis$$

$$x = I = plot\ on\ x\ axis$$

$$m = \frac{1}{\mu_{max} K_i} = slope$$

$$c = \frac{1}{\mu_{max}} + \frac{K_s}{\mu_{max}} . \frac{1}{S_e} = intercept$$

3.4Procedures for Wastewater Characterization

3.4.1 Measurement of pH

The pH of all wastewater samples was measured at the time of collection by using portable battery operated pH meter model MP220. The calibration was carried out with two standard butter solution of pH 4.0 and 7.0. The pH of the samples should lie between these values. The sample temperature is determined at the same time. The reading is taken after the indicated value remains constant

for about 1 min. After each measurement, the electrode of the pH meter was washed with distilled water and was cleaned with tissue paper.

3.4.2 Test for Cyanide

1t is carried out to determine the Cyanogenic glucosides level in cassava, garri, cassava wastewater or any other plant extract as the case might be. It can also be carried out to evaluate the effect of various processing methods on the concentration of free cyanide. The hydrogen cyanide released during the hydrolysis of cyanogenic glucoside is a poisonous substance. It has a boiling point of 25.7°C and gaseous at room temperature. The main apparatus used for the determination of free cyanide concentration in cassava wastewater or garri extract was expandable ion analyser or ion-selective Electrode (EA920). Others included a cyanide electrode, reference electrode and beakers. The procedure involved the preparation of two standards that differ in concentration by a factor of ten. However, the standards were selected in such a way that the cyanide concentration in the samples for analysis, 1ppm and 100ppm were used. The electrodes were then immersed in the first standard and the concentration was entered into the memory of the Dogtem. The electrodes were later immersed in the second standard of 100ppm and the concentration was equally entered into memory of the system. The electrode was immersed into each of the samples and when the ion-analyzer had the word “READY or four points on the screen, the concentration of the sample was read. The cyanide concentration obtained were given in parts per million (ppm).

3.4.3 Determination of Total Solids

These are the solids present in the sample of the wastewater solution. They were determined by evaporating a known volume of unfiltered solution at a temperature of 105^{o}C in the oven.

Materials**:**

Porcelain dish (100 ml), steam bath, drying oven, muffle furnace, desiccator, Goochcrucible, analytical balance, glass fiber filter disk, filtration apparatus, pipettes, measuring cylinders.

Procedure**:**

1. Ignite a clean evaporating dish at 550^{0}C in a muffle furnace for 1 hr.
2. Cool the dish, weigh and keep it in a desiccator.
3. Transfer carefully 50 ml of sample into the dish and evaporate to dryness on asteam bath.
4. Place the evaporated sample in an oven adjusted at 1030C and dry it for 1 hr.
5. Repeat drying at 103^{0}C till constant weight is obtained.
6. Determine the total solids with the following formula:

mg/l total solids = ((A-B) * 106) / ml sample, where

A = weight of residue + dish

B = weight of dish

3.4.4 Determination of Dissolved Solids

These are all solids present in the sample solution filtered through 1.2µm filter. They were determined by evaporating a known volume of filtrate sample at a temperature of 105^{o}C in the oven.

1. Mg/l total dissolved solids = total solids – total suspended solids

3.4.5 Determination of Suspended Solids

These are all solids present in the sample that remain on 1.2µm filter. They were determined by filtering a known volume of sample and placing the filter and filter container at a temperature of 105^{o}C in the oven for 24 hours to evaporate the water.

Procedure

1. Place a filter disk on the bottom of a clean Gooch crucible.
2. Pour 20 ml distilled water and apply vacuum. Repeat the process two more times.
3. Remove crucible to an oven and dry it for 1 hr at 1030C.
4. After drying, the crucible is kept in a desiccator.
5. Weigh the crucible and place it on a suction unit.
6. Pour 25 ml of sample. Wash pipette with distilled water and pour the washingalso into the crucible.
7. After filtration, dry the crucible at 1030C for 1 hr
8. Weigh till constant weight is obtained.

9. Determine the total suspended solids with the following formula:

$$\text{Mg/l total suspended solids} = ((\text{A-B}) * 10^6) / \text{ml sample}$$

where: A = weight of residue and crucible

B = weight of crucible

Or

Total Suspended Solids, mg/L = $(B-A)(1000mg/g)/samplevolume,L$

where A = weight of filter (dried at 103°C) + aluminum boat, g

B = weight of filter + aluminum boat + residue (dried at 103°C), g

C = weight of aluminum boat + filter and residue (combusted at 500°C), g

Also, calculate the percentage of TVSS relative to TSS in the activated sludge.

Compare to the range of typical reported values: 80% - 90%.

3.4.6 Determination of Fixed Solids

These are all solids that remain after firing a sample in 550°C muffle furnace.

Total Fixed Suspended Solids, mg/L = $(C-A)(1000mgg)/samplevolume,L$

where A = weight of filter (dried at 103°C) + aluminum boat, g

B = weight of filter + aluminum boat + residue (dried at 103°C), g

C = weight of aluminum boat + filter and residue (combusted at 500°C), g

Also, calculate the percentage of TVSS relative to TSS in the activated sludge. Compare to the range of typical reported values: 80% - 90%.

3.4.7 Determination of Volatile Solids

These are all solids removed by firing a sample in 550°C muffle furnace.

Total Volatile Suspended Solids, mg/L = $(B-C)(1000mgg)/samplevolume,L$

where A = weight of filter (dried at 103°C) + aluminum boat, g

B = weight of filter + aluminum boat + residue (dried at 103°C), g

C = weight of aluminum boat + filter and residue (combusted at 500°C), g

Also, calculate the percentage of TVSS relative to TSS in the activated sludge. Compare to the range of typical reported values: 80% - 90%.

3.4.8 Turbidity Determination

To determine turbidity, turbidimeter (nephelometer) was used in this experiment, while formazine primary standard was employed to calibrate the nephelometer.

Procedure

1. Fill one turbidity tube to the *50* mL line with clear water, either from the tap or bottled water.

2. Fill the other turbidity tube to the 50 mL line with the sample water.

3. Hold the tubes side-by-side in the light, and look through them vertically (from the top down). Compare their cloudiness by observing the fuzziness of the black dot at the bottom of the tube.

4. Shake the Standard Turbidity Reagent vigorously and add *0.5* mL (which is marked by a line on the pipette) to the tube *of clear water.* The reagent will make the clear water turn slightly cloudy or turbid. Stir the water in each tube with the stirring rods.

5. Compare the turbidity again by looking, down into the water in each tube at the black dot. *If* the sample water is still more turbid than the clear water, continue adding, the Turbidity Reagent by *0.5* mL increments until both tubes appear equally cloudy.

6. Compute the Jackson Turbidity Units of the sample. Each 0.5 mL of Turbidity Reagent that you added to the dear water equals 5 Jackson Turbidity Units.

$$0.5\ mL = 5\ JTUs$$

7. Record your results on the *Data Recording Form.*

8. Dispose of the waste liquid by pouring it down the drain.

9. Wash, dry and put away the test equipment.

Interpreting Results

- Do you consider the amount of turbidity you found to be a sign of a healthy or unhealthy water system?

- What do you think accounts for the level of turbidity you found?

- If you find high turbidity, look around the site to try to find the source of turbidity

* Would you expect to find more or less turbidity during another season?

Water bodies with only sparse plant and animal life 0 JTU

Drinking, water <0.5 JTU

Typical Groundwater <1.0 JTU

3.4.9 Alkalinity Determination

Alkalinity is the measure of hydroxide and carbonate ion content of wastewater sample. Wastewater sample was titrated with standard H_2SO_4 using indicator until the pink coluor of the solution changed to colourless. This is the indication of end point.

Procedure

Preparation of the Meter

Follow Method ULM-191-2, *pH Measurement of Photographic Processing Solutions* (or any subsequent pH method), for making pH measurements below pH 9

$$Total Alkalinity. for the specified sample size = \frac{[mL, proposed sample size][mL, std\ 0.1\ NH_2SO_4 for\ 1\ litre]}{1000}$$

Or

All calculations are based on the following equations:

$$Alkalinity, MgCaCO_3/1 = \frac{AxNx\ 50.000}{mlsample}$$

Where, A = ml of acid used for titration to pH 4.5

N = Normality of acid (0.1 N H_2SO_4)

Report alkalinity (mg $CaCO_3$/I)

3.4.10 Determination of Chemical Oxygen Demand (COD)

The sample of the wastewater was mixed with excess Potassium dichromate and Sulphuric acid and the mixture was heated under total reflux condition for 2hours. The amount of potassium dichromate reduced gave a measure of the amount of oxidizable organic material.

Apparatus. Reflux apparatus, consisting of a 300-mi round bottom flask with ground glass neck size 24/40 and a Friedrichs style condenser ; a hot plate with 1300-W rating ; 500-mi Erienmeyer flask.

Reagents

- ✓ Sulphuric acid-silver sulphate solution. Dissolve 22 g silver sulphate (Ag_2SO_4) in a 9-lb (4.1-kg) bottle of concentrated sulphuric acid (H_2S0_4). It will take 1 to 2 days for the silver sulphate to dissolve.
- ✓ Potassium dichromate solution, 0.25 N. Dissolve 12.259 g potassium dichromate ($K_2Cr_2O_7$) previously dried at 103°C for 2 h, in distilled water and make up to 11.
- ✓ Ferron indicator solution. Dissolve 1.485 g of 1, 10 phenomathroline ($C_{12}H_8N_2.H_2O$) together with 0.695 g ferrous sulphate crystals ($FeSO_4.7H_20$) in water and make up to 100 ml.

- ✓ Ferrous ammonium sulphate solution, 0.25 N. Dissolve 98 g ferrous ammonium sulphate [$Fe(NH_4)_2 (SO_4)_2. 6H_2O$] in distilled water. Add 20 ml concentrated sulphuric acid, cool, and make up to 11. This solution must be standardized against potassium dichromate daily.

- ✓ Mercuric sulphate ($HgSO_4$) analytical grade crystals.

Procedure

- ✓ Place a 20-ml sample in the round bottom flask, add 0.4 g mercuric sulphate, and add up by pipetting 10 ml potassium dichromate solution. Carefully add 30 ml sulphuric acid silver sulphate solution, a little at a time, mixing after each addition. Be sure the reflux mixture is mixed thoroughly before heat is applied. If this is not done, the mixture may be blown out of the condenser.

- ✓ Add a few clean glass beads to prevent bumping and attach the flask to the condenser. Reflux the mixture for 2 h. Cool, and then wash down the condenser with approximately 25 ml distilled water.

- ✓ Transfer the contents to a 500-ml Erlenmeyer flask, washing out the reflux flask 4 to 5 times with distilled water. Dilute the mixture to approximately 140-ml; cool and titrate the excess dichromate with ferrous ammonium sulphate solution, using ferroin indicator. Generally, two or three drops of the indicator are added to the sample just before titrating.

- ✓ Take as the end point the sharp color change from blue-green to reddish brown, even though the blue-green may reappear within minutes.
- ✓ A blank consisting of 20 ml of distilled water Instead of the sample, together with the reagents, is refluxed and titrated in the same manner.

Calculations

$$Mg/1\ COD\ = \frac{(a-b)x\ c\ x\ 8.000}{m1\ of\ sample}$$

in which;

COD = oxygen consumed from potassium dichromate,

a = ferrous ammonium sulphate solution used for blank, m1,,

b = ferrous ammonium sulphate solution used for sample, m1 and

c = normality of ferrous ammonium sulphate solution

CHAPTER FOUR

RESULTS AND DISCUSSIONS

4.1 Results of Experiments

The kinetic coefficients obtained for the various experiments are shown in Tables 4.9 to 4.12. The kinetic coefficients: Y, K_d, μ and K_s were obtained based on the Monod and Michaelis Menten models (Muhammad, 2006).

Table 4.1: Definition of the Cases of Cassava Wastewater Treatment

Case	Vw	L/W	N_b	Q	HRT	S_o	X_o	I
1	10	0.4	3	0.4	25	2189	10680	120
2	10	0.5	4	0.3148	31.7662	2060	10560	109
3	10	0.6	5	0.2796	35.76538	2000	10503	98
4	10	0.7	6	0.2444	40.91653	1970	10467	88
5	10	0.8	7	0.2092	47.80115	1930	10410	76
6	10	0.9	8	0.1739	57.50431	1900	10032	64
7	10	1	9	0.1287	77.70008	1850	9600	52
8	10	1.1	10	0.1035	96.61836	1810	9207	43
9	10	1.2	11	0.0683	146.4129	1750	8796	31
10	10	1.3	12	0.0331	302.1148	1700	8400	20

Table 4.2: Record of Effluent COD and Suspended Solids for the Different Cases Studied

Case	S	X
1	408	412.896
2	384	388.608
3	368	372.416
4	352	356.224
5	332	335.984
6	308	311.696
7	300	303.6
8	276	279.312
9	240	242.88
10	204	206.448

Table 4.3a: Estimation of Parameters for the Various Experimental Cases

Case					
1	S, mg/l	408	327.9912	247.9824	126.48
	S_o, mg/l	2189	1521.355	969.727	547.25
	X_o, mg/l	10680	10017.84	9505.2	9174.12
	SRT, d	2.25	3.3	6.6	18.3
2	S, mg/l	384	308.6976	233.3952	119.04
	S_o, mg/l	2060	1431.7	912.58	515
	X_o, mg/l	10560	9905.28	9398.4	9071.04
	SRT, d	2.265	3.322	6.644	18.422
3	S, mg/l	368	295.8352	223.6704	114.08
	S_o, mg/l	2000	1390	886	500
	X_o, mg/l	10503	9851.814	9347.67	9022.077
	SRT, d	2.2875	3.355	6.71	18.605
4	S, mg/l	352	282.9728	213.9456	109.12
	S_o, mg/l	1970	1369.15	872.71	492.5
	X_o, mg/l	10467	9818.046	9315.63	8991.153
	SRT, d	2.295	3.366	6.732	18.666
5	S, mg/l	332	266.8948	201.7896	102.92
	S_o, mg/l	1930	1341.35	854.99	482.5
	X_o, mg/l	10410	9764.58	9264.9	8942.19
	SRT, d	2.3175	3.399	6.798	18.849
6	S, mg/l	308	247.6012	187.2024	95.48
	S_o, mg/l	1900	1320.5	841.7	475
	X_o, mg/l	10032	9410.016	8928.48	8617.488
	SRT, d	2.325	3.41	6.82	18.91
7	S, mg/l	300	241.17	182.34	93
	S_o, mg/l	1850	1285.75	819.55	462.5
	X_o, mg/l	9600	9004.8	8544	8246.4
	SRT, d	2.3475	3.443	6.886	19.093
8	S, mg/l	276	221.8764	167.7528	85.56
	S_o, mg/l	1810	1257.95	801.83	452.5
	X_o, mg/l	9207	8636.166	8194.23	7908.813
	SRT, d	2.35125	3.4485	6.897	19.1235
9	S, mg/l	240	192.936	145.872	74.4
	S_o, mg/l	1750	1216.25	775.25	437.5
	X_o, mg/l	8796	8250.648	7828.44	7555.764
	SRT, d	2.3625	3.465	6.93	19.215
10	S, mg/l	204	163.9956	123.9912	63.24
	S_o, mg/l	1700	1181.5	753.1	425
	X_o, mg/l	8400	7879.2	7476	7215.6
	SRT, d	2.37	3.476	6.952	19.276

Table 4.3 shows that the experiment was performed 4 times for each case of given initial S_o, S, X_o and SRT.

Table 4.3b: Estimation of Parameters for the Various Experimental Cases

Case					
1	S, mg/l	489.6	448.8	408	367.2
	I, mg	108	120	132	144
	Q, l/min	0.48	0.46	0.4	0.38
2	S, mg/l	460.8	422.4	384	345.6
	I, mg	98.1	109	119.9	130.8
	Q, l/min	0.37776	0.36202	0.3148	0.29906
3	S, mg/l	441.6	404.8	368	331.2
	I, mg	88.2	98	107.8	117.6
	Q, l/min	0.33552	0.32154	0.2796	0.26562
4	S, mg/l	422.4	387.2	352	316.8
	I, mg	79.2	88	96.8	105.6
	Q, l/min	0.29328	0.28106	0.2444	0.23218
5	S, mg/l	398.4	365.2	332	298.8
	I, mg	68.4	76	83.6	91.2
	Q, l/min	0.25104	0.24058	0.2092	0.19874
6	S, mg/l	369.6	338.8	308	277.2
	I, mg	57.6	64	70.4	76.8
	Q, l/min	0.20868	0.199985	0.1739	0.165205
7	S, mg/l	360	330	300	270
	I, mg	46.8	52	57.2	62.4
	Q, l/min	0.15444	0.148005	0.1287	0.122265
8	S, mg/l	331.2	303.6	276	248.4
	I, mg	38.7	43	47.3	51.6
	Q, l/min	0.1242	0.119025	0.1035	0.098325
9	S, mg/l	288	264	240	216
	I, mg	27.9	31	34.1	37.2
	Q, l/min	0.08196	0.078545	0.0683	0.064885
10	S, mg/l	244.8	224.4	204	183.6
	I, mg	18	20	22	24
	Q, l/min	0.03972	0.038065	0.0331	0.031445

4.2 Evaluation of Kinetic Coefficients without Inhibition

Seven Coefficients were determined, viz: endogenous decay coefficient, per min; Cell yield coefficient, ratio of the mass of cells formed to the mass of substrate consumed, mg/mg; Maximum rate of substrate utilization per unit

mass of micro-organisms, per min; Half velocity constant, substrate concentration at one-half of the maximum growth rate, mg/l; Overall COD removal rate constant, per min; Michaelis-Menten constant, mg/l; Inhibition constant, mg/l.

From Table 4.4, Graphs of $Q(S_o-S)/V_wX_o$ against 1/SRT were plotted and the intercepts and slopes of the graphs were read for the 10 cases, k_d and Y for each of the cases were determined using the intercept and slope using: K_d = intercept/slope and Y = 1/slope. It was observed that the kinetic coefficients changed with changes in N_b, L/w and I concentrations (Tables 4.4, 4.5 and 4.6). Generally, the values of kinetic constants presented in Tables 4.9 to 4.12 are within the normal range of ABR process found in literature. The Figs. 4.1 and 4.2 show the variation of kinetic coefficient with the inhibition coefficient, K_i. The K_d and Y intersects in Fig 4.2 at a value of 2000 $mins^{-1}$.The maximum growth rate was estimated to be between 0.138 to 0.142min^{-1} for cassava wastewater treatment. This value is a little lower than the values above in literature. This can be attributed to improved efficiency obtainable in the ABR which results from increasing number of baffles and it simulates a condition of several treatment units in series.

Table 4.4: Determination of Endogenous decay coefficient, k_d and Cell yield Coefficient, Y

Case						Intercept	Slope	K_d	Y
	1/SRT	0.444	0.303	0.152	0.055				
1	$Q(S_o - S)/V_wX_o$	0.567	0.429	0.289	0.183	0.135	0.975	0.138	1.026
	1/SRT	0.442	0.301	0.151	0.054				
2	$Q(S_o - S)/V_wX_o$	0.425	0.321	0.216	0.137	0.101	0.735	0.137	1.360
	1/SRT	0.437	0.298	0.149	0.054				
3	$Q(S_o - S)/V_wX_o$	0.369	0.279	0.188	0.120	0.088	0.645	0.136	1.550
	1/SRT	0.436	0.297	0.149	0.054				
4	$Q(S_o - S)/V_wX_o$	0.321	0.243	0.164	0.104	0.077	0.562	0.137	1.779
	1/SRT	0.431	0.294	0.147	0.053				
5	$Q(S_o - S)/V_wX_o$	0.273	0.207	0.140	0.089	0.066	0.482	0.137	2.076
	1/SRT	0.430	0.293	0.147	0.053				
6	$Q(S_o - S)/V_wX_o$	0.235	0.178	0.121	0.077	0.057	0.414	0.138	2.414
	1/SRT	0.426	0.290	0.145	0.052				
7	$Q(S_o - S)/V_wX_o$	0.177	0.134	0.091	0.058	0.043	0.315	0.137	3.175
	1/SRT	0.425	0.290	0.145	0.052				
8	$Q(S_o - S)/V_wX_o$	0.147	0.112	0.076	0.048	0.036	0.261	0.138	3.828
	1/SRT	0.423	0.289	0.144	0.052				
9	$Q(S_o - S)/V_wX_o$	0.100	0.076	0.052	0.033	0.025	0.178	0.139	5.624
	1/SRT	0.422	0.288	0.144	0.052				
10	$Q(S_o - S)/V_wX_o$	0.050	0.038	0.026	0.017	0.013	0.089	0.142	11.19

From Table 4.5, Graphs of $SRT/(1+k_d*SRT)$ against 1/S were plotted and the intercepts and slopes of the graphs were read for the 10 cases, k and k_s for each of the cases were determined using the intercept and slope using: k = 1/intercept and k_s = slope/intercept.

Determination of k_d and Y

For Case 1, read from Table 4.4, the graph of

$Q(S_o-S)/(V_wX_o)$ against 1/SRT was plotted as shown in Fig. 4.1:

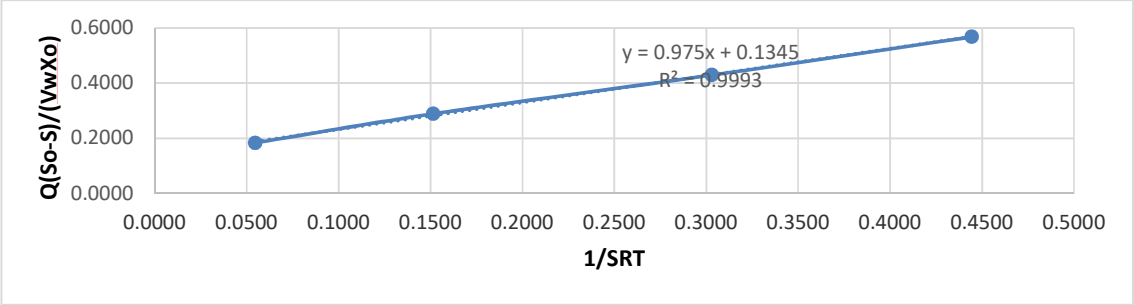

Fig. 4.1 Plot of $Q(S_o-S)/(V_wX_o)$ against 1/SRT

The intercept was read as 0.135 and the slope was determined as 0.975.

k_d was calculated as intercept/slope = 0.135/0.975 = 0.138

Y was computed as 1/slope = 1/0.975 = 1.026.

This was done for the nine remaining cases to determine k_d and Y for the nine cases.

Table 4.5: Determination of Maximum rate of Substrate Utilization, k and Half Velocity Constant, k_s

Case						Intercept	Slope	k	k_s
	1/S	0.002	0.003	0.004	0.008				
1	SRT/(1+K_d*SRT)	1.717	2.268	3.455	5.192	0.492	611.5	2.03	1243
	1/S	0.003	0.003	0.004	0.008				
2	SRT/(1+K_d*SRT)	1.729	2.283	3.478	5.229	0.495	579.6	2.02	1171
	1/S	0.003	0.003	0.004	0.009				
3	SRT/(1+K_d*SRT)	1.744	2.303	3.507	5.268	0.503	559.1	1.99	1111
	1/S	0.003	0.004	0.005	0.009				
4	SRT/(1+K_d*SRT)	1.747	2.306	3.507	5.258	0.512	532.8	1.95	1040
	1/S	0.003	0.004	0.005	0.010				
5	SRT/(1+K_d*SRT)	1.760	2.321	3.525	5.274	0.527	502.6	1.90	953
	1/S	0.003	0.004	0.005	0.010				
6	SRT/(1+K_d*SRT)	1.761	2.320	3.516	5.244	0.542	462.0	1.85	853
	1/S	0.003	0.004	0.005	0.011				
7	SRT/(1+K_d*SRT)	1.778	2.342	3.549	5.294	0.547	454.4	1.83	831
	1/S	0.004	0.005	0.006	0.012				
8	SRT/(1+K_d*SRT)	1.776	2.338	3.536	5.260	0.559	414.0	1.79	740
	1/S	0.004	0.005	0.007	0.013				
9	SRT/(1+K_d*SRT)	1.777	2.336	3.524	5.221	0.579	355.7	1.73	615
	1/S	0.005	0.006	0.008	0.016				
10	SRT/(1+K_d*SRT)	1.773	2.327	3.498	5.156	0.602	296.7	1.66	493

From Table 4.6, Graphs of $Q(So-S)/V_w$ against S were plotted, the intercepts were all set at zero and the slopes of the graphs were read for the 10 cases, K_r for each of the cases was determined using the slope using: K_r = slope. This method was illustrated by Haydar and Aziz (2009).

Determination of k and k_s

For Case 1, read from Table 4.5, the graph of $SRT/(1+K_d*SRT)$ against 1/S was plotted as shown in Fig. 4.2:

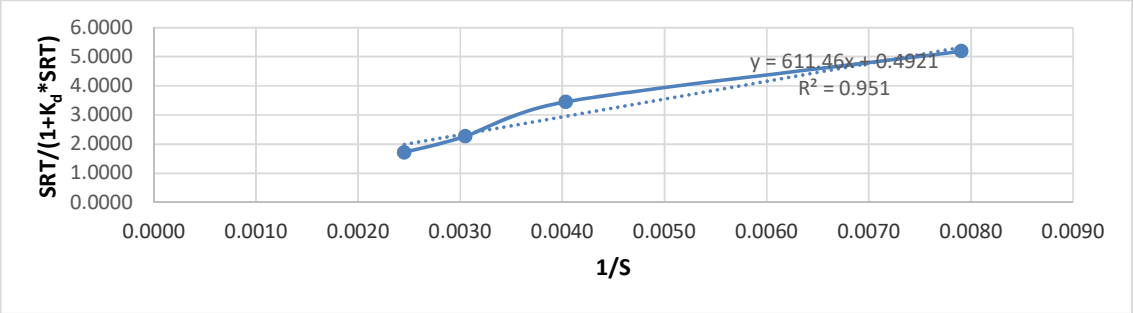

Fig. 4.2 Plot of $SRT/(1+K_d*SRT)$ against 1/S

The intercept was read as 0.492 and the slope was determined as 611.5.

Then k was calculated as 1/intercept = 1/0.492 = 2.03

K_s was computed as slope/intercept = 611.5/0.492 = 1243.

This was done for the nine remaining cases to determine k and k_s for the nine cases.

Table 4.6:Determination of Overall COD Removal Rate Constant, K_r

Case						Intercept	Slope	K_r
	S	408.0	328.0	248.0	126.5			
1	$Q(S_o - S)/Vw$	6055.4	4296.1	2742.6	1683.1	0	13.577	13.577
	S	384.0	308.7	233.4	119.0			
2	$Q(S_o - S)/Vw$	4484.6	3181.7	2031.2	1246.5	0	10.683	10.683
	S	368.0	295.8	223.7	114.1			
3	$Q(S_o - S)/Vw$	3878.6	2753.4	1759.3	1079.0	0	9.646	9.646
	S	352.0	283.0	213.9	109.1			
4	$Q(S_o - S)/Vw$	3361.2	2389.2	1529.5	937.0	0	8.747	8.747
	S	332.0	266.9	201.8	102.9			
5	$Q(S_o - S)/Vw$	2841.6	2023.0	1298.2	794.1	0	7.849	7.849
	S	308.0	247.6	187.2	95.5			
6	$Q(S_o - S)/Vw$	2353.2	1679.2	1081.3	660.0	0	7.018	7.018
	S	300.0	241.2	182.3	93.0			
7	$Q(S_o - S)/Vw$	1695.6	1209.9	779.1	475.5	0	5.192	5.192
	S	276.0	221.9	167.8	85.6			
8	$Q(S_o - S)/Vw$	1349.5	965.1	623.5	379.8	0	4.499	4.499
	S	240.0	192.9	145.9	74.4			
9	$Q(S_o - S)/Vw$	876.6	629.0	408.4	248.0	0	3.369	3.369
	S	204.0	164.0	124.0	63.2			
10	$Q(S_o - S)/Vw$	420.9	303.1	197.8	119.7	0	1.908	1.908

From Table 4.7, Graphs of 1/Q against 1/S were plotted and the intercepts and slopes of the graphs were read for the 10 cases, K_m for each of the cases was determined using the intercept and slope using: K_m = slope/intercept

Determination of K_r

For Case 1, read from Table 4.6, the graph of $Q(S_o-S)/Vw$ against S was plotted as shown in Fig. 4.3:

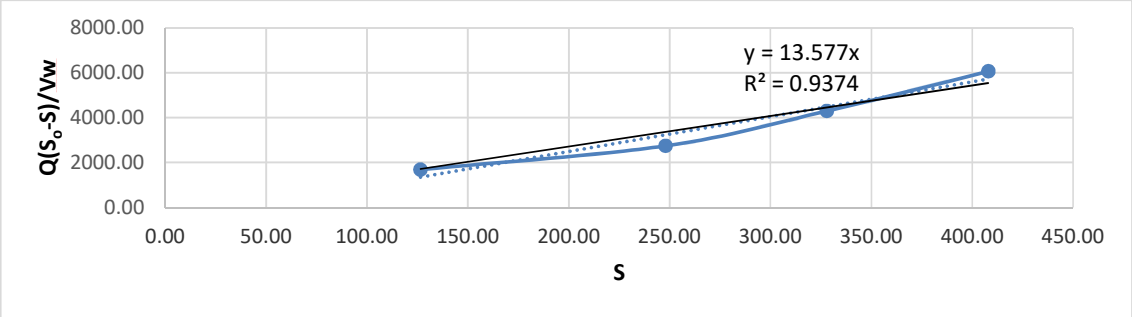

Fig. 4.3 Plot of $Q(S_o-S)/V_w$ against S

The intercept was set at 0 and the slope was determined as 13.577.

Then K_r was calculated as the slope = 13.577

This was done for the nine remaining cases to determine K_r for the nine cases.

Table 4.7: Michaelis-Menten Constant, K_m

Case						Intercept	Slope	Km
	1/S	0.0020	0.0022	0.0025	0.0027			
1	1/Q	2.0833	2.1739	2.5000	2.6316	0.302	866.1	2865.88
	1/S	0.0022	0.0024	0.0026	0.0029			
2	1/Q	2.6472	2.7623	3.1766	3.3438	0.384	1035.7	2697.14
	1/S	0.0023	0.0025	0.0027	0.0030			
3	1/Q	2.9804	3.1100	3.5765	3.7648	0.432	1117.5	2584.41
	1/S	0.0024	0.0026	0.0028	0.0032			
4	1/Q	3.4097	3.5580	4.0917	4.3070	0.495	1222.9	2472.50
	1/S	0.0025	0.0027	0.0030	0.0033			
5	1/Q	3.9834	4.1566	4.7801	5.0317	0.578	1347.5	2331.72
	1/S	0.0027	0.0030	0.0032	0.0036			
6	1/Q	4.7920	5.0004	5.7504	6.0531	0.695	1503.8	2163.43
	1/S	0.0028	0.0030	0.0033	0.0037			
7	1/Q	6.4750	6.7565	7.7700	8.1790	0.939	1979.2	2107.10
	1/S	0.0030	0.0033	0.0036	0.0040			
8	1/Q	8.0515	8.4016	9.6618	10.1704	1.168	2264.2	1938.53
	1/S	0.0035	0.0038	0.0042	0.0046			
9	1/Q	12.2011	12.7316	14.6413	15.4119	1.770	2983.6	1685.74
	1/S	0.0041	0.0045	0.0049	0.0054			
10	1/Q	25.1762	26.2709	30.2115	31.8016	3.652	5233.0	1432.84

Determination of K_m

For Case 1, read from Table 4.7, the graph of 1/Q against 1/S was plotted as shown in Fig. 4.4:

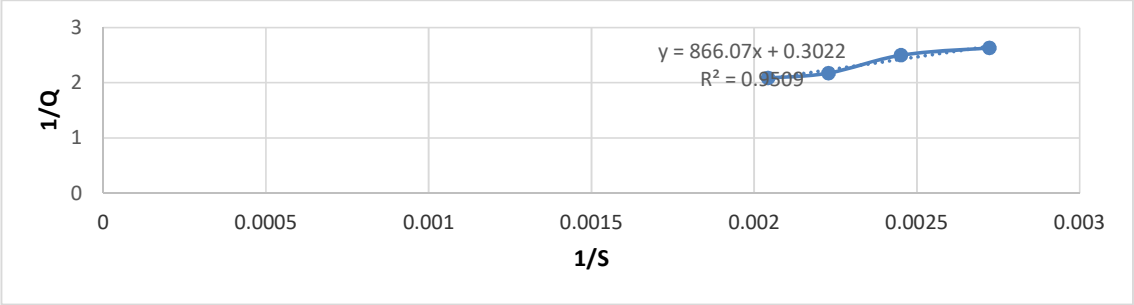

Fig. 4.4 Plot of 1/Q against 1/S

The intercept was read as 0.302 and the slope was determined as 866.1.

K_m was calculated as slope/intercept = 866.1/0.302 = 2865.88

This was done for the nine remaining cases to determine K_m for the nine cases.

4.3 Evaluation of Kinetic Coefficients with Inhibition

According to FSU (2014), inhibition constant is determined with the values and plots of 1/Q, 1/S, $1/Q_{app}$ and I in their different orders as shown in this section.

Plots of 1/Q against 1/S were made at given inhibitor concentration for the different phases of the 10 cases. The intercepts of the plot on 1/Q axes were read as $1/Q_{app}$ for each phase of each of the 10 cases. Plots of Inhibitor concentration against $1/Q_{app}$ were made for the 10 cases (Tables 4.8 to 4.11) and K_i was read as the additive inverse of the intercepts. Q_{app} = Apparent flow rate, l/min (Table 4.12).According to Fig. 4.3, the COD removal efficiency was lower than the COD removal efficiency under non-inhibitory condition (Table 4.14). At first glance, the second shoulder clearly indicates the occurrence of inhibition. Here the COD removal efficiency dropped from 88% to 84% between a cyanide concentration of 10 to 50mg/l. it remained constant between 50 and 70mg/l of cyanide until it further dropped to 82%, at which no further decline in COD removal efficiency. This was observed at cyanide concentration of 110mg/l.

Table 4.8: Phase 1 at particular inhibitor concentration for each of the 10 cases

Case		Phase 1			
1	S, mg/l	587.52	538.56	489.6	440.64
	I, mg	108			
	Q, l/min	0.576	0.552	0.48	0.456
2	S, mg/l	552.96	506.88	460.8	414.72
	I, mg	98.1			
	Q, l/min	0.453312	0.434424	0.37776	0.358872
3	S, mg/l	529.92	485.76	441.6	397.44
	I, mg	88.2			
	Q, l/min	0.402624	0.385848	0.33552	0.318744
4	S, mg/l	506.88	464.64	422.4	380.16
	I, mg	79.2			
	Q, l/min	0.351936	0.337272	0.29328	0.278616
5	S, mg/l	478.08	438.24	398.4	358.56
	I, mg	68.4			
	Q, l/min	0.301248	0.288696	0.25104	0.238488
6	S, mg/l	443.52	406.56	369.6	332.64
	I, mg	57.6			
	Q, l/min	0.250416	0.239982	0.20868	0.198246
7	S, mg/l	432	396	360	324
	I, mg	46.8			
	Q, l/min	0.185328	0.177606	0.15444	0.146718
8	S, mg/l	397.44	364.32	331.2	298.08
	I, mg	38.7			
	Q, l/min	0.14904	0.14283	0.1242	0.11799
9	S, mg/l	345.6	316.8	288	259.2
	I, mg	27.9			
	Q, l/min	0.098352	0.094254	0.08196	0.077862
10	S, mg/l	293.76	269.28	244.8	220.32
	I, mg	18			
	Q, l/min	0.047664	0.045678	0.03972	0.037734

- The determination of K_i involved much more rigorous method than determining the other coefficients.

- Now there were 4 phases of the experiment for each of the 10 cases instead of only one phase as it was for other coefficients.

- This is because an intermediate parameter called $1/Q_{app}$, (Q_{app} = apparent flow rate) has to be determined before/from which K_i is then determined.

- $1/Q_{app}$ is read as the intercept on 1/Q axis when the plot of 1/Q against 1/S was made. This is shown in the next slide.

K_i for Case 1

For Phase 1 of Case 1, at inhibitor concentration of 108, the plot of 1/Q against 1/S is generated as shown in Fig. 4.5:

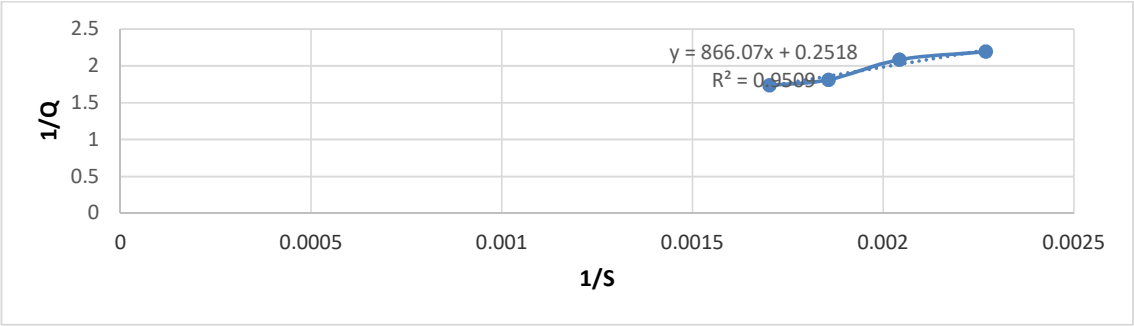

Fig. 4.5 Plot of 1/Q against 1/S

The intercept on 1/Q axis is read as 0.2518 which is called $1/Q_{app}$ for Phase 1 of Case 1 at I = 108

Table 4.9: Phase 2 at particular inhibitor concentration for each of the 10 cases

Case		Phase 2			
1	S, mg/l	538.56	493.68	448.8	403.92
	I, mg	120			
	Q, l/min	0.552	0.529	0.46	0.437
2	S, mg/l	506.88	464.64	422.4	380.16
	I, mg	109			
	Q, l/min	0.434424	0.416323	0.36202	0.343919
3	S, mg/l	485.76	445.28	404.8	364.32
	I, mg	98			
	Q, l/min	0.385848	0.369771	0.32154	0.305463
4	S, mg/l	464.64	425.92	387.2	348.48
	I, mg	88			
	Q, l/min	0.337272	0.323219	0.28106	0.267007
5	S, mg/l	438.24	401.72	365.2	328.68
	I, mg	76			
	Q, l/min	0.288696	0.276667	0.24058	0.228551
6	S, mg/l	406.56	372.68	338.8	304.92
	I, mg	64			
	Q, l/min	0.239982	0.229983	0.199985	0.189986
7	S, mg/l	396	363	330	297
	I, mg	52			
	Q, l/min	0.177606	0.170206	0.148005	0.140605
8	S, mg/l	364.32	333.96	303.6	273.24
	I, mg	43			
	Q, l/min	0.14283	0.136879	0.119025	0.113074
9	S, mg/l	316.8	290.4	264	237.6
	I, mg	31			
	Q, l/min	0.094254	0.090327	0.078545	0.074618
10	S, mg/l	269.28	246.84	224.4	201.96
	I, mg	20			
	Q, l/min	0.045678	0.043775	0.038065	0.036162

K_i for Case 1

For Phase 2 of Case 1, at inhibitor concentration of 120, the plot of 1/Q against 1/S is generated as shown in Fig. 4.6:

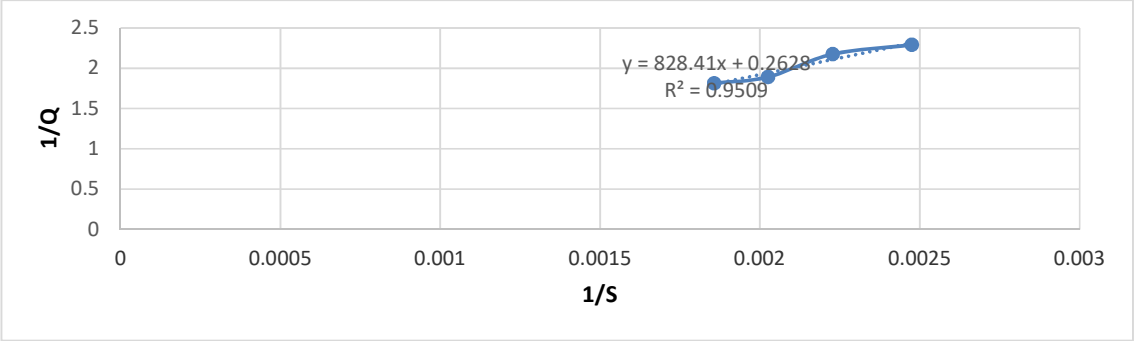

Fig. 4.6 Plot of 1/Q against 1/S

The intercept on 1/Q axis is read as 0.2628 which is called $1/Q_{app}$ for Phase 2 of Case 1 at I = 120.

Table 4.10: Phase 3 at particular inhibitor concentration for each of the 10 cases

Case	Phase 3				
	S, mg/l	489.6	448.8	408	367.2
	I, mg	132			
1	Q, l/min	0.48	0.46	0.4	0.38
	S, mg/l	460.8	422.4	384	345.6
	I, mg	119.9			
2	Q, l/min	0.37776	0.36202	0.3148	0.29906
	S, mg/l	441.6	404.8	368	331.2
	I, mg	107.8			
3	Q, l/min	0.33552	0.32154	0.2796	0.26562
	S, mg/l	422.4	387.2	352	316.8
	I, mg	96.8			
4	Q, l/min	0.29328	0.28106	0.2444	0.23218
	S, mg/l	398.4	365.2	332	298.8
	I, mg	83.6			
5	Q, l/min	0.25104	0.24058	0.2092	0.19874
	S, mg/l	369.6	338.8	308	277.2
	I, mg	70.4			
6	Q, l/min	0.20868	0.199985	0.1739	0.165205
	S, mg/l	360	330	300	270
	I, mg	57.2			
7	Q, l/min	0.15444	0.148005	0.1287	0.122265
	S, mg/l	331.2	303.6	276	248.4
	I, mg	47.3			
8	Q, l/min	0.1242	0.119025	0.1035	0.098325
	S, mg/l	288	264	240	216
	I, mg	34.1			
9	Q, l/min	0.08196	0.078545	0.0683	0.064885
	S, mg/l	244.8	224.4	204	183.6
	I, mg	22			
10	Q, l/min	0.03972	0.038065	0.0331	0.031445

K_i for Case 1

For Phase 3 of Case 1, at inhibitor concentration of 132, the plot of 1/Q against 1/S is generated as shown in Fig. 4.7:

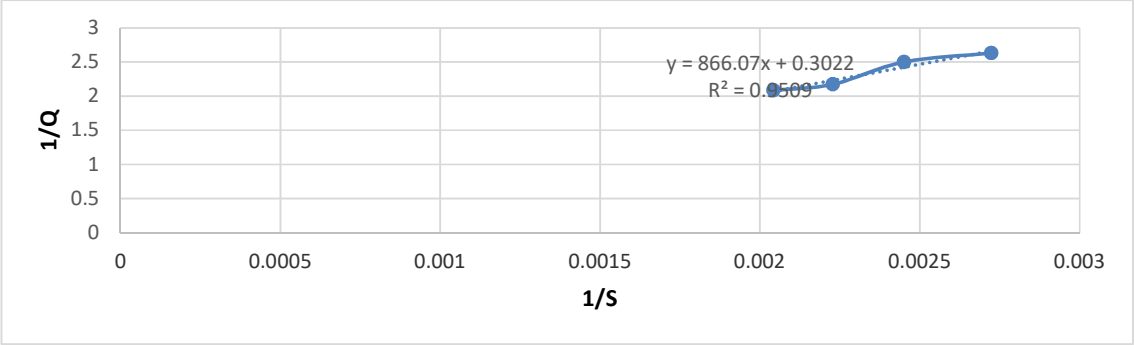

Fig. 4.7 Plot of 1/Q against 1/S

The intercept on 1/Q axis is read as 0.3022 which is called $1/Q_{app}$ for Phase 3 of Case 1 at I = 132.

Table 4.11: Phase 4 at particular inhibitor concentration for each of the 10 cases

Case	Phase 4				
	S, mg/l	440.64	403.92	367.2	330.48
	I, mg	144			
1	Q, l/min	0.456	0.437	0.38	0.361
	S, mg/l	414.72	380.16	345.6	311.04
	I, mg	130.8			
2	Q, l/min	0.358872	0.343919	0.29906	0.284107
	S, mg/l	397.44	364.32	331.2	298.08
	I, mg	117.6			
3	Q, l/min	0.318744	0.305463	0.26562	0.252339
	S, mg/l	380.16	348.48	316.8	285.12
	I, mg	105.6			
4	Q, l/min	0.278616	0.267007	0.23218	0.220571
	S, mg/l	358.56	328.68	298.8	268.92
	I, mg	91.2			
5	Q, l/min	0.238488	0.228551	0.19874	0.188803
	S, mg/l	332.64	304.92	277.2	249.48
	I, mg	76.8			
6	Q, l/min	0.198246	0.189986	0.165205	0.156945
	S, mg/l	324	297	270	243
	I, mg	62.4			
7	Q, l/min	0.146718	0.140605	0.122265	0.116152
	S, mg/l	298.08	273.24	248.4	223.56
	I, mg	51.6			
8	Q, l/min	0.11799	0.113074	0.098325	0.093409
	S, mg/l	259.2	237.6	216	194.4
	I, mg	37.2			
9	Q, l/min	0.077862	0.074618	0.064885	0.061641
	S, mg/l	220.32	201.96	183.6	165.24
	I, mg	24			
10	Q, l/min	0.037734	0.036162	0.031445	0.029873

K_i for Case 1

For Phase 4 of Case 1, at inhibitor concentration of 144, the plot of 1/Q against 1/S is generated as shown in Fig. 4.8:

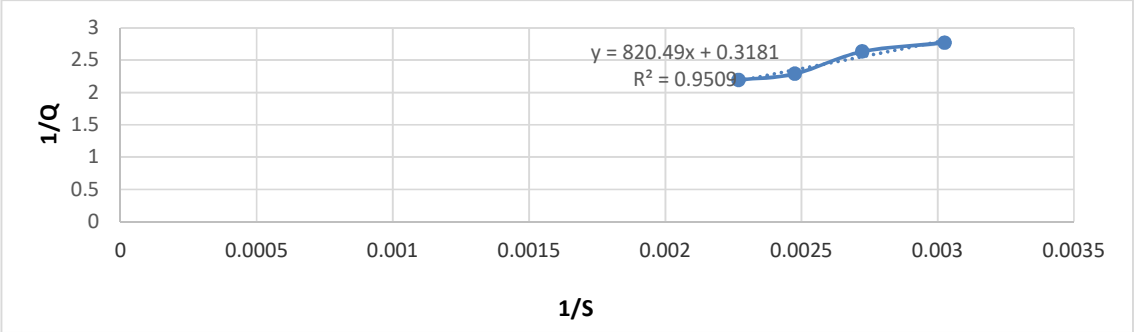

Fig. 4.8 Plot of 1/Q against 1/S

The intercept on 1/Q axis is read as 0.3181 which is called $1/Q_{app}$ for Phase 4 of Case 1 at I = 144.

This was repeated for the remaining nine cases. The resulting values of k_i are summarized in Table 4.12.

Table 4.12: Computation of Inhibitor Constant, k_i

Cases						K_i
1	1/Qapp	0.2518	0.2628	0.3022	0.3182	9.9989
	I	108	120	132	144	
2	1/Qapp	0.32	0.3339	0.384	0.4042	9.2079
	I	98.1	109	119.9	130.8	
3	1/Qapp	0.3603	0.376	0.4324	0.4551	8.3002
	I	88.2	98	107.8	117.6	
4	1/Qapp	0.4122	0.4301	0.4946	0.5207	7.4252
	I	79.2	88	96.8	105.6	
5	1/Qapp	0.4815	0.5025	0.5779	0.6083	6.3827
	I	68.4	76	83.6	91.2	
6	1/Qapp	0.5793	0.6045	0.6951	0.7317	5.4414
	I	57.6	64	70.4	76.8	
7	1/Qapp	0.7263	0.7579	0.8716	0.9174	4.3996
	I	46.8	52	57.2	62.4	
8	1/Qapp	0.9733	1.0156	1.168	1.2295	3.6196
	I	38.7	43	47.3	51.6	
9	1/Qapp	1.4749	1.5391	1.7699	1.8631	2.6198
	I	27.9	31	34.1	37.2	
10	1/Qapp	3.0435	3.1758	3.6522	3.8444	1.6901
	I	18	20	22	24	

The values of k_i shown in Table 4.12 were obtained for the various cases by plotting $1/Q_{app}$ against I and taking the additive inverse of the intercept. From Table 4.12 it can be seen that the values of k_i decreased with decreasing inhibitor concentration.

The COD removal efficiency of the reactor was estimated for each of the 10 cases as:

$RE = (S_o - S)/S_o$The values are presented in Table 4.13.

Table 4.13: Estimation of COD Removal Efficiency (RE)

Case	S_o	S	RE
1	2189	408	0.813614
2	2060	384	0.813592
3	2000	368	0.816
4	1970	352	0.82132
5	1930	332	0.827979
6	1900	308	0.837895
7	1850	300	0.837838
8	1810	276	0.847514
9	1750	240	0.862857
10	1700	204	0.88

The COD removal efficiency (RE) is observed to increase with increasing number of baffles as shown in Table 4.13.

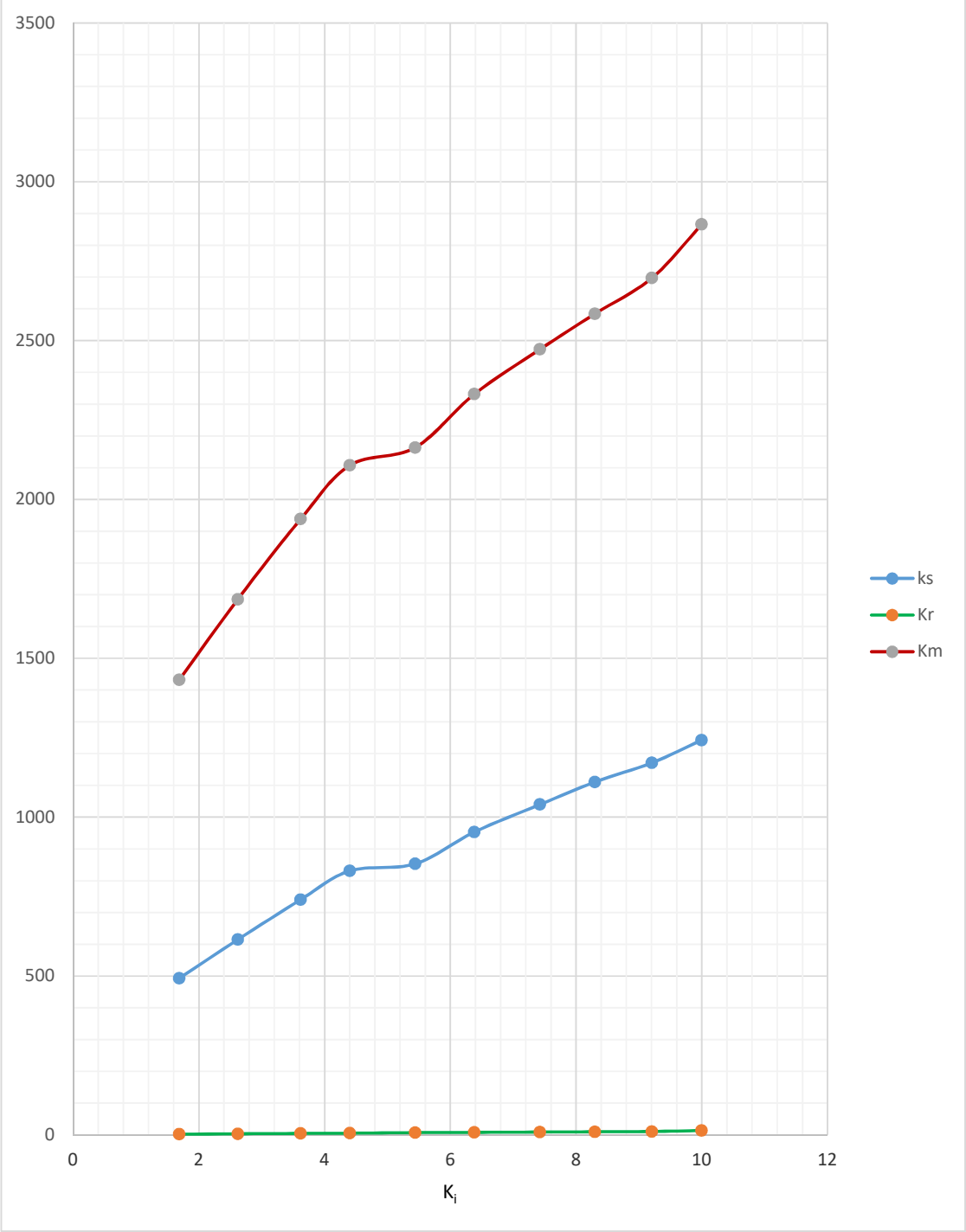

Fig.4.9: Plot of k_s, K_r, K_m against K_i

Fig 4.9 shows the variation of k_s, K_r and K_m as K_i varies. K_i is the inhibition constant which represents how potent an inhibitor is. It increases as the

concentration of the inhibitor increases. It is the concentration required to produce half maximum inhibition. Inhibitor tends to inhibit the growth or survival of more micro-organisms in the waste water, it also slows down the utilisation of substrate COD allowing more COD remain in the system. Since addition of inhibitor allows more substrate to remain in system, k_s, which is the concentration of the substrate at half of growth rate, therefore increases as more inhibitor is added. This can be read from the plot which shows that as inhibition constant which is a representation of inhibitor concentration, increases, k_s also increases.

K_r which is the overall COD removal constant also increases as K_i increases as shown in the plot. Addition of inhibitor hastens COD removal but does not guarantee total removal of COD. K_r is a representation of how fast the COD removal is not how well and it is easily read from the plot that it increases as K_i increases which entails faster COD removal as K_i increases.

K_m (the Michaelis constant; sometimes represented as k_s instead) is the substrate concentration at which the reaction velocity is 50% of the maximum velocity. It is virtually the same with k_s so it shows the same trend of increasing with K_i just as k_s shows.

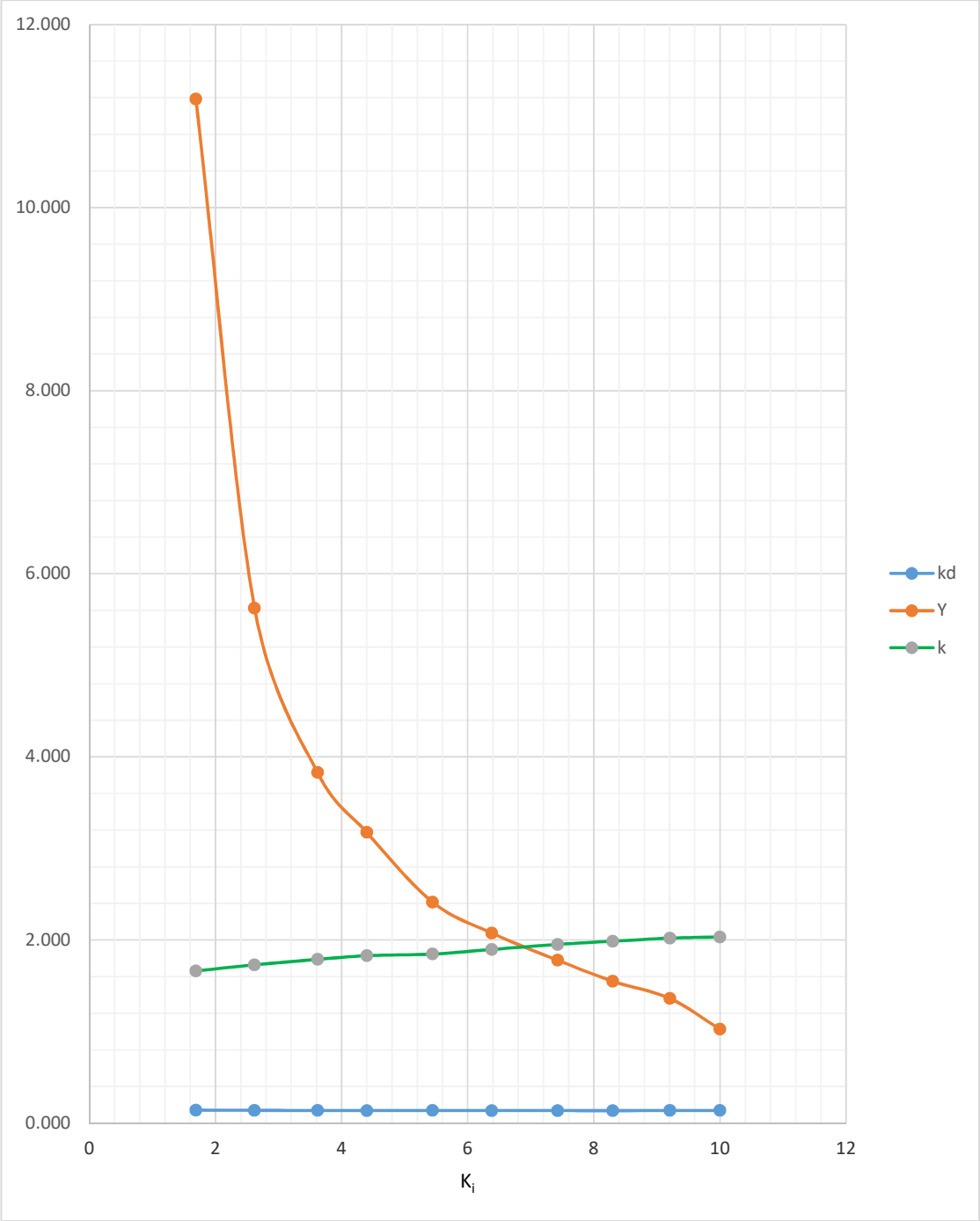

Fig.4.10: Plot of k_d, Y, k against K_i

Fig 4.10 shows the changes in k_d, Y and k as K_i changes. k_d represents the decay or decrease in cells of micro-organisms present in the wastewater as the reaction is on. Fig 4.10 shows that as the inhibition constant which represents the inhibition concentration increases, cells decrease in mass faster and this decrease in cells mass is called endogenous decay. k also increases with K_i since

inhibition slows down the growth of micro-organisms in the system making the amount of organisms to remain little and this then means that substrate utilisation per unit mass of the organisms will be high. This is read from the graph that as K_i increases, k also increases.

Y is the cell yield coefficient representing the number and mass of cells. Since inhibition causes a decrease in cells mass, as inhibition increases, cells decay thus making the cell yield to be low. This is read from Fig 4.2 showing that cell yield decreases as K_i increases.

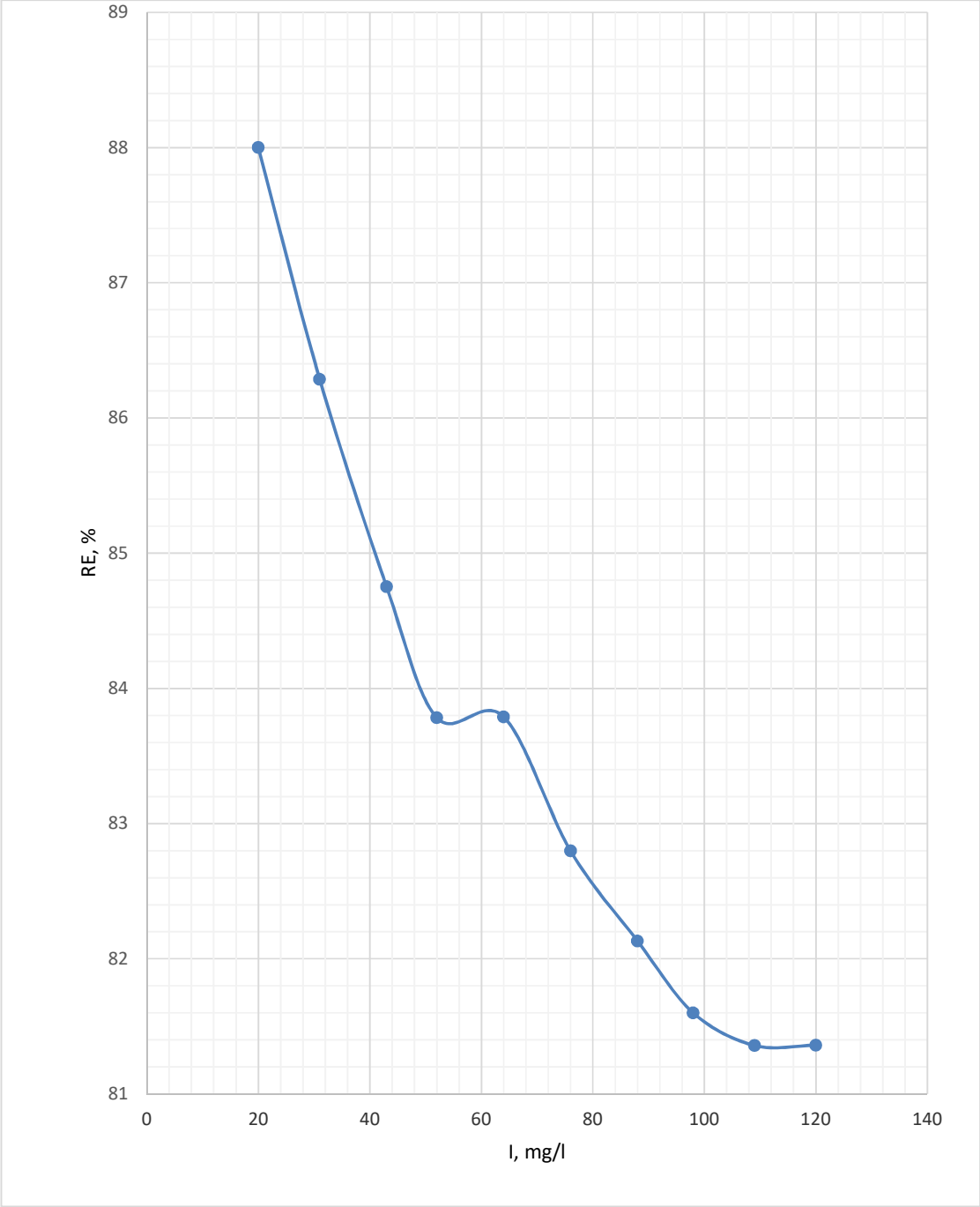

Fig.4.11: Effect of Cyanide Inhibitor on COD Removal Efficiency

COD removal efficiency represents how well COD is removed from the wastewater in the course of the reactions. Addition of inhibitor though hastens COD removal, also has the side effect of making the system not able to remove large quantities of COD out of the system and this results in decrease in total

COD removal of the reactor. From Fig 4.11, it can be seen that as inhibition concentration increases, the overall COD removal efficiency decreases.

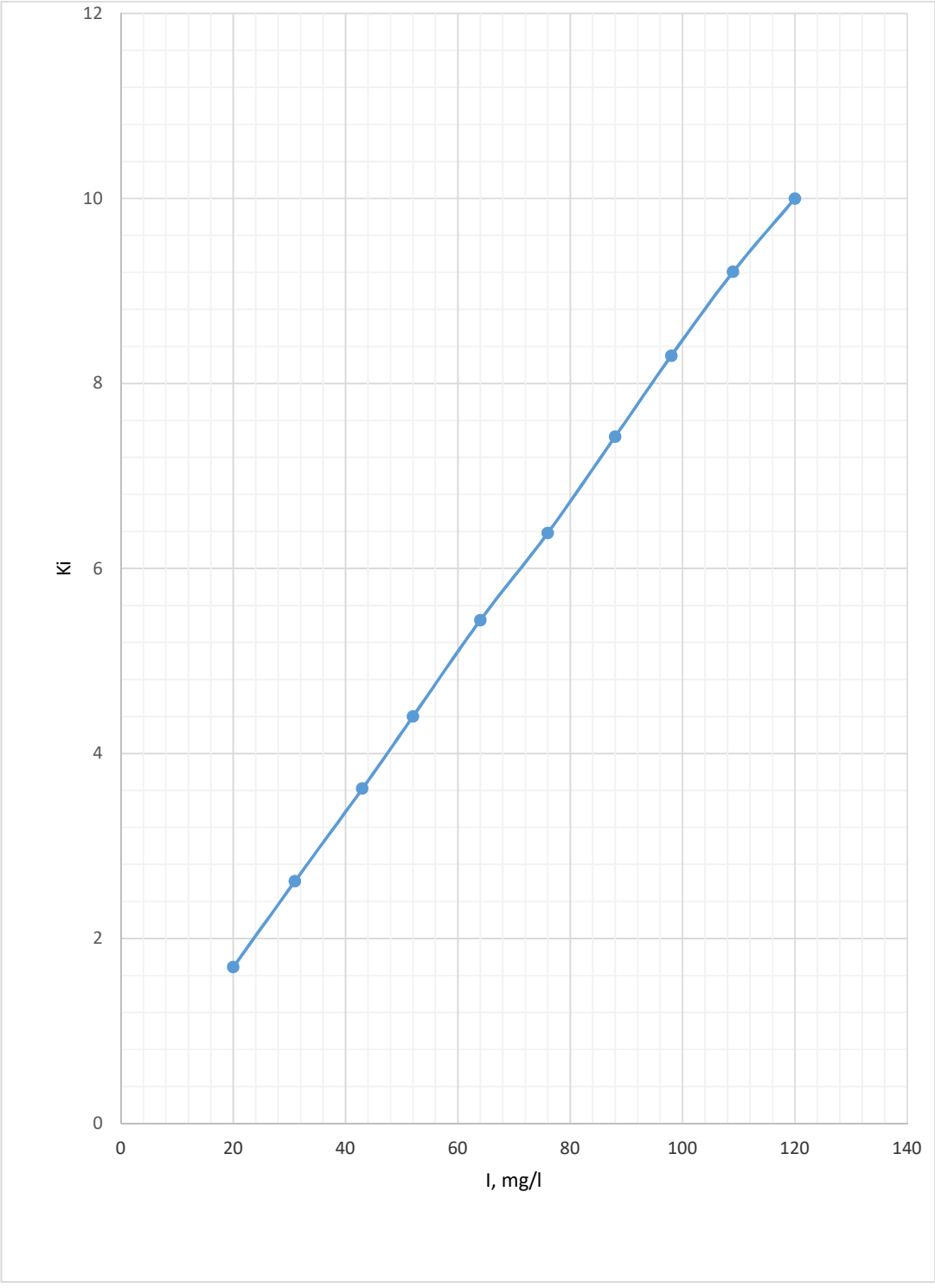

Fig.4.12: Plot of K_i against I

K_i is the inhibition constant which represents how potent an inhibitor is. It is the concentration required to produce half maximum inhibition. It increases as the concentration of the inhibitor increases. This is shown in Fig 4.12 which is the plot of inhibition constant against inhibition concentration.

4.4Calibration and Validation of Model for Cassava Wastewater Treatment

Table 4.14: Computation of Model Parameters

Case	L/W	N_b	K_i	Q	RE
1	0.4	3	9.9989	0.4	0.813614
2	0.5	4	9.2079	0.3148	0.813592
3	0.6	5	8.3002	0.2796	0.816
4	0.7	6	7.4252	0.2444	0.82132
5	0.8	7	6.3827	0.2092	0.827979
6	0.9	8	5.4414	0.1739	0.837895
7	1	9	4.3996	0.1287	0.837838
8	1.1	10	3.6196	0.1035	0.847514
9	1.2	11	2.6198	0.0683	0.862857
10	1.3	12	1.6901	0.0331	0.88

The data in Table 4.14 was used to generate a correlation to govern the effect of the four parameters L/W, N_b, K_i and Q on the Removal Efficiency, RE.

Upper limits of the four parameters, L/W, N_b, K_i and Q were set at 10, 20, 30 and 0.8 respectively, while the lower limits were set at 0.001, 1, 0.01 and 0.01 respectively. RE was assigned upper and lower limits of 0.99 and 0.7 respectively.

Table 4.15: RE and L/W, N_b, K_i, Q involving the Upper and Lower Limits

RE	L/W	N_b	K_i	Q
0.7	0.001	1	30	0.8
0.8136	0.4	3	9.9989	0.4
0.8136	0.5	4	9.2079	0.3148
0.816	0.6	5	8.3002	0.2796
0.8213	0.7	6	7.4252	0.2444
0.828	0.8	7	6.3827	0.2092
0.8379	0.9	8	5.4414	0.1739
0.8378	1	9	4.3396	0.1287
0.8475	1.1	10	3.6196	0.1035
0.8629	1.2	11	2.6198	0.0683
0.88	1.3	12	1.6901	0.0331
0.99	10	20	0.01	0.01

$RE = f(L/W, N_b, K_i, Q)$

$$RE = m\left(\frac{L}{W}\right)^{a_1}(N_b)^{a_2}(K_i)^{a_3}(Q)^{a_4} \quad (4.1)$$

$$\text{In}(RE) = \text{In}(m) + a_1(\text{In}L/W) + a_2(\text{In}N_b) + a_3(\text{In}K_i) + a_4(\text{In}Q) \quad (4.2)$$

Representing In(RE), In(m), In(L/W), In(N_b), In(K_i) and In(Q) with R, a_0, L, N, C and Q respectively, Equation 4.2 becomes:

$$R = a_0 + a_1L + a_2N + a_3C + a_4Q \quad (4.3)$$

$$\Sigma R = a_0n + a_1\Sigma L + a_2\Sigma N + a_3\Sigma C + a_4\Sigma Q \quad (4.4)$$

$$\Sigma LR = a_0\Sigma L + a_1\Sigma L^2 + a_2\Sigma LN + a_3\Sigma LC + a_4\Sigma LQ \quad (4.5)$$

$$\Sigma NR = a_0\Sigma N + a_1\Sigma LN + a_2\Sigma N^2 + a_3\Sigma NC + a_4\Sigma NQ \quad (4.6)$$

$$\Sigma CR = a_0\Sigma C + a_1\Sigma LC + a_2\Sigma NC + a_3\Sigma C^2 + a_4\Sigma CQ \quad (4.7)$$

$$\Sigma QR = a_0\Sigma Q + a_1\Sigma LQ + a_2\Sigma NQ + a_3\Sigma CQ + a_4\Sigma Q^2 \quad (4.8)$$

The value of n in Equation 4.4 is the number of cases for the analyses which is 12 (10 cases plus the set upper and lower limits).

The values of ΣR to ΣQ^2 were gotten from Appendix 2 and were inserted into Equations 4.4 to 4.8 to produce Equations 4.9 to 4.13 as shown:

$$-2.16 = 12a_0 - 6.87a_1 + 23.37a_2 + 16.09a_3 - 23.3a_4 \quad (4.9)$$

$$2.93 = -6.87a_0 + 54.92a_1 + 4.11a_2 - 39.9a_3 - 7.33a_4 \quad (4.10)$$

$$-3.58 = 23.37a_0 + 4.11a_1 + 53.38a_2 + 19.33a_3 - 54.9a_4 \quad (4.11)$$

$$-4.42 = 16.09a_0 - 39.9a_1 + 19.33a_2 + 66.74a_3 - 7.33a_4 \quad (4.12)$$

$$3.27 = -23.3a_0 - 7.33a_1 + -54.9a_2 + -7.33a_3 + 60.83a_4 \quad (4.13)$$

Equations 4.9 to 4.13 were then solved simultaneously to give a_0, a_1, a_2, a_3 and a_4 as -0.1858657, 0.019319, 0.0011, -0.012 and -0.016 respectively.

Since $\ln(m) = a_0 = -0.1858657$, $m = e^{-0.1858657} = 0.83038504$

Putting the values of m, a_1, a_2, a_3 and a_4 in Equation 4.1 changes it to:

$$\mathbf{RE = (0.83038504(L/W)^{0.019319}N_b^{0.0011}) / (K_i^{0.012}Q^{0.016})} \quad (4.14)$$

The correlation coefficient of Equation 4.1, $R^2 = 0.997$

The correlation given in Equation 4.14 was used in developing a Microsoft Visual Basic Program for estimating Removal Efficiency. The sample of the program is as shown in Plate 4.1:

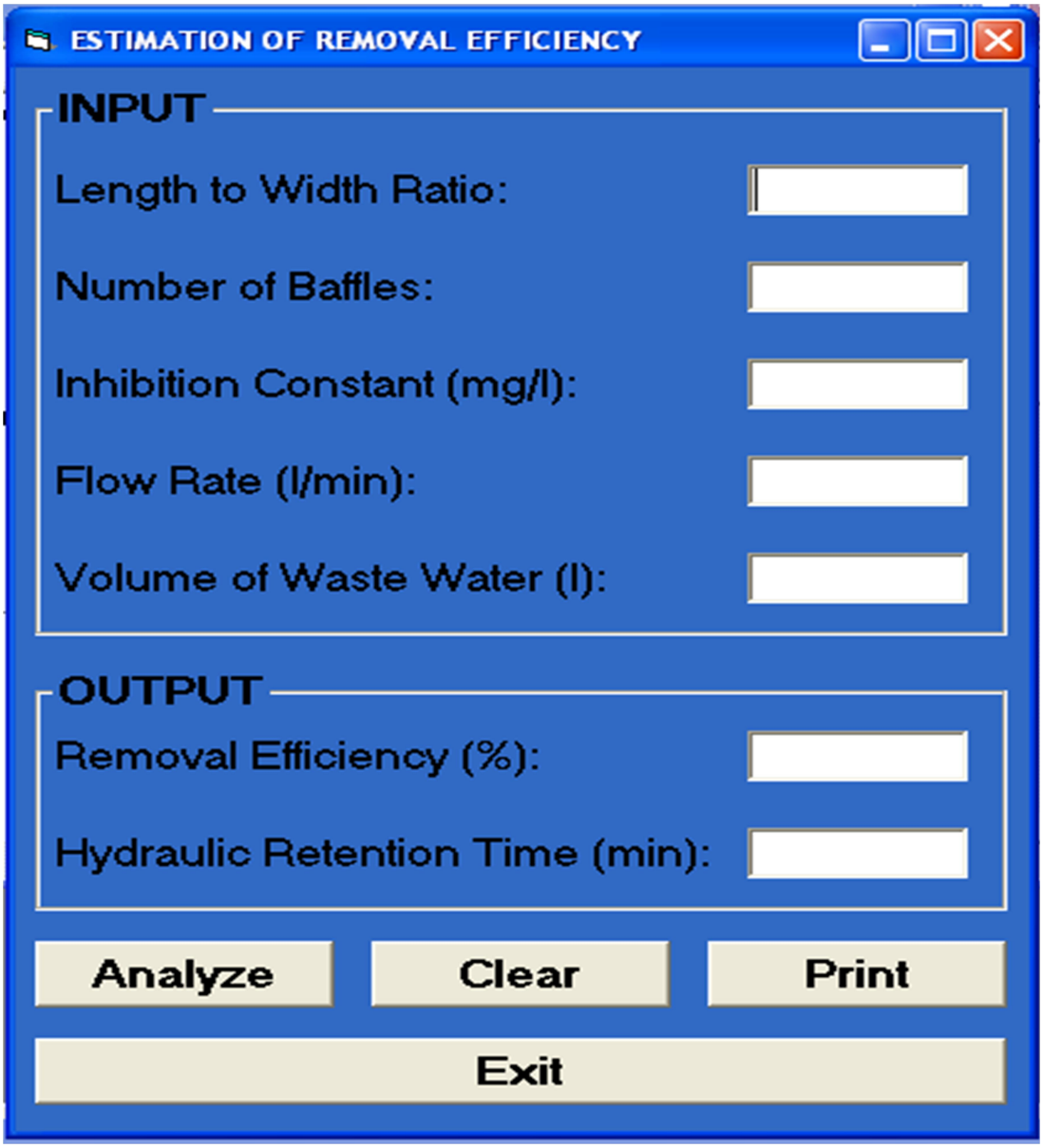

Plate.4.1: Microsoft Visual Basic Program for Estimating Removal Efficiency

4.5Results of Acidity, Alkalinity, Turbidity and pH Determination

4.5.1 Results of Acidity, Alkalinity, Turbidity and pH Determination for Reactor 1

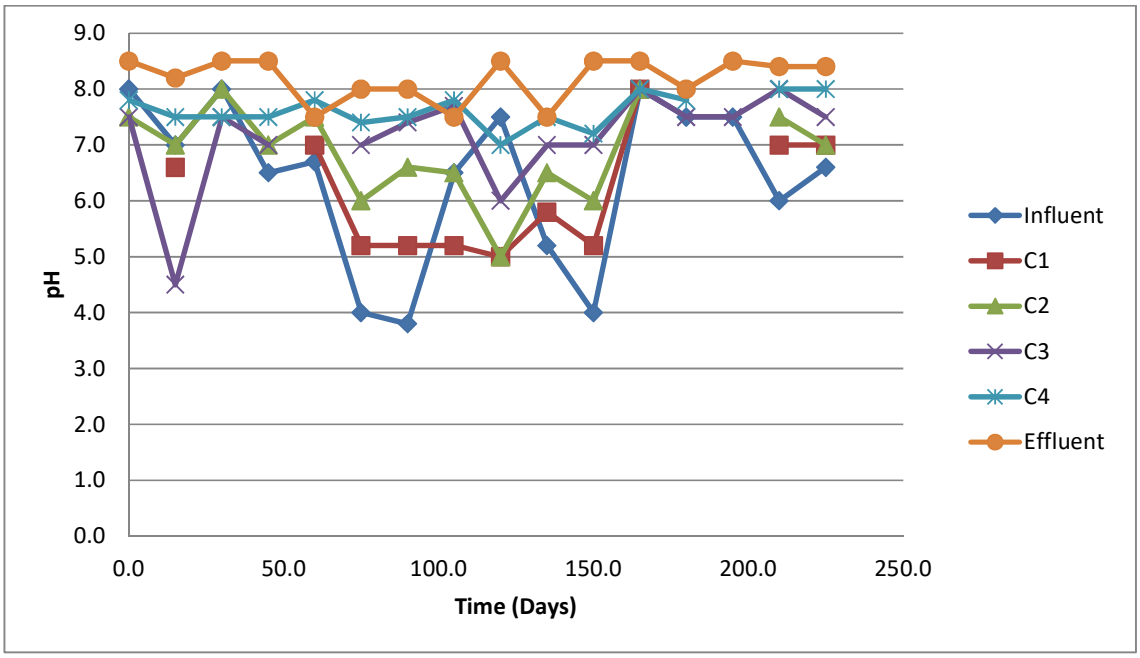

Fig.4.13:pH behaviour as a function of time

Feed tank pH was adjusted with sodium bicarbonate at the start-up period and in cases where ABR performance strongly decreased. In general, pH increased along the four compartments as the acids generated were consumed until the end of treatment which indicates a possible buffering ability for ABR (Fig4.13). The effluent pH remained fairly stable (not fluctuating with time) while the influent pH fluctuated, maybe as a result of manual addition of potassium cyanide.COD conversion during the start-up period was obtained up to 61%, with HRT of 3 days (OLR of 1.5 kgCOD/m^3.d). After each increase in OLR, the COD concentration in effluent increased. When the OLR was increased to 2.5, 5

and 10 kgCOD/ m^3.d at HRT in the range of 1.43-2.45 days the efficiency of COD removal was achieved as 67%, 55% and 40%, respectively.

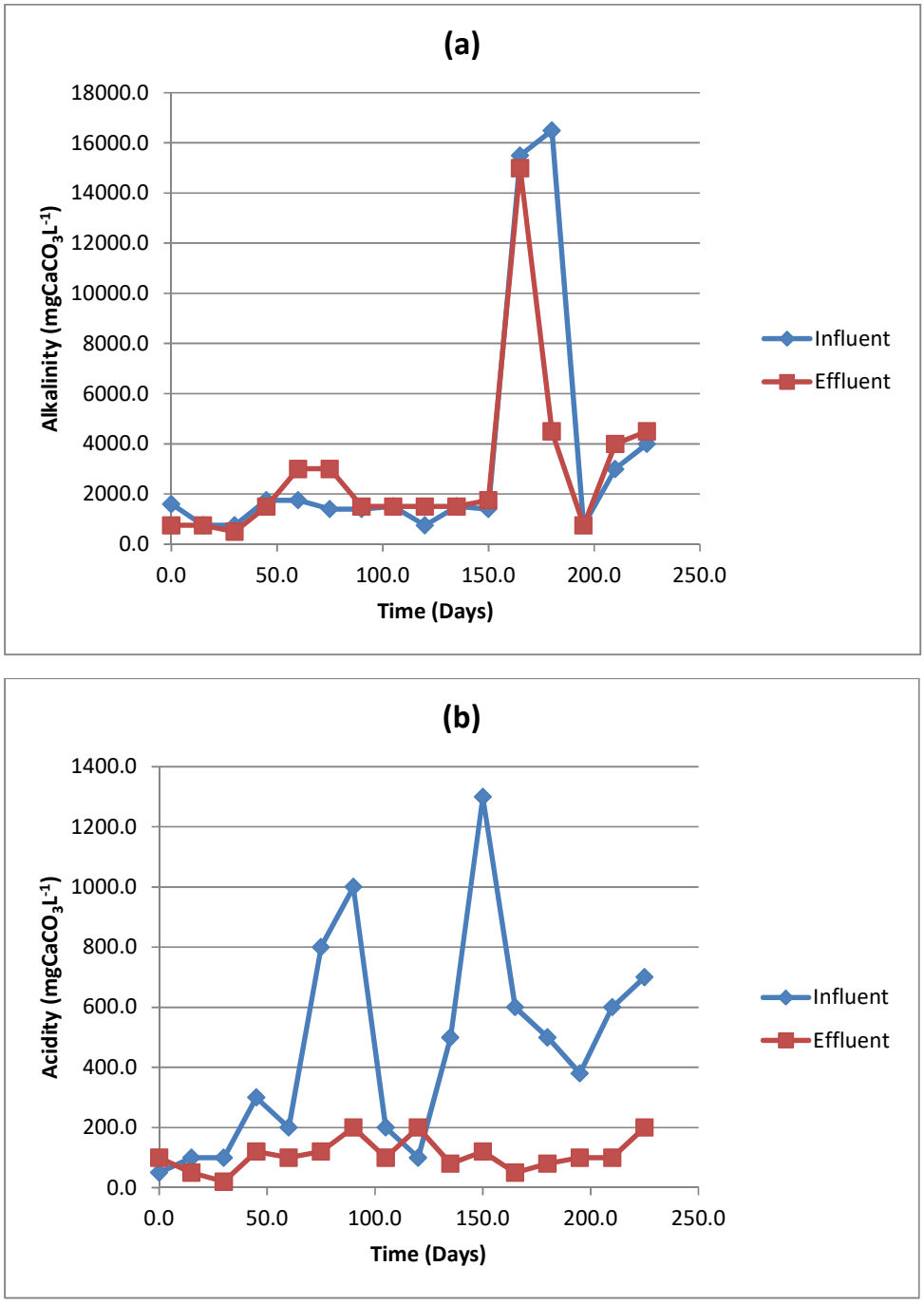

Fig.4.14:(a) Alkalinity and (b) Acidity behaviour as a function of time

Fig.4.14 shows the behavior of these two variables as a function of time. Alkalinity levels remained within close limits between the influent and effluent. However there was a very sharp increase in alkalinity level at a HRT of about 150 days before returning to normal level. This is attributable to system shock. The effluent acidity level remained lower than the influent value except at start up and at HRT of between 100 and 150 days. This showed that acidogenesis was effective during system operation. Turbidity varied significantly along compartments, however generally decreased in the end of treatment which means that ABR retains particulate material, as shown in Fig.4.15.

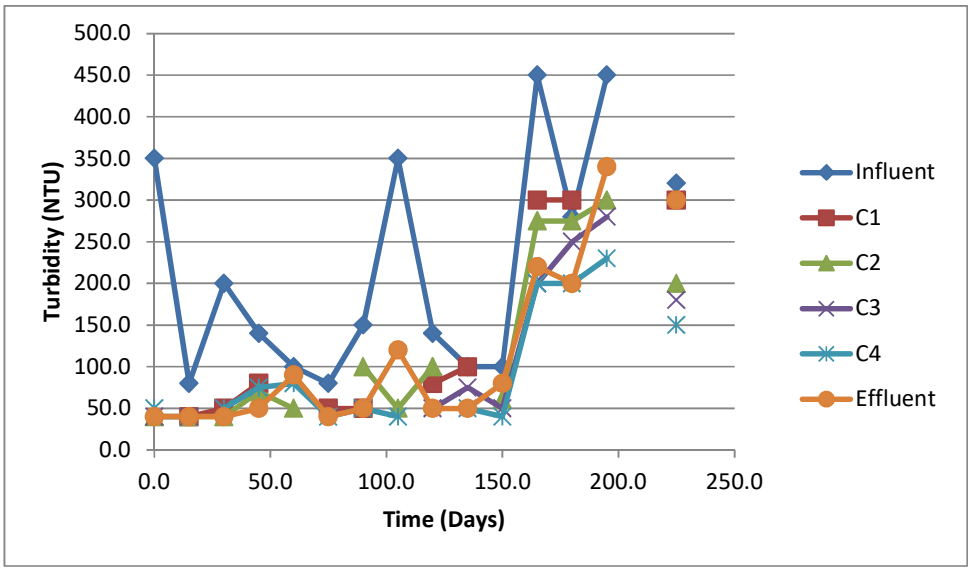

Fig.4.15:Turbidity behaviour as a function of time

4.5.2 Results of Acidity, Alkalinity, Turbidity and pH Determination for Reactor 2

As shown in Fig. 4.16, the feed alkalinity after pH adjustment was approximately 1000-3000 mg/L. while the effluent alkalinity was always in the range of 2000-5000 mg/L. The results of pH variations along with the reactor

showed that the pH decreases in compartments 1 and 2 up to pH<6.5 during the reactor operation. However, although the pH in compartments 3-5 returned to near neutrality, compartment 1 stayed at approximately pH=6.4 for the rest of the experiment. This is clearly shown in Fig.4.17.

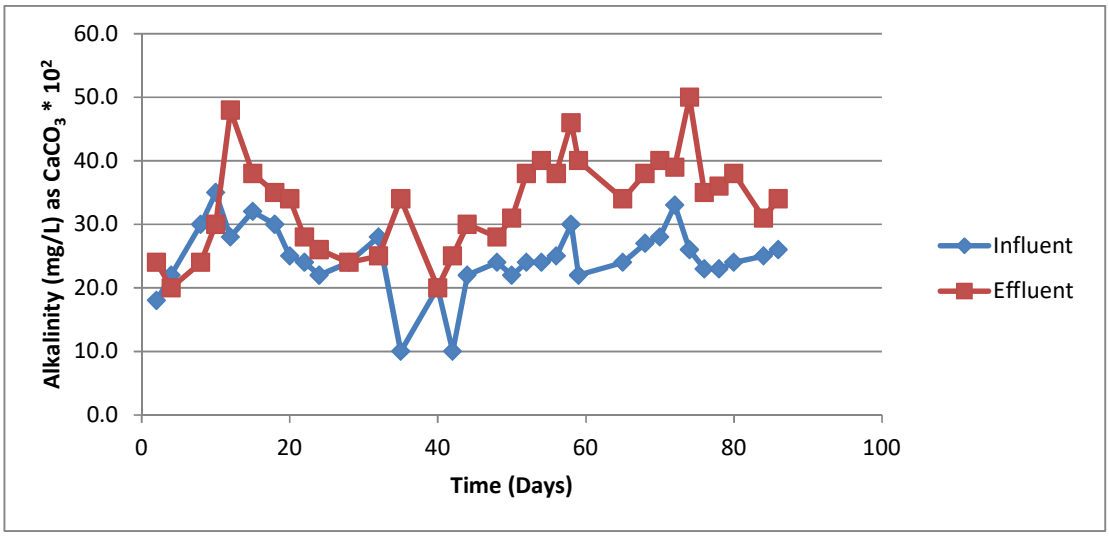

Fig4.16:Influent and effluent alkalinity during reactor operation period

Acidogenic groups are much more active in the first compartments. Therefore, acidity is also higher compared to its values at the last compartment. On the other hand, alkalinity tends to be constant along the experiment. This is better observed at the last compartments due to a higher methanogenic activity.

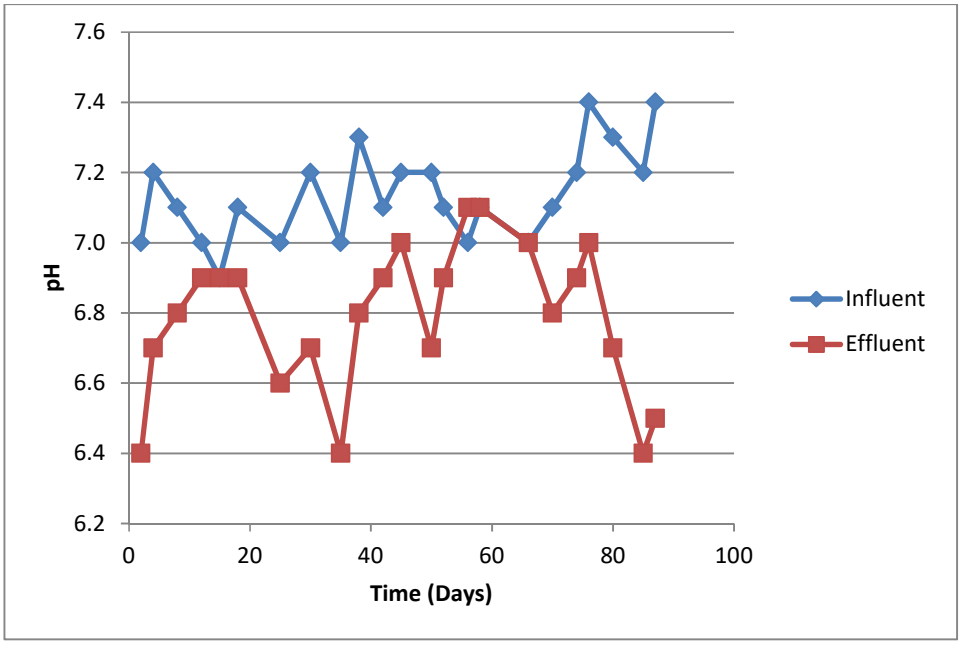

Fig.4.17:pH variation profile during reactor operation period

4.5 Results of Acidity, Alkalinity, Turbidity and pH Determination for Reactor 3

The pH values of influent and effluent were found to be in the range of 7.2—82 and 6.8—7.5 respectively at various HRTs tested. The pH in the Comparments1, 2 and3 were in the acidic range, whereas the other chambers exhibited a neutral range of pH. It was observed that during every shift to the next lower HRT the pH in first three chambers dropped rapidly, while other compartments were found to be the least affected. This indicated that accumulation of fatty acids was restricted upto compartments 1 to 3 only, unaffecting the methanogenosis occurring in rest of the chambers. This was due to the fact that the hydrolysis, acidogenesis and acetogenesis occurring in the initial chambers. It was observed that in spite of variations in the pH of feed wastewater, the pH values of treated effluent were constant at a particular HRT.

The constant effluent pH values implied the effective consumption of volatile fatty acids by methanogens. The alkalinity levels reveal a potential anaerobic process performance. Lower values of effluent alkalinity warn about the impending reactor failure. During the transition period (i.e. the period between shift of HRT to next lower HRT and time of acclimatization at that new HRT), alkalinity levels were observed to be lowered. Low effluent alkalinity coincided with lower COD reduction efficiencies. However, once the transition period was over, the reactor performance at a particular HRT was stable. The alkalinity of influent and treated effluent was in the range of 230—330 mg/L and 252-400 mg/L as $CaCO_3$. At higher HRTs (HRT>0.25 day), the effluent alkalinity levels were 10—18% more than the influent alkalinity. It was observed that these ratios varied between 0.22 and 0.35 at the RRTs above 0.25. However the values were 0.55 and 0.69 at the HRTs of 0.17 and 0.13days respectively.

4.6 Comparison with Other Works

Several authors have studied the effect of aspect ratio (L/w) on COD removal in ABR system and reported that the optimum aspect ratio for COD removal is the range of 0.5 to 1.5 (Marquardt, 1995; Parker and Doyle III, 1997; Fredrickson et al., 1970).Zamamiri (2002) studied the influence of number of baffles on COD removal efficiency in bioreactors and obtained the range of value 2 and 15.This is in agreement with the results obtained in this study. Mantzaris (2002), studied the effect of cyanide concentration on COD removal efficiency and obtained similar graphs as the one shown in Fig. 4.3.

CHAPTER FIVE

CONCLUSION AND RECOMMENDATIONS

5.1 Conclusion

The state-of-the-art in the field of ABR for treatment of wastewater is reviewed in this study, based on a substantial number of relevant references published recently; it can be concluded that the ABR could be applied to treat various wastewaters with satisfactory results if integrated with proper technology. As a high-rate anaerobic reactor, ABR has considerable potential for wastewater treatment. The objective of this study was evaluation of the performance of the ABR during various hydraulic and loading conditions of Cassava wastewater. Conclusions are enumerated viz:

i. The mathematical model for cassava wastewater treatment was successfully calibrated and validated in an ABR system.
ii. When fitted to experimental data, the Monod and Michaelis-menten models showed a good prediction of the ABR system.
iii. Kinetic coefficients obtained in the study were in agreement with results cited in literature. The effect of N_b and L/W on the COD removal efficiency showed that the values increased as COD removal efficiency.
iv. Similarly, the impact of N_b and L/W ratio on the cyanide concentration revealed optimum values

5.2 Recommendations

This study points the need for further investigations in the following areas:

i. Further studies are required for the optimization of methane production from cassava wastewater treatment in ABR
ii. The stoichiometry of the ABR system in Modeling cassava wastewater treatment deserves to be investigated.
iii. The optimum values obtained in this study should be implemented and tested in a pilot plant scale to confirm the success of the developed model.
iv. Further studies should address population and species of microorganisms need for enhanced treatment of the cassava wastewater.
v. Investigation is needed for the economy of the ABR system.
vi. The ability of the system to withstand shock loading needs to be investigated.

5.3 Contributions to Knowledge

A new model for COD removal from Cassava wastewater treatment was developed using ABR system. Other contributions to knowledge include:

i. Evaluation of optimum number of baffles and aspect ratio for the treatment of cassava wastewater, before discharge to the environment.

ii. Successful calibration of Monod and Michaelis-Menten Models using cassava wastewater as process system.

iii. A relationship between cyanide inhibition and removal efficiency was established for cassava wastewater treatment.

iv. The study also obtained values of inhibition constants for varying concentrations of cyanide in cassava wastewater treatment.

v. In addition, the effects of inhibition of various kinetic coefficients for cassava waste water were established.

REFERENCES

Agrawal, P., Koshy, G. and Ramseier, M. (1989). An algorithm for operating a fed-batch fermenter at opitimum specific growth-rate. Biotech. Bioeng., 33:115-125.

Agunwamba, J.C., Oti, N.C. and Aguwa, I. (2001). "Treatablility of cassava wastwater and sewage: batch reactor studies". J. Sci. Engr. Tech 8(1) pp 3096-3107.

Agunwamba, J.C. (2004). "Degradation of glucoside in cassava Wastewater,. African J. of Science 5(i):1174— 1185.

Akinrele, R. H. (1986). Seasonal succession in marine bacterioplancton species found among colony-forming bacteria. Appl. Environ. Microbial. 63, 3359 – 3366.

Akunna J. C and Clark, M. (2000). Performance of a granular-bed anaerobic baffled reactor (GRABBR) treating whisky distillery wastewater. Bioresour. Technol. 74: 257-261.

Andrews, J. F. (1968). "A mathematical model for the continuous culture of microorganisms utilizing inhibitory substrates." Biotechnol. Bioengr 10, pp. 707-723.

Andrews, J.F. (1969). Dynamic model of the anaerobic digestion model. *J. Sanit. Engng.* Div. Proc. Am. Soc. Civ. Engrs, SA 1, 95-116.

Andrews, J.F. (1971). Kinetic models of biological waste treatment processes. *Biotechnol. Bioengng. Symp*., 2, 5-33.

Angelidaki, I. (1992). Anaerobic thermophilic biogass process: the effect of lipids and ammonia. Ph.D. Thesis, Copenhagen, The Technical University of Denmark. Pp 105-115.

Angelidaki, I. and Ahring, B.K. (1992). Effects of free long-chain fatty acids on thermophilic anaerobic digestion. *Appl. Microbiol. Biotech.,* 37, 808-812.

Angelidaki, I., Ellegaard, L. and Ahring, B.K. (1993). A mathematical model for dynamic simulation of anaerobic digestion of complex substrates: focusing on ammonia inhibition. *Biotechnology and Bioengineering*, 42, 159-166.

Angenent, L. T., Abel, S. J and Sung, S., (2002). Effect of an organic shock load on the stability of an anaerobic migrating blanket reactor. J. Environ. Eng., 128 (12): 1109-1120.

Annachhatre, A. P and Amatya, P. L., (2000). UASB treatment of tapioca starch wastewater. J. Environ. Eng. 126 (12):1149-1152.

Aoyama, A., Doyle III, F.J., and Venkatasubramanian, V. (1995). Control-affine fuzzy neural network approach for nonlinear process control. Proc. J. Cont., 5:375-386.

APHA. (1998) Standard Methods for the Examination of Water and Wastewater, 17th Edition, American Public Health Association, Washington, DC. Pp 45-49.

Arguedas, O. C and Cooke, D. P. (1982). Biodegradation of three and four ring polycyclic aromatic hydrocarbons under aerobic and denitrifying conditions. Environ. Sci. Technol. 32, 2633 – 2639.

Bachmann, V.L., Beard, P.L. and Mc Cart (1985). Performance characteristics of anaerobic baffled reactor, Wat. Res. 19 (1) 99-106.

Bailey, J.E. and Ollis, D.F. (1986). Biochemical Engineering Fundamentals. McGraw-Hill, New York, Second edition. Pp 108.

Baloch, M.l., Akunna, J.C. and Collier, P.J. (2007). The performance of a phase separated granular bed bioreactor treating brewery wastewater. Bioresour. Technol. 98: 1849-1 855.

Barber, W.P.T. and Stuckey, D.C. (1999). The use of the anaerobic baffled reactors (ABR) for wastewater treatment: A review. Water Res., 33:1559-15 78.

Bengtsson, I. L. and Triet, C. K. (1994). Emulsifying agents from bacteria isolated during screening for cells with hydrophobic surfaces. Appl. Microbial. Biotechnol. 32, 521 – 525.

Bodkhe, S.Y., (2009). A modified anaerobic baffled reactor for municipal wastewater treatment. J. Environ. Manage. 90: 2488-2493.

Bryant, M.P. (1979). Microbial methane production - theoretical aspects. *J. Anim. Sci*., 48, 193-201.

Bryers, J.D. (1985). Structured modelling of the anaerobic digestion of biomass particulates. *Biotechnology and Bioengineering*, 27, 638-649.

Cereda, S. H and Takahashi, T. O. (1996). Microbial co-oxidations involving hydrocarbons. Microbiol. Rev. 43, 59 – 72.

Costello, D.J., Greenfield, P.F. and Lee, P.L. (1991a). Dynamic modelling of a single-stage high-rate anaerobic reactor- I. Model derivation. *Wat. Res*., 25, 847-858.

Costello, D.J., Greenfield, P.F. and Lee, P.L. (1991b). Dynamic modelling of a single-stage high-rate anaerobic reactor- II. Model verification. *Wat. Res*., 25, 859-871.

De Azevedo, S.F., Dahm, B. and Oliveira, F.R. (1997). Hybrid modeling of biochemical processes: A comparison with the conventional approach. Comput. Chem. Eng., (Suppl.):S751-S756.

Domach, M.M., leung, S.K., Cahn, R.E., Cocks, G.G. and Shuler, M.L, (1984). Computer model for glucose-limited growth of a single cell of Escherichia coli B/r-A. Biotechnology and Bio-engineering, 26:20-216.

Doyle, F.J., Ogunnaike, B.A and Pearson, R.K. (1995). Nonlinear model-based control using second order Volterra Model. Automatica, (31):697-714.

Draaijer, H., Mass, J., Schaapman, J.E. and Khan, A. (1992). Performance of the 5 MLD UASB Reactor for Sewage Treatment at Kampur, India. Water Sci. Technol. 23(7): 123-133.

Eastman, J.A. and Ferguson, J.F. (1981). Solubilization of particulate organic carbon during the acid phase of anaerobic digestion. *Journal WPCF*, 53, 352-366.

Ekundayo, J.A. (1980). In; Fungal Biotechnology. Eds.: Smith JE, Berry DR, Kristiasen B. London: Academic Press. pp. 244-270.

ERM (1996): Strategic environmental Assessment. Agricultural and consumer protection. FAO, www.fao.org/docrep/007/y2413e/y2413ed.htm

Faisal, M and Unno, H. (2001). kinetic analysis of palm oil mill wastewater treatment by modified anaerobic baffled reactor Biochem. Eng. J, 9 25.51, 200l.

FAO. (2004). Feasibility of anaerobic biodegradation of PAHs in dredged river sediments. Water Sci. Technol. 38, 41 – 48.

Feng, H.J., Hua, L.F., Mahmood, Q., Qiu, C.D., Fang, C.R and Shen, D.S. (2008). Anaerobic domestic wastewater treatment with bamboo carrier anaerobic baffled reactor. Int. Biodeter. Biodegr. 62: 232-238.

Fredrickson, A.G., Megee III, R.D. and Tsuchiya, H.M. (1970). Mathematical models for fermentation processes. Adv. Appl. Microbial., 13:419.

FSU (2014): Kinetics: Inhibition of an Enzymes Activity – Background: The Inhibitor Constant; BCH4053L, Biochemistry Laboratory Manual; Retrieved, 2014 from www.chem.fsu.edu/chemlab/bch4053l/index.html

Gavala, H.N., Skiadas, I.V., Bozinis, N.A. and Lyberatos, G. (1996). Anaerobic codigestion of agricultural industries wastewaters. *Wat. Sci. Tech*., 34, 67-75.

Goldstein, W.S. and Spencer, K.C. (1985).Inhibition of Cyanogenesis by Tannins, Journal of Chemical Ecology, 11: 847-856.

Graef, S.P. and Andrews, J.F. (1974). Stability and control of anaerobic digestion. *Journal WPCF*, 46, 667-682.

Grover, R., Marwaha, S. S and Kennedy, J. F. (1999). Studies on the use of an anaerobic baffled reactor for the continuous anaerobic digestion of pulp and paper mill black liquors. Process Biochem., 39: 653-657.

Haydar, S. and Aziz, J.A. (2009): Kinetic Coefficients for the Biological Treatment of Tannery Wastewater using Activated Sludge Process; Pak Journal of Engineering and Applied Science Vol 5 July 2009 (p 39 – 43).

Henson, M.A. (1998). Nonlinear model predictive control: Current status and future directions. Comput. Chem. Eng., 23:187-202.

Hill, C.G. Jr. (1977). An Introduction to Chemical Engineering Kinetics and Reactor Design. Wiley, New York. Pp 132-135.

Hill, D.T. and Barth, C.L. (1977). A dynamic model for simulation of animal waste digestion. *Journal WPCF*, 10, 2129-2143.

Hulshoff Pol, L.W., Lopes, C.I.S, Lettinga, O. and Lens, L.N.P (2004). Anaerobic sludge granulation. Water Res. 38: 1376-1389.

Hutnan, M., Drtil, M., Mrafkova, A.L., Derco, J and Buday, J. (1999). Comparison of startup and anaerobic wastewater treatment in UASB, hybrid and baffled reactor. Bioproc. Eng. 21: 439-445.

Ihekoronye, U. A. and Ngoddy, O. J. (1985). Maintenance energy of bacteria in growing cultures. Proc. R. Soc. Lond. (Biol.) 163, 224 – 231.

Jeong, J.W., Snay, J. and Ataai, M.M. (1990) A mathematical method for examining growth and sporulation process of Bacillus subtilis. Bioeng., 35:160-184,

Jewel, V. J. (1987). "Anaerobic Sewage Treatment." Environmental Sc:. & Tech, 21(1), - pp. 14-21.

Kalogo, Y., Mbouche, J. and Verstraete, W. (2001). Physical and Biological Performance of Self-inoculated UASB Reactor Treating Raw Domestic Sewage. J. Environ. Eng. 127(2): 179-183.

Kalyuzhnii, S.V. and Fedorovich, V.V. (1997). Integrated mathematical model of UASB reactor for competition between sulphate reduction and methanogenesis. *Wat. Sci. Technol*., 36, 201-208.

Kalyuzhnyi, S., Santos, L and Martinez, J. R. (1998). Anaerobic Treatment of Raw and Preclarified Potato-Maize Wastewater in a UASB Reactor. Bioresource. Technol., 66: 195-199.

Karl-Heinz, B. (2000). Bioreaction Engineering Modeling and control, Chapter 2: Bioprocess Models. Petersburg, Springer. Pp 44-105.

Kennedy, K. and Barriault, M. (2005). Effect of recycle on treatment of aircraft de-icing fluid in an anaerobic baffled reactor. Water SA 31: 377-384.

Khabbaz, M., Vossoughi, M. and Shakari, M. (2004). Performance of an Anearobic Baffled Reactor for Olive Mill Oil Wastewater Treatment. Proc. of 9th Iranian Chemical Engineering Congress. Iran University of Science and Technology, 23-25 November, 2004. Pp 3044-3063.

Kleinstreuer, C. and Powegha, T. (1982). Dynamic simulator for anaerobic digestion process. *Biotechnology and Bioengineering*, 24, 1941-1951.

Kong, H.L and Wu, H.F. (2008). Pretreatment of textile dyeing wastewater using an anoxic baffled reactor. Bioresour. Technol. 99: 7886-7891.

Krishna, G.V.T., Kumar, P. and Kumar, P. (2007). Treatment of low-strength soluble wastewater using an anaerobic baffled reactor (ABR). J. Environ. Manage. 90: 1-11.

Langenhoff, A. M. and Stuckey, D. C. (2000). Treatment of dilute wastewater using an anaerobic baffled reactor: effect of Low temperature. Water. Res., 34 (15): 3867-3875.

Langenhoff, A.M. and Stuckey, D.C. (2000). Treatment of dilute wastewater using an anaerobic baffled reactor: effect of low temperature. Water Res. 34: 3867-3875.

Lawrence, A.W. (1971). Application of process kinetics to design of anaerobic processes. In: *Anaerobic Biological Treatment Processes,* F.G. Pohland (ed.). Advances in Chemistry Series No.105, 163-189, AmericanChemical Society, Washington D.C.

Lettinga, G., Zehnder, A. B., Grotenhuis, J. T. C. and Hulshoff Pol L. W. (1998). Granular Anaerobic Sludge: Microbiology and Technology. Wageningen. The Netherlands: Centre for Agricultural Publishing and Documentation. Pp 23-34.

Lettinga, G.A., Van Velsen, F.M., de Zeeuw, W.J. and Hobma, S.W. (1979). The application of anaerobic digestion to the industrial pollution treatment. In: *Anaerobic Digestion,* Stafford et al. (eds.), 167-186. Applied Science Publishers, London, England.

Lettinga, G.A., van Velsen, F.M., Hobma, S.W., de Zeeuw, W.J. and Klapwijk, A. (1980). Use of the Upflow Sludge Blanket (USB) reactor concept for

biological wastewater treatment. *Biotechnology and Bioengineering*, 22, 699-734.

Lineweaver, H. and Burk, D. (1934): The Determination of Enzyme Dissociation Constants. Journal of the American Chemical Society**56** (3): 658–666.

Li, O., OuYang, F. and Yang, L.Z. (2001). Study on the performance of ABR reactor: review and summary. China Biogas. 19: 9-14 (Chinese).

Liu, X.L., Ren, N.Q. and Wan, C.L. (2007). Hydrodynamic characteristics of a four-compartment periodic anaerobic baffled reactor. J. Environ. Sci. 19: 1159-1165.

Ljung, L. (1987). System identification: theory for the user. PTR Prentice Hall, Englewood Cliffs, NJ. Pp 87-102.

Maner, B. and Doyle III, F.J. (1997). Polymerization control using autoregressive plus Volterra-based MPC. AIChE J., 43:1763-1784.

Mantzaris, N.V., Srienc, F., and Daoutidis, P. (2002). Nonlinear productivity control using a multi staged cell population balance model. Chem. Eng. Sci, 57:1-14

Marquardt, W. (1995) towards a process modeling methodology. In methods of model based process control, Pp 3-40. Kluwer academic publishers..

McCarty, P. L. (1 964a). “Anaerobic Waste Treatment Fundamentals, Part III, Toxic Materials and Their Control,” Public Works 95(November): pp. 91-94.

McCarty, P. L. (1964b). “Anaerobic Waste Treatment Fundamentals, Part II, Environmental Requirements and Control.” Public Works 95(October): pp. 123-126.

McCarty, P. L. (1964c). “Anaerobic Waste Treatment Fundamentals, Part IV, Process Design.’ Public Works 95(December): pp. 95-99.

McCarty, P. L. (1975). “Stoichiometry of biological reactions.” Frog. Water Technol. 7. pp. 157-112.

McCarty, P. L. and Smith, D. P. (1986). “Anaerobic Wastewater Treatment.” Environment: CJ Sd. & Technology 20(12), pp. 1200-1206.

Moletta, R., Verrier, D. and Albagnac, G. (1986). Dynamic modelling of anaerobic digestion. *Wat. Res*., 20, 427-434.

Monod, J. (1948). “The growth of bacterial cultures.” Ann Rev: microbial. 3, pp. 371—394. Namkung. E. and B. E. Rittmann (1986). “Soluble microbial products formation kinetics by biofilms.” Water Res. 20, pp. 795—806.

Monod, J. (1949). The growth of bacterial cultures. Annu. Rev. Microbiol., 3:371.

Mosey, F., E. (1983). Mathematical modelling of the anaerobic digestion process: regulatory mechanisms for the formation of short-chain volatile acids from glucose. *Wat. Sci. Technol*., 15, 209-232.

Muhammad, H.A. (2006): Determination of Biokinetic Coefficients of an Immersed Membrane Bioreactor; Journal of Membrane Science 271 (2006) 47 – 58.

Nartey, N. C. (1973). Influence of hydrodynamic conditions on naphthalene dissolution and subsequent biodegradation. Biotechnol. Bioeng. 57, 145 – 154.

Nachaiyasit, S. and Stucky, D. C., (1997a). The effect of shock loads on the performance of an anaerobic baffled reactor (ABR), 1. Step change in feed concentration at constant retention time. Water. Res., **31** (11): 2737-2746

Noguera, D. R. (1991). "Soluble microbial products (SMP) modeling in biological processes." M. S. Thesis, Dept. Civil Engr.. University of Illinois at Urbana-Champaign, Urbana. Illinois. Pp 57.

Noguera, D. R., Araki, N. and Rittmann, B. E. (1994). 'Soluble microbial products in anaerobic chemostats." Biotechnol. Bioengr 44, pp. 1040—1047.

O'Rourke, J. T. (1968). Kinetics of Anaerobic Treatment at Reduced Temperatures. Stanford University. Pp 403.

Obadina, A. O., Oyewole, O. B., Sanni, L. O. and Abiola, S. S. (2006). Fungalenrichment of cassava peels proteins. Afri. J. Biotechnol. 5(3): 302-304.

Odunfa, E. B. (1985). Significance of bacterial surface-active compounds in interaction of bacteria with interfaces. Microbial. Rev. 60, 151 – 166.

Okafor, N. (1992). Commercialization of fermented foods in Sub-SaharanAfrica. In Application of Biotechnology to traditional fermented foods.pp. 165-169. National Academy press, USA.

Parker, R.S. (1999). Model-Based Analysis and Control for Biosystems. PhD. thesis, Department of Chemical Engineering, University of Delaware. Pp 146-150.

Parker, R.S. and Doyle III, F.J., (2001). Optimal control of a continuous bioreactor using an empirical non-linear model. Ind. Eng. Chem. Res., 40:1939-1951.

Parkin, G. F. and Owen, W. F. (1986). “Fundamentals of Anaerobic Digestion of Wastewater Sludges.” J. Environmental Eng.. 112(5), pp. 867-920.

Peretti, S.W. and Bailey, J.E. (1985). Mechanistically detailed model of cellular metabolism for glucose-limited growth of Escherichia coli B/r-A. Biotech. Bioeng., 28:1672-1689.

Pick-Ford, J. (1977) Sewage Treatment in Developing Countries, Water Pollution Control Vol. 78 NIl pp. 40.

Psichogios, D. and Ungar, L.H. (1992). A Hybrid neural network-first principles approach to process modeling. AIChE, J., 38:1499-1511.

Pullammanapallil, P., Owens, J.M., Svoronos, S.A., Lyberatos, G. and Chynoweth, D.P. (1991). Dynamic model for conventionally mixed anaerobic digestion reactors. AIChE Annual Meeting, paper 277c, 43-53.

Rittmann, G. E., and Soez, P. B. (1993). "Modeling biological processes involved in degradation of hazardous organic substrates." In Biotmeaunent of' Industrial and Hazardous Wastes, eds. J. M. Levin and .M. Dealt. Nes4 York: McGraw-Hill, pp. 113—136.

Salami, A. K. and Egwim, C. (1997). Diffusion – the crucial process in many aspects of the biology of bacteria. Adv. Microb. Ecol. 11, 37-69.

Sallis, P. J and Uyanik, S. (2003). Granule development in a spilt-feed anaerobic baffled reactor. Bioresource. Technol., 89: 255-265.

Schroepfer, G. J. (1955). "The Anaerobic Contact Process as Applied to Packinghouse Waste." Sewage and Industrial Wastes, 27. pp. 460-486.

Siegriest, H., Renggli, D. and Gujer, W. (1993). Mathematical modelling of anaerobic mesophilic sewage sludge treatment. *Wat. Sci. Technol*., 27, 25-36.

Skiadas, I.V. and Lyberatos, G. (1998). The periodic anaerobic baffled reactor. Water Sd. Technol. 38: 401-408.

Smith, P.H., Bordeaux, F.M., Goto, M., Shiralipour, A., Wilke, A., Andrews, J.F., Ide, S. and Barnett, M.W. (1998). Biological production of methane from biomass. In: Methane from biomass. *A treatment approach.*

Speece, R. E. (1983). Anaerobic biotechnology for industrial wastewater treatment. *Environ. Sci. Technol*., 17, 416A-426A.

Speece, R. E. (1996). Anaerobic Biotechnology for Industrial Wastewaters. Nashville: Archae Press. Pp 201-208.

Steinmeyer, D.E. and Shuler, M.L. (1989). Structured model for Saccharomyces Cerevisiae. Chem. Eng. Sci., 44:2017-2030.

Swyen, C. F. and Wiston, E. (1971). Anaerobic biodegradation of naphthalene, phenanthrene and biphenyl by a denitrifying enrichment culture. Water Res. 35, 291 – 299.

Tholudor, A. and Ramirez, W.F. (1996). Optimization of fed-batch bioreactors using neural network parameter function models. Biotech. Prog., 12:302-309.

Tsuchiya, H.M., Fredrickson, A.G. and Aris, R. (1996). Dynamics of miocrobial cell populations. Adv. Chem. Eng., 6:125.

Uyanik, S., Sallis, P.J. and Anderson, G.K. (2002b). The effect of polymer addition on granulation in an anaerobic baffled reactor (ABR). Part II: compartmentalization of bacterial populations. Water Res. 36: 944-955.1542

Uyanik, S., Sallis, P.J, and Anderson, G.K. (2002a). The effect of polymer addition on granulation in an anaerobic baffled reactor (ABR). Part 1:process performance. Water Res. 36: 933-943.

Viet, Y. B. (1998). Impact of inoculation protocols, salinity and pH on the degradation of polycyclic aromatic hydrocarbons (PAHs) and survival of PAH-degrading bacteria introduced into soil. Appl. Environ. Microbial. 64, 359 – 362.

Vijayaraghavan, k. and Remanujan, T.(1999). Effect of Chloride and Condensable Tannin in Anaerobic Degradation of Tannery Wastewaters. Bioprocess Eng. 20: 499-503.

Vyssides, F.A., van Lier, J.B. and Macario, A.J.L. (2005). Diversity and population dynamics of bacteria in a granular consortium. *Appl. Environ*., 57, 1728-1734.

Wang H.Y., Cooney C.L., and Wang D.I.C. (1977). Computer aidede baker's yeast fermentations biotech. Bioeng., 19:69-86.

Weng, C.N. and Jeris, J.S. (1976). Biochemical mechanisms in the methane fermentation of glutamic and oleic acids. *Wat. Res.,* 10, 9-18.

Williams, F.M. (1967). A model of cell growth dynamics. Theor, J. Boil.,15:190.

Wisnewski, P.A., Doyle III, F.J., and Kayihan, F. (1997). Fundamental continuous pulp digester model for simulation and control. AIChE, J., 43:3175-3192.

Woffside, I. R and Shifter, K. M. (1959). Development of fungal inocula for bioaugmentation of contaminated soils. Appl. Environ. Microbial. 62, 2045 – 2052.

Wrenn, B. A. and Rittman, B. E. (1995). “Evaluation of a model ‘or the effects of substrate interactions on the kinetics of reductive dechlorination.” Biodegrodammon 7: pp. 49—64.

Yang, R.D. and Humphrey, A.E. (1975). Dynamic and steady state studies of phenol biodegradation in pure and mixed cultures. Biotech. Bioeng., 17:1211.

Young, J. C. and McCarty, P. L. (1969). ‘The Anaerobic Filter for Waste Treatment.” J. Water pollution Control Federation 41. pp. R l60-R 173.

Zamamiri, A.M., Zhang Y. and Hjortso, M.A. (2002). Dynamics analysis of an age distribution model of oscillating yeast cultures. Chem. Eng. Sci, 57:2169-218.

APPENDICES

Appendix 1: Values for Generation of Regression Model

RE	L/W	Nb	Ki	Q
0.7	**0.001**	**1**	**30**	**0.8**
0.8136	**0.4**	**3**	**9.9989**	**0.4**
0.8136	**0.5**	**4**	**9.2079**	**0.3148**
0.816	**0.6**	**5**	**8.3002**	**0.2796**
0.8213	**0.7**	**6**	**7.4252**	**0.2444**
0.828	**0.8**	**7**	**6.3827**	**0.2092**
0.8379	**0.9**	**8**	**5.4414**	**0.1739**
0.8378	**1**	**9**	**4.3396**	**0.1287**
0.8475	**1.1**	**10**	**3.6196**	**0.1035**
0.8629	**1.2**	**11**	**2.6198**	**0.0683**
0.88	**1.3**	**12**	**1.6901**	**0.0331**
0.99	**10**	**20**	**0.01**	**0.01**

V_w = Wastewater volume for each case, l

V_r = Reactor volume, l

L/W = Length-width ratio

N_b = Number of baffles

Q = Flow rate, l/min

HRT = Hydraulic retention time, min = V_w/Q

S_o = Influent COD at the start of each of the experimental case, mg/l

X_o = Influent suspended solids at the start of each case, mg/l

I = Inhibitor (cyanide) Concentration at the start of each case, mg/l

Appendix 2: Values for Generation of Regression Model

R	L	N	C	Q	LR	L^2	LN	LC	LQ	NR	N^2	NC	NQ	CR	C^2	CQ	QR	Q^2
-0.36	-6.91	0.00	3.40	-0.22	2.46	47.73	0.00	-23.50	1.54	0.00	0.00	0.00	0.00	-1.21	11.57	-0.76	0.08	0.05
-0.21	-0.92	1.10	2.30	-0.92	0.19	0.84	-1.01	-2.11	0.84	-0.23	1.21	2.53	-1.01	-0.48	5.30	-2.11	0.19	0.84
-0.21	-0.69	1.39	2.22	-1.16	0.14	0.48	-0.96	-1.54	0.80	-0.29	1.92	3.08	-1.60	-0.46	4.93	-2.57	0.24	1.34
-0.20	-0.51	1.61	2.12	-1.27	0.10	0.26	-0.82	-1.08	0.65	-0.33	2.59	3.41	-2.05	-0.43	4.48	-2.70	0.26	1.62
-0.20	-0.36	1.79	2.01	-1.41	0.07	0.13	-0.64	-0.72	0.50	-0.35	3.21	3.59	-2.53	-0.39	4.02	-2.83	0.28	1.99
-0.19	-0.22	2.57	2.71	-1.59	0.04	0.05	-0.57	-0.60	0.36	-0.48	6.58	6.95	-4.09	-0.51	7.34	-4.32	0.30	2.54
-0.18	-0.11	2.08	1.69	-1.75	0.02	0.01	-0.22	-0.18	0.18	-0.37	4.33	3.52	-3.64	-0.30	2.87	-2.96	0.31	3.06
-0.18	0.00	2.20	1.47	-2.05	0.00	0.00	0.00	0.00	0.00	-0.39	4.83	3.23	-4.51	-0.26	2.16	-3.01	0.36	4.21
-0.17	0.10	2.30	1.29	-2.27	-0.02	0.01	0.22	0.12	-0.22	-0.38	5.30	2.96	-5.22	-0.21	1.66	-2.92	0.38	5.15
-0.15	0.18	2.40	0.96	-2.68	-0.03	0.03	0.44	0.18	-0.49	-0.35	5.75	2.31	-6.44	-0.14	0.93	-2.59	0.40	7.21
-0.13	0.26	2.94	0.52	-3.41	-0.03	0.07	0.77	0.14	-0.89	-0.38	8.67	1.55	-10.0	-0.07	0.28	-1.79	0.44	11.62
-0.01	2.30	3.00	-4.61	-4.61	-0.02	5.30	6.90	-10.61	-10.61	-0.03	8.98	-13.8	-13.8	0.05	21.22	21.22	0.05	21.22
ΣR=	**ΣL=**	**ΣN=**	**ΣC=**	**ΣQ=**	**ΣLR=**	**ΣL^2=**	**ΣLN=**	**ΣLC=**	**ΣLQ=**	**ΣNR=**	**ΣN^2=**	**ΣNC=**	**ΣNQ=**	**ΣCR=**	**ΣC^2=**	**ΣCQ=**	**ΣQR=**	**ΣQ^2=**
-2.16	-6.87	23.37	16.09	-23.3	2.93	54.92	4.11	-39.90	-7.33	-3.58	53.38	19.33	-54.9	-4.42	66.74	-7.33	3.27	60.83

Where, R = ln(RE)

L = ln(L/W)

N = ln(N_b)

C = ln(Ki)

Q = ln(Q)

APPENDIX 3:pH Behaviour as a Function of Time

Acidity (mgCaCO3L-1)		
Time (Days)	**Influent**	**Effluent**
0.0	**50.0**	**100.0**
15.0	**100.0**	**50.0**
30.0	**100.0**	**20.0**
45.0	**300.0**	**120.0**
60.0	**200.0**	**100.0**
75.0	**800.0**	**120.0**
90.0	**1000.0**	**200.0**
105.0	**200.0**	**100.0**
120.0	**100.0**	**200.0**
135.0	**500.0**	**80.0**
150.0	**1300.0**	**120.0**
165.0	**600.0**	**50.0**
180.0	**500.0**	**80.0**
195.0	**380.0**	**100.0**
210.0	**600.0**	**100.0**
225.0	**700.0**	**200.0**

APPENDIX 4: (a) Alkalinity and (b) Acidity Behaviour as a Function of Time

Alkalinity ($mgCaCO_3L^{-1}$)		
Time (Days)	**Influent**	**Effluent**
0.0	**1600.0**	**750.0**
15.0	**750.0**	**750.0**
30.0	**750.0**	**500.0**
45.0	**1750.0**	**1500.0**
60.0	**1750.0**	**3000.0**
75.0	**1400.0**	**3000.0**
90.0	**1400.0**	**1500.0**
105.0	**1500.0**	**1500.0**
120.0	**750.0**	**1500.0**
135.0	**1500.0**	**1500.0**
150.0	**1400.0**	**1750.0**
165.0	**15500.0**	**15000.0**
180.0	**16500.0**	**4500.0**
195.0	**750.0**	**750.0**
210.0	**3000.0**	**4000.0**
225.0	**4000.0**	**4500.0**

APPENDIX 5 : Turbidity Behaviour as a Function of Time

	Turbidity (NTU)					
Time (Days)	Influent	C_1	C_2	C_3	C_4	Effluent
0.0	350.0	-	40.0	40.0	50.0	40.0
15.0	80.0	40.0	40.0	40.0	-	40.0
30.0	200.0	50.0	40.0	-	50.0	40.0
45.0	140.0	80.0	70.0	-	75.0	50.0
60.0	100.0	-	50.0	-	80.0	90.0
75.0	80.0	50.0	-	-	40.0	40.0
90.0	150.0	50.0	100.0	-	50.0	50.0
105.0	350.0	-	50.0	-	40.0	120.0
120.0	140.0	80.0	100.0	50.0	-	50.0
135.0	100.0	100.0	-	75.0	50.0	50.0
150.0	100.0	-	60.0	50.0	40.0	80.0
165.0	450.0	300.0	275.0	200.0	200.0	220.0
180.0	280.0	300.0	275.0	250.0	200.0	200.0
195.0	450.0	-	300.0	280.0	230.0	340.0
210.0	-	-	-	-	-	-
225.0	320.0	300.0	200.0	180.0	150.0	300.0

APPENDIX 6:Influent and Effluent Alkalinity during Reactor Operation Period

	Alkalinity (mg/L) as $CaCO_3$ * 10^2	
Time (days)	Influent	Effluent
2	18.0	24.0
4	22.0	20.0
8	30.0	24.0
10	35.0	30.0
12	28.0	48.0
15	32.0	38.0
18	30.0	35.0
20	25.0	34.0
22	24.0	28.0
24	22.0	26.0
28	24.0	24.0
32	28.0	25.0
35	10.0	34.0
40	20.0	20.0
42	10.0	25.0
44	22.0	30.0
48	24.0	28.0
50	22.0	31.0
52	24.0	38.0
54	24.0	40.0
56	25.0	38.0
58	30.0	46.0
59	22.0	40.0
65	24.0	34.0
68	27.0	38.0
70	28.0	40.0
72	33.0	39
74	26.0	50
76	23.0	35
78	23.0	36
80	24.0	38

APPENDIX 7: pH Variation Profile during Reactor Operation Period

	pH	
Time (days)	Influent	Effluent
2	7.0	6.4
4	7.2	6.7
8	7.1	6.8
12	7.0	6.9
15	6.9	6.9
18	7.1	6.9
25	7.0	6.6
30	7.2	6.7
35	7.0	6.4
38	7.3	6.8
42	7.1	6.9
45	7.2	7.0
50	7.2	6.7
52	7.1	6.9
56	7.0	7.1
58	7.1	7.1
66	7.0	7.0
70	7.1	6.8
74	7.2	6.9
76	7.4	7.0
80	7.3	6.7
85	7.2	6.4
87	7.4	6.5